



Proceedings of the
International Conference on
Creep and Deformation Characteristics
in Geomaterials

24-25 August 2015, Gothenburg, Sweden

Edited by:

Jelke Dijkstra
Minna Karstunen
Jean-Philippe Gras
Mats Karlsson

Acknowledgment

The conference is organised as part of the activities of the Marie Curie Industry Academia Partnerships and Pathways project on Creep of Geomaterials (CREEP PIAP-GA-2011-286397). Financial support from the European Community under the 7th Framework Programme is gratefully acknowledged.

CREEP partners:

Norwegian University of Science and Technology (NTNU), Trondheim, Norway
Chalmers University of Technology, Gothenburg, Sweden
Shanghai Jiao Tong University, Shanghai, China
Cold and Arid Regions Environmental and Engineering Research Institute,
Chinese Academy of Sciences, Lanzhou, China
Deltares, Delft, the Netherlands
Norwegian Geotechnical Institute, Oslo, Norway

© The copyright of the keynote presentations and the extended abstracts within this proceedings lies with the authors.

International Conference on
Creep and Deformation Characteristics
in Geomaterials

978-91-980974-8-1 (Print)
978-91-980974-9-8 (Pdf)

Published by Chalmers University of Technology 2015

Table of Contents

Preface	iii
Committees	v
Invited Keynote Presentations	1
Material creep, characteristic times, and patience <i>I. Einav</i>	3
Experimental study of viscoplastic mechanisms in clay under complex loading <i>P.-Y. Hicher</i>	5
Creep effects on the clays from Mexico basin <i>E. Ovando-Shelley</i>	7
Extended Abstracts	15
Numerical analysis of an embankment on soft soil <i>A. Amavasai, J.-P. Gras, J. Dijkstra & M. Karstunen</i>	17
Implementation of a critical state soft soil creep model with shear stiffness <i>M.A. Haji Ashrafi & G. Grimstad</i>	21
A framework for peat behaviour based on hyperplasticity principles <i>D. Boumezerane, G. Grimstad & A. Makdisi</i>	25
A new concept in developing a constitutive model for frozen soils <i>S. A. Ghoreishian Amiri, M. Kadivar & G. Grimstad</i>	29
On estimation of parameters describing soil structure and anisotropy for CREEP-SCLAY1S <i>J.-P. Gras, J. Dijkstra & M. Karstunen</i>	33
Is creep analysis creeping into practice? <i>G. Grimstad, M. Mehli & S.A. Degago</i>	35
A procedure for determining long-term creep rates of soft clays by triaxial testing <i>H.P. Jostad & J. Yannie</i>	39
Effect of sample disturbance on evaluated creep parameters for a high plasticity clay <i>M. Karlsson, A. Bergström, J. Dijkstra & A. Emdal</i>	43
Creep of sand in filled open cast mining pits <i>F. Levin & S. Vogt</i>	47

Thermo-hydro-mechanical simulation of an energy pile in soft clay with a rate-dependent anisotropic constitutive model	51
<i>Y. Li, J. Dijkstra & M. Karstunen</i>	
Viscoplastic subloading modelling of strain rate change effects in London clay	55
<i>J.R. Maranhã, C. Pereira & A. Vieira</i>	
Creep mechanisms in soil and crystalline rock and mathematical formulation of them based on stochastic mechanics	59
<i>R. Pusch</i>	
Back calculation of triaxial extension creep tests on a tertiary clay	63
<i>N. Sivasithamparam, H.P. Jostad & P. Fornes</i>	
A probabilistic approach for calculation of land subsidence on a macro-scale	67
<i>J. Sundell, L. Rosén, C. Alén, M. Karlsson & E. Haaf</i>	
An overlay model for peat	71
<i>J.A.M. Teunissen & C. Zwanenburg</i>	
Modelling deep foundations in soft Gothenburg clay	75
<i>T. Wood & M. Karstunen</i>	
A hypoplastic creep model for frozen soil	79
<i>G.F. Xu, W. Wu & J.L. Qi</i>	
A new elasto-viscoplastic model for 1-d compressive behavior of clays	85
<i>Y. Yuan & A.J. Whittle</i>	
Undrained triaxial relaxation tests on a fibrous peat	89
<i>L. Zhang, B.C. O'Kelly & T. Nagel</i>	

Preface

Geotechnical engineering often involves designing structures built on, in or of natural or improved soils. Increasingly, long-term behaviour needs to be accounted for in the consideration of stability and deformation of geotechnical structures. In the context of major infrastructure projects, long-term refers to a period of decades. Given that the soil often governs the response of geotechnical structures, an in-depth understanding of the material behaviour is of paramount importance. An additional complication is that the material response is influenced by the stress history of the material, resulting from geological, environmental and building processes.

The fact that natural soils are complex geomaterials makes analysis of geotechnical problems challenging. In particular, the rate-dependent behaviour in clays, peats and frozen soils is poorly captured in existing models, both on the particulate level and on the continuum scale.

The aim of the conference is to provide an international forum for presenting and discussing the latest developments in modelling, monitoring, analysing and managing long-term deformations in geotechnical engineering. Creep and rate-dependency is also an important mechanism in other engineering materials, such as concrete and polymers.

Active discussion will be facilitated through a contribution of keynote presentations and submitted contributions. The invited keynote presenters are: Prof. Efraín Ovando-Shelley (Universidad Nacional Autónoma de México, Mexico), Prof. Itai Einav (The University of Sydney, Australia), Prof. Pierre-Yves Hicher (École Centrale de Nantes, France) and Prof. Kenneth Runesson (Chalmers University of Technology).

Given most academics want to publish their original research in international scientific journals, we have opted for extended abstracts only, available in Open Access. The proceedings contains some highlights of the research done under the CREEP project, achieved through intense collaboration between industry and academia, as well as contributions from other parties interested in the topic.

Jelke Dijkstra
Minna Karstunen
Jean-Philippe Gras
Mats Karlsson

Committees

Organizing Committee

Associate Prof. Jelke Dijkstra, Chair (Chalmers University of Technology, Sweden)
Prof. Minna Karstunen, Vice-Chair (Chalmers University of Technology, Sweden)
Dr Jean-Philippe Gras, (Chalmers University of Technology, Sweden)
Dr Mats Karlsson, (Chalmers University of Technology, Sweden)

Scientific Committee

Prof. Gustav Grimstad (Norwegian University of Science and Technology, Norway)
Prof. Minna Karstunen (Chalmers University of Technology, Sweden)
Prof. Jilin Qi (CAREERI, China)
Associate Prof. Jelke Dijkstra (Chalmers University of Technology, Sweden)
Associate Prof. Zhenyu Yin (Shanghai Jiao Tong University, China/Ecole Centrale de Nantes, France)
Dr S. Ali Ghoreishian Amiri (Norwegian University of Science and Technology, Norway)
Dr Thomas Benz (Norwegian University of Science and Technology, Norway)
Dr Djamalddine Boumezerane (Norwegian University of Science and Technology, Norway)
Dr Samson Degago (NPRA, Norway)
Dr Jean-Philippe Gras (Chalmers University of Technology, Sweden)
Dr Evert den Haan (Deltares, the Netherlands)
Dr Hans-Petter Jostad (Norwegian Geotechnical Institute, Norway)
Dr Mats Karlsson (Chalmers University of Technology, Sweden)
Dr Nallathamby Sivasithamparam (Norwegian Geotechnical Institute, Norway)
Dr Cor Zwanenburg (Deltares, the Netherlands)

Invited Keynote Presentations

MATERIAL CREEP, CHARACTERISTIC TIMES, AND PATIENCE

I. Einav

School of Civil Engineering, University of Sydney, Sydney, Australia

INTRODUCTION

In materials science, creep is the tendency of a solid material to move slowly under the influence of mechanical stresses (Wikipedia, 17 June, 2015). The word “slowly” is also adopted in Oxford and Merriam Webster dictionaries. But when saying “slowly” these definitions miss a reference – slowly relative to what? Therefore, during my talk I will start by proposing to extend the above definition:

“Creep is the tendency of a solid material to move slowly relative to human patience, under the influence of mechanical stresses”.

Since the notion of creep depends on both material characteristic times and the time entrenched in patience, the term creep motion may be scientifically confusing. Rather than classifying deformation to be of creep nature or not, it could be more relevant to avoid a reference to patience and simply classify deformations in terms of the various characteristic times.

During my talk I will present a variety of new experimental results revealing rate dependent load-deformation curves reminiscent of what might be thought as creep-like materials. Although the various experiments present similar trends, the physical processes behind those vary, and include gradual brittle failure effect on compression of soft porous media, diffusion and inertia effects on capillary forces, and asperity morphing effect on surface-to-surface contacts. Through discrete element model a further of such trend will be related to gradual melting and solidification, relevant to fault gouge materials. The key characteristic times behind these various processes will be identified; regimes of observed phenomena will be related with non-dimensionless groups denoting the relative magnitudes of the various characteristic times. Finally, I will identify the challenges for future constitutive models in order to capture these rich behaviours.

ACKNOWLEDGEMENTS

The author would like to acknowledge the contributions from Y. Gan , F. Guillard & P. Rognon (School of Civil Engineering, University of Sydney, Sydney, Australia) and J.R. Valdes (Department of Civil, Construction, and Environmental Engineering, San Diego State University, San Diego, USA).

EXPERIMENTAL STUDY OF VISCOPLASTIC MECHANISMS IN CLAY UNDER COMPLEX LOADING

P.-Y. Hicher

LUNAM University, Ecole Centrale de Nantes, UMR CNRS GeM, France

INTRODUCTION

A series of triaxial tests has been performed on a saturated compacted clay. Cyclic tests at very small to small strain amplitudes ($<10^{-3}$) and monotonic undrained triaxial tests at different strain rates demonstrate the influence of the material viscous properties, which appear to be independent of the strain amplitude and of the condition of loading: monotonic or cyclic.

Then, stress relaxation and creep tests at various loading stages including primary loading, unloading and reloading were performed and the results were analyzed in terms of viscoplastic mechanisms. Performed during a primary loading, the stress relaxation tests show a constant decrease of the deviatoric stress with time down to a constant stress value.

The result can be seen as in agreement with the viscoplastic theory developed by Perzyna based on the overstress concept. This approach commonly used in geomechanics has proven to be efficient for modeling the time-dependent behavior of soils. When the stress relaxation test is performed during an unloading phase, the stress decrease can still be observed if the unloading amplitude remains small. However, the stress decrease is smaller than the one observed during primary loading. The overstress theory can also be applied to this case if we consider that the unloading amplitude was small enough for the stress state to remain beyond the yield surface and, therefore, that the primary viscoplastic mechanism continues to be mobilized during the stress relaxation phase.

In the case of a large stress reversal, the stress increases during the stress relaxation phase, indicating the existence of a kinematic viscoplastic mechanism which develops during unloading. Similar results were obtained during reloading: for small reloading amplitude, the stress continued to increase whereas for larger reloading, the stress decreased during the stress relaxation phases, in agreement with the concept of a kinematic viscoplastic mechanism which takes effect also during the reloading phase. Interestingly, more complex cases were observed for intermediate unloading (reloading). In these cases, the stress started to decrease (increase) at the beginning of the relaxation phase following an unloading (reloading) and after a given time began to increase (decrease) until reaching a stabilized condition. These results seem to indicate the existence of several mechanisms (at least two) acting simultaneously, linked to the memory of the different loading phases.

Undrained creep tests were also performed in order to complement the results obtained during stress relaxation tests. The results bear out the existence of viscoplastic mechanisms. Creep during primary loading or reloading show an increase of the deviatoric strain with time, whereas creep at different unloading stages show a decrease of the deviatoric strain with time, in agreement with the concept of kinematic hardening defined by the stress relaxation tests.

A creep test performed after a moderate unloading showed a slight decrease of the strain followed by a continuous increase, which confirms the notion of a double kinematic mechanism acting simultaneously to create conflicting evolutions of the deviatoric strain during creep phases, as during stress relaxation phases.

CONCLUSIONS

In conclusion, this set of experimental results improves our understanding of the time-dependent behavior of clayey soils subjected to complex loading.

CREEP EFFECTS ON THE CLAYS FROM MEXICO BASIN

E. Ovando-Shelley

Instituto de Ingeniería, Universidad Nacional Autónoma de México, Mexico

INTRODUCTION

The Basin of Mexico, sometimes called the Valley of Mexico, lies over a surface of about 7160 km², surrounded by volcanic ranges. The lower parts of the basin, some 2050 km², were once occupied by a system of interconnected lakes, the largest of which was Lake Texcoco. The central part of Mexico City is set on the southwestern portion of the basin and it mainly rests over lacustrine clays. The lake system is practically nonexistent nowadays because it has been desiccated progressively over the last 400 years or so.

Mexico City Clays were deposited as floccules of very small particles in lakes where salinity varied. In the northern portion, the Texcoco Lake water was rich in salts but in the south, the Xochimilco and Chalco lakes contained very small amounts of dissolved minerals. Sodium ions must have certainly had an influence on the micro structural array of these clays but re-search into these aspects is scarce. Pioneering investigations into these matters are due to Marsal & Mazari (1959) and Girault (1964) who found that the clays they studied were mostly amorphous.

The behaviour of these clays can be affected by the rate at which loads and deformations are imposed upon them. In this paper we examine succinctly these effects all of which relate to time-dependent stress-strain characteristics that are typical of materials subjected to creep. The clays in the Basin of Mexico underlie a rather large urbanized area and, consequently, geotechnical engineers in the city have had to deal with these materials and have had to devise ad hoc foundation solutions to cope with these materials. We briefly examine and discuss some of these solutions herein.

GRAVIMETRIC AND VOLUMETRIC RELATIONSHIPS

Natural water contents and Atterberg limits in Mexico City Clays are notoriously large. These materials have been pointed out as extremely plastic clays that, correspondingly, display very low shear strengths and rather large compressibilities.

The highest water contents in the city lake area are found in high the Upper Clay Formation, down to a depth of about 20 m. Water contents in these clays vary considerably, de-pending on the location of individual sites. In general, soils towards the edges of the former lake are less humid than in the central part a situation that has been favoured by the existence of sands and sandy silts interspersed with the upper clays in the so called transition zone. Sites in the built area, having been subjected to external overburdens and exposed to the effects of regional consolidation have less pore water than the so called virgin clays, which are typical of the less or newly urbanized areas, like those found in the former Texcoco Lake in which external loads have not been applied on the surface but in which regional consolidation has also had an important effect. The following data

give an idea of the distribution of water content in the upper 20m of the First Clay Formation, in different parts of the city:

- Downtown Mexico City (Cathedral, 2001) 150 to 250%
- Densely built area (colonia Roma, first 20m, 1986) 200 to 300%
- Texcoco lake bed (2001) 400 to 600%

COMPRESSIBILITY

Result of tests performed on a strain-controlled oedometer are given in the graphs displayed in Figure 1, which have vertical effective stress as abscissae and liquidity index (LI) as ordinates (López, 2002). These tests were performed on samples retrieved from the urban area at a site belonging to the virgin lake, applying different strain rates. In general compressibility curves tend to move towards the right in σ'_v -LI space as strain rate increases, which is a feature common to most soils but is more notorious in materials from the Basin of Mexico, thus re-reflecting their viscous character. From these tests the apparent preconsolidation pressure can be expressed in terms of strain rate, r , plasticity index, PI and liquidity index:

$$\sigma'_c = 45 PI (r)^{0.27 LI} \quad (1)$$

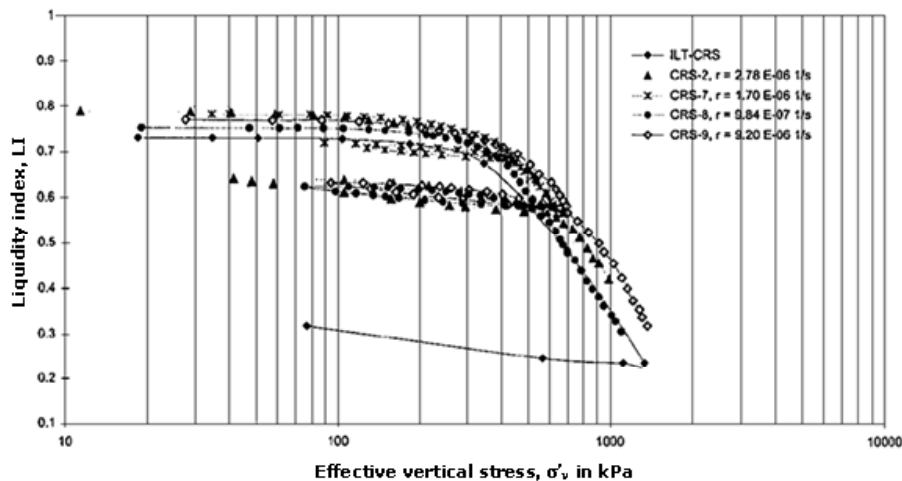


Figure 1 Liquidity index against Effective vertical stress (Tests at different strain rates)

Effective stress changes brought by pumping to extract water from the deep aquifers, have produced changes in water content, as the ensuing regional consolidation process in the Basin of Mexico goes on. These changes have also modified stress and stress-path dependent me-chemical parameters, like compressibility or stiffness and shear strength. The effects of effec-tive stress changes due to water extraction on index and mechanical properties have been dis-cussed elsewhere (Ovando-Shelley et al, 2003, 2007). In applying the model, the following set of differential equations must be integrated:

$$c_{ve} \frac{\partial^2 u}{\partial z^2} = \frac{\partial u}{\partial t} - \frac{1}{m_{ve}} g(u, \varepsilon_z) \quad (2)$$

$$\frac{\partial \varepsilon_z}{\partial t} = -m_{ve} \frac{\partial u}{\partial t} + g(u, \varepsilon_z) \quad (3)$$

$$g(u, \varepsilon_z) = \frac{\psi / v_o}{t_o} \exp \left[- \left(\varepsilon_z - \varepsilon_{zo}^{vp} \right) \frac{v_o}{\psi} \right] \left(\frac{\sigma'_z}{\sigma'_{zo}} \right)^{\frac{\lambda}{\psi}} \quad (4)$$

where, c_{ve} is a consolidation coefficient associated to elastic deformations, equal to $k/(m_{ve}\gamma_w)$; k is the soil's permeability and m_{ve} is the volumetric compressibility along the elastic portion of the one dimensional stress-strain curve, equal to $\partial \varepsilon_z^e / \partial \sigma'_z = (\kappa/v_o)/(\sigma'_z)$; $\kappa/v_o = C_{ve}/2.3$, where C_{ve} is the slope along the compressibility curve in log time versus strain; finally κ/v_o is the slope of a reference one dimensional stress-strain curve.

The graphs in Figure 2 show typical compressibility curves obtained from one dimensional compression tests on Mexico City clays. Samples were extracted from the urbanized area, from the same site and from the same stratum in three different dates, 1952, 1986 and 2001. The effects of regional consolidation are evident in that voids ratio of the latter specimens is lower and, correspondingly, their apparent preconsolidation pressure is larger. Yet, the virgin consolidation line of the three specimens tested is approximately the same. Further discussion into these aspects may be found in other publications (Ovando et al. 2003, 2007).

Intrinsic soil properties have been referred to the compressibility and strength characteristics that are inherent to the soil and independent of its natural state. They provide, according to Burland (1990), a reference framework for assessing and interpreting the significance of these same properties as exhibited by natural clays.

Normalized compression curves in I_v versus σ'_v space given in Figure 3 are plotted using normalized compression curves from a variety of sites published previously (Burland, 1990) including as a means for making comparisons, curves obtained from the testing of natural and reconstituted clays from Mexico City and Lake Texcoco; data from tests performed on Colombian clays from Bogota are also included. The parameter void index, I_v is

$$I_v^* = \frac{(e - e_{100}^*)}{e_{100}^* - e_{1000}^*} = \frac{(e - e_{100}^*)}{C_c^*} \quad (5)$$

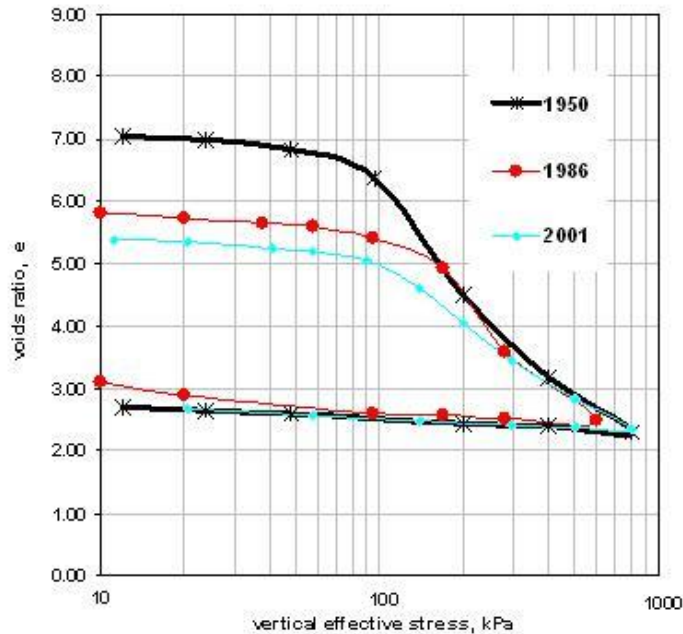


Figure 2. Compressibility curves obtained from one-dimensional compression tests on Mexico City Clay samples retrieved from the same stratum at the same site at three different dates.

Viscosity of the Basin of Mexico clays also influences the behaviour of these soils during long term loading. When external loads are applied stepwise, it has traditionally been customary to separate the primary and the secondary stages of consolidation, implicitly assuming that both processes are uncoupled. This was the approach originally put forth, among others, by Zeevaert (1971) who developed a formulation assuming a Kelvin type rheological model for the Mexico City Clays.

Nonetheless, it has also been established that both processes, primary and secondary consolidation, are coupled and that they occur simultaneously, assuming that the soil is a viscous material. One such model has been applied recently to study regional subsidence in the city (Ovando et al 2008). It is a one dimensional consolidation model in which the soil under-going the consolidation process is assumed to be an elasto-viscoplastic material (Yin and Graham, 1994, 1996).

SHEAR STRENGTH AND UNDRAINED BEHAVIOUR

Most bearing capacity problems in common foundation engineering practice in Mexico City are usually solved relying heavily on estimations of undrained shear strength from traditional UU compression tests. Shear strength in the lacustrine clays from the Basin of Mexico is typically very low, as it can be expected a priori given the extremely high water contents found in these materials.

Given the geological conditions prevailing in the former lake bed and the recent effective stress increments produced by water pumping from the aquifer, the clays in Mexico City can be assumed to be normally consolidated and strength will increase over time on account of these effective stress increments brought about by regional consolidation.

CU compression tests show that ϕ (total stress) values range from about 16° to slightly more than 22°. CU tests with pore pressure measurement yield ϕ' values that often exceed 40°.

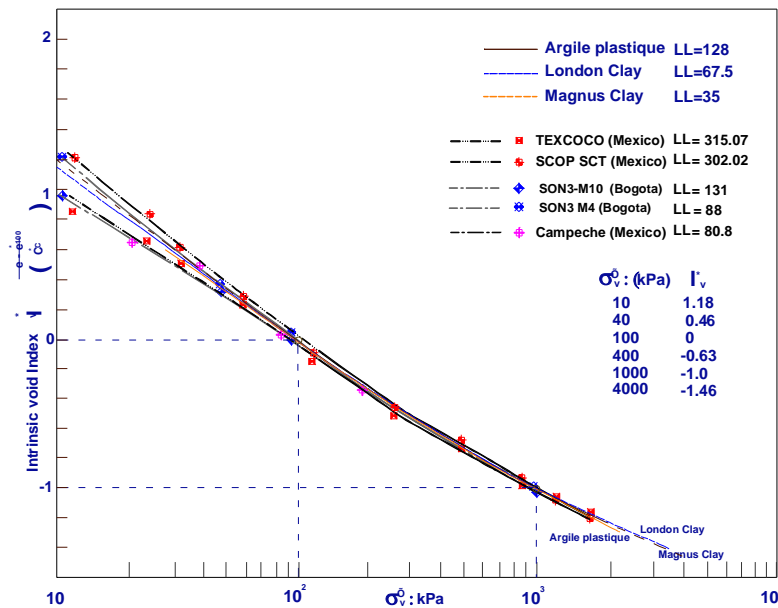


Figure 3 Normalized intrinsic compression line, Burland (1990). Added Data shown includes clays of the former Texcoco, Lake, from the urban zone in Mexico City (SCOP-SCT centre), the city of Bogota, Colombia and the Campeche Sound in the Gulf of Mexico.

From the results of a set of CU tests carried out in order to investigate the applicability of the Modified Cam Clay model to Mexico City Clay, it was concluded that it can be used to provide a fair description of the behaviour of isotropically consolidated Mexico City Clay in a normally consolidated or a slightly overconsolidated state (Giraldo, 1996). The model did not work well for overconsolidated samples with $OCR > 4$. Extending these concepts further, Valderrama (2013) put forth an elasto-plastic model in which the size of the yield surface is rate-dependent:

$$f = (q - \alpha \cdot p')^2 - (M^2 - \alpha^2)[(p_0^Y) - p']p' = 0 \quad (6)$$

α is the inclination of the elliptic yield curve with respect to the isotropic line in q - p' space, $\alpha = 1$ when the sample is isotropically consolidated and $\alpha < 1$; M , q and p' have their usual meanings. The rate parameter Y modifies p_0' , the maximum mean effective stress as seen in Figure 4 (a). Y may be obtained from the graph in Figure 4 (b), a plot of Y normalized with respect to Y_0 (the value of Y corresponding to an arbitrary reference deformation rate of 0.0001 mm/min). Experimental data shown there were obtained from test on natural and reconstituted Mexico City and Texcoco Lake clay samples.

The effects of strain rate on stress-strain curves and on small strain stiffness measured are illustrated in Figures 5a and 5b, respectively. As shown there rate affects most notoriously normalized stiffness (G/p').

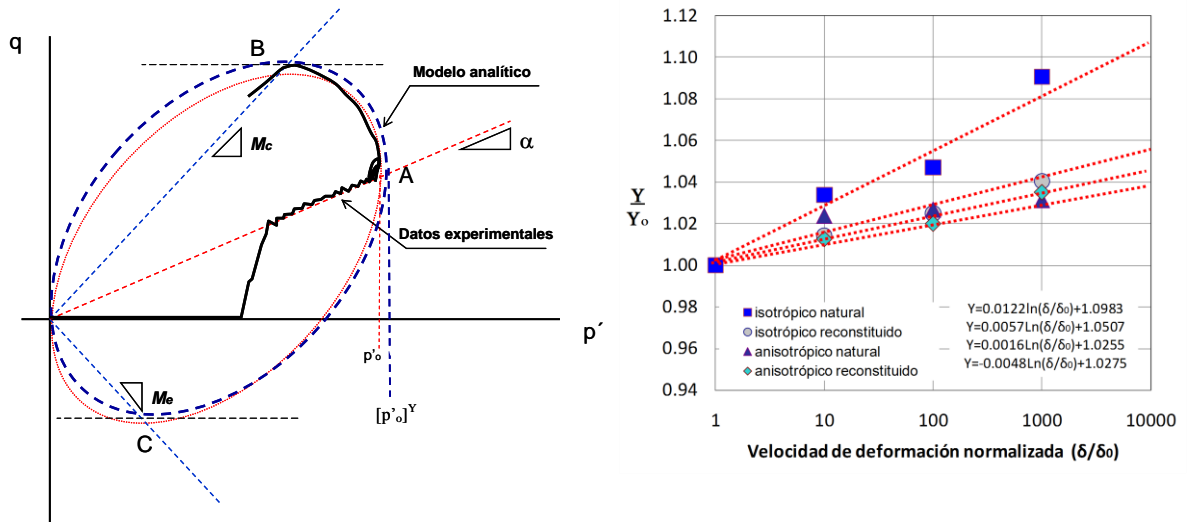


Figure 4. Left hand graph (a): strain-dependent yield surface. Right hand graph (b): graphical representation of the rate parameter Y for natural and reconstituted clay.

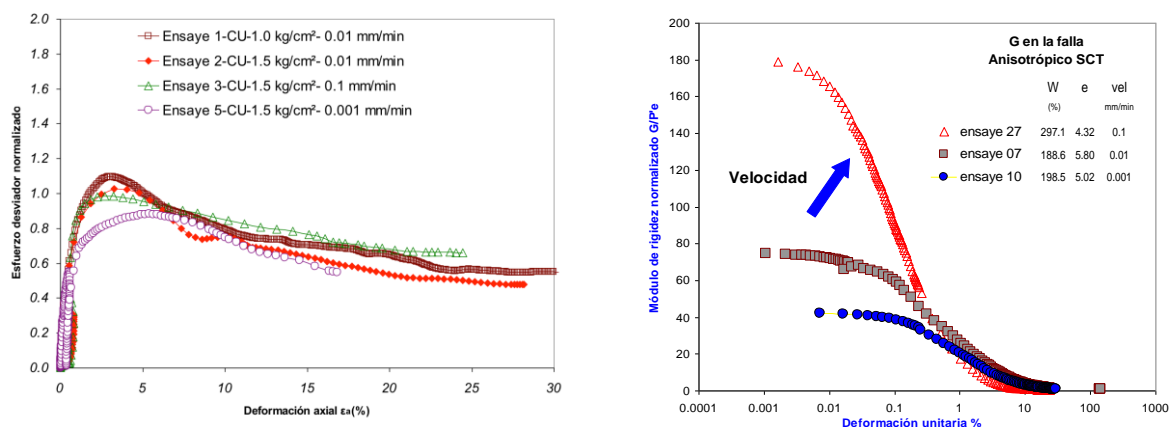


Figure 5 Illustration of rate effect on stress-strain curves (a) and normalized stiffness curves (G/p') against axial strain (b).

FINAL REMARKS

The totality of the area formerly occupied by the lakes is now sinking on account the intense exploitation of the aquifers that underlie the soft clayey soils. Deep well pumping produces the depletion of pore water pressures and that, in turn, increases effective stress in the clay masses. The ensuing consolidation process changes the index and mechanical properties of the soils, both under static and under dynamic conditions.

Compressibility of these clays is very large and depends strongly on loading patterns and strain rate, as described here. Viscosity is shown to be a parameter of major importance in describing consolidation under one dimensional loading of these materials. Intrinsic properties of soils from the Basin of Mexico are scarcely known but the results shown here also confirm the existence of a unique, normalized compressibility curve expressed in terms of the intrinsic voids index. This curve appears to be valid for a large variety of soils, as demonstrated here.

Shear strength and the overall stress-strain-pore pressure behaviour are also rate dependent and some of the main features of the static undrained behaviour of these soils can be modelled reasonably well with classical plasticity models. One such model was adapted to include rate effects by introducing a rate factor that modifies the shape and size of the yield surface.

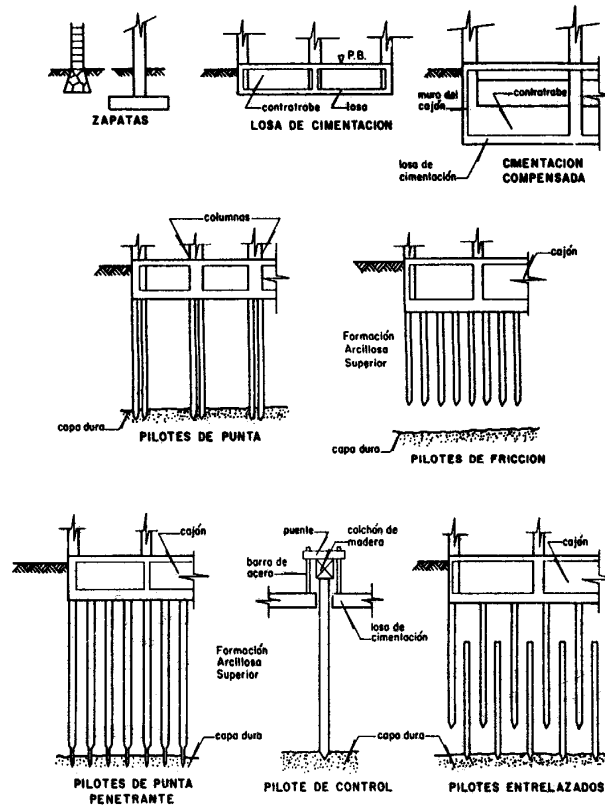


Figure 6. Foundation types commonly used in Mexico City.

Practical engineers have had to devise solutions in order to cope with difficult subsoil conditions in Mexico City. Some of the most common foundation types used in the city are illustrated in Figure 6: a) traditional surface footings, continuous or isolated, (upper row, left); b) box foundations (upper row, centre); c) compensated box foundations (upper row, right); d) point bearing piles (middle row, left); d) friction piles as settlement reducing elements, together with box foundations (middle row, right); e) friction piles with penetrating tips (bottom row, left); f) piles with devices for controlling loads (bottom row, centre); g) overlapping piles (bottom row, right).

All of the solutions have advantages and limitations that have to be assessed having as a reference the unique characteristics of the Mexico City and Texcoco clays, namely their extremely high compressibility and low shear strength. These materials are highly rate dependent, as shown here and this dependency must be borne in mind in any foundation project, especially in regard to dynamic loading situations brought about during earthquakes, a situation not covered in this paper but of paramount importance. Regional subsidence associated to water pumping from deep aquifers brings about effective stress increments that modify soil

properties, both static and dynamic. Modification of these properties as well as the expected settlements must also be accounted for in the design of foundations, given due consideration to the interaction of the foundation with its environment both under static and under seismic loads.

REFERENCES

- Burland, J.B., (1990). On the compressibility and shear strength of natural clays. *Géotechnique* 40(3): 329-378.
- Giraldo, M. C. 1996. Evaluación de un modelo elastoplástico para predecir el comportamiento de la arcilla de la ciudad de México. Tesis de maestría, División de Estudios de Posgrado, Facultad de Ingeniería, UNAM, agosto.
- Girault, P. 1964. Mineralogía de las arcillas del Valle de México. *Revista Ingeniería*, Facultad de Ingeniería, UNAM.
- López Velázquez Ó. 2002. Compresibilidad unidimensional de la arcilla de la ciudad de México bajo diferentes condiciones de carga y determinación del coeficiente K₀. Tesis de Maestría, División de estudios de posgrado, Facultad de Ingeniería, UNAM, Mexico
- Marsal, R. J. & Graue, R; 1969. El subsuelo del Lago de Texcoco, volumen Nabor Carrillo; D.F.:167-202.
- Ovando-Shelley E., Romo, M. P. & Ossa, A. 2007. The sinking of Mexico city: Its effects on soil properties and seismic response. *Soil Dynamics and Earthquake Engineering*, 27(4):333-343.
- Valderrama, Y. 2013. Modelo elastoplástico de Suelos naturales y reconstituidos de la Cuenca de México. Tesis docotoral, UNAM, Facultad de Ingeniería, División de Estudios de Posgrado (en elaboración).
- Yin JH, Graham J. 1994. Equivalent times and one dimensional elastic viscoplastic modelling of time dependent stress-strain behaviour of clays. *Canadian Geotechnical Journal*, 31(1):42-52.
- Yin JH, Graham J. 1996. Elastic visco-plastic modelling of one dimensional consolidation. *Géotechnique*, 46(3):515-27.
- Zeevaert L. 1971. *Foundation engineering for difficult subsoil conditions*. New York: Van Nostrand Reinhold Co.

Extended Abstracts

NUMERICAL ANALYSIS OF AN EMBANKMENT ON SOFT SOIL

A. Amavasai, J.-P. Gras, J. Dijkstra, M. Karstunen

Department of Civil and Environmental Engineering, Chalmers University of Technology, Gothenburg, Sweden

INTRODUCTION

This paper aims at benchmarking, an advanced constitutive model for natural soft soil incorporating anisotropy, structure and viscous characteristics, against well-documented long term field observations. The test embankment constructed at Haarajoki, Finland in 1997 by the Finnish National Road Administration (Vepsäläinen et al. 1997) is chosen as the benchmark case for validating CREEP-SCLAY1S, which is an extension of the CREEP-SCLAY model (Sivasithamparam et al. 2015) due to availability of long term data. Half of the area is improved with prefabricated vertical drains, and the other half, considered in this paper is unimproved. Emphasis is given to consistent parameter determination for the model from existing laboratory results in a completely automated manner, using a series of newly developed MATLAB algorithms. Laboratory experiments and embankment construction are simulated in Tochnog Professional (2015). The sensitivity of parameters, boundary, permeability and mesh on the embankment analysis are also investigated.

PROFILE

The soil deposit in Haarajoki exhibits high variation due to its history of intermittent saline and fresh water influx. The 2 m thick dry crust layer is heavily overconsolidated, differing from the soft soil layers as shown in Figure 1.

The embankment is 2.9 m high and 100 m long, constructed at an average of 0.5 m lifts on every 2 days. The embankment is 8 m wide with slopes at a gradient of 1:2. The phreatic level is at the ground surface. The embankment material varies from sandy gravel to gravel with a density of 21 kN/m³. The dry crust layer is 2 m thick followed by 18 m thick soft clay deposit. Deposits such as silt and till can be found beneath the soft clay layer.

PARAMETER DERIVATION

The quality of laboratory tests for most of the soil samples from Haarajoki exhibit poor standard, suffering from sampling effects, noise in data and lack key information. Based on the index tests provided, the soil deposits from Haarajoki have been divided into 6 layers. Data from incremental loading tests of Haarajoki samples are digitized and stored in separate arrays. The data is then manipulated and by using a set of newly developed algorithms in MATLAB necessary parameters for CREEP-SCLAY1S are derived in automated manner.

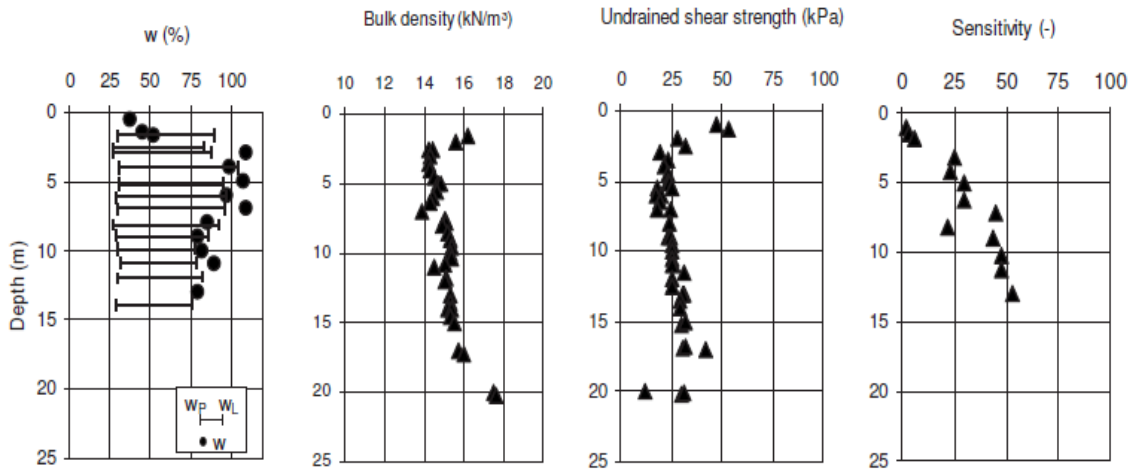


Figure 1: Illustration of Haarajoki soil profile Yildiz et al. (2009)

EXPERIMENTAL SIMULATION

Laboratory experiments are simulated to validate the newly derived parameters before furthering to embankment simulation, as shown in Figure 2. The geometry of the sample is modelled in Gmsh (2005) mesh generating software, and boundary conditions in the different experiments. The match is very good.

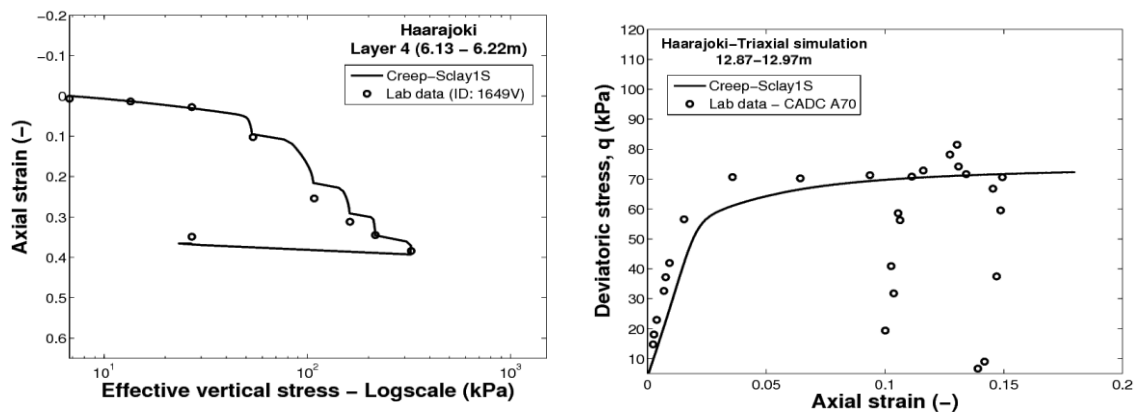


Figure 2: Comparison of simulation with laboratory data for (a) oedometer incremental loading experiment for samples from Layer-4 (b) drained triaxial experiment for sample from layer-5

EMBANKMENT SIMULATION

Plane strain analysis has been considered for embankment simulation. The right half of the geometry is modelled due to symmetrical boundary condition. A length of 50m from embankment centreline has been considered to prevent boundary effects. Boundary conditions are applied according to field conditions and numerical assumptions. Stage construction of embankment is simulated in Tochnog. Mohr Coulomb model is used for modelling the embankment. Due to differential desiccation rate, the dry crust layer has been divided into three linear elastic layers with large elastic stiffness on its top layer. The results are in good accordance with the field measurements, as shown in Figure 4. The excess pore

pressure after 1500 days is predicted to be around 28 kPa and the settlement to be 0.42m, which agree with field observations.

In order to identify the most critical region, the settlement along embankment centreline (point A) is plotted at different times as shown in Figure 4. It is clearly evident that the dry crust is the most critical region followed by initial soft soil layers (2 -5m). Sensitivity analysis further reveals that the stiffness of dry crust also significantly affects the rate of pore pressure dissipation.

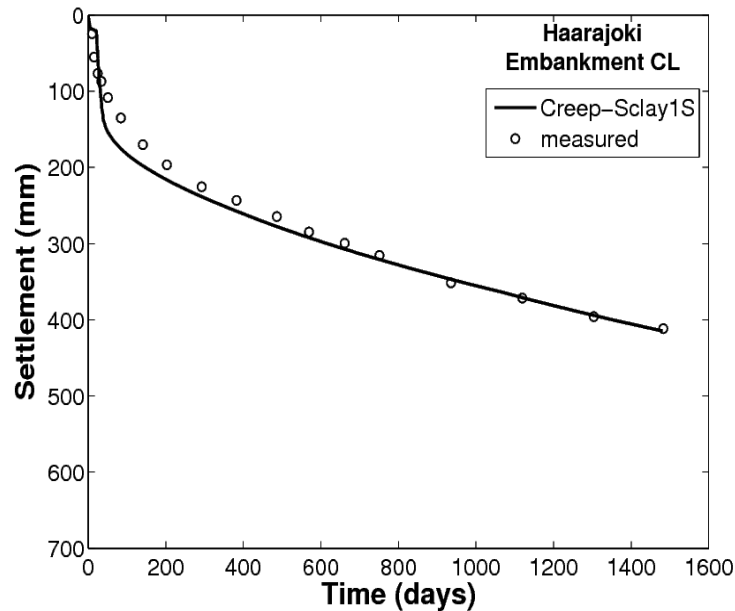


Figure 3: Comparison of simulation with field measurement along embankment centreline.

CONCLUSIONS

The element level simulations with the newly derived model parameters have shown to be in close agreement with the laboratory test data for the 1D incremental oedometer test and the drained triaxial test. On the other hand, the CRS tests showed larger discrepancies resulting from the complexities of the CRS test that require high quality samples, which were not available. Adaptation of the new model parameter set is shown to lead to the best predictions of the test embankment so far. The predictions are in good accordance with field measurements for settlement and pore-pressure distribution.

The most influential parameters for embankment simulation includes the permeability, dry crust stiffness and modified creep index. Dry crust has been found to be the most sensitive layer followed by initial soft soil layer (2-4m depth). The automated method of parameter derivation is efficient and did not require optimization in this project. The CREEP-SCLAY1S model, combined with consistent parameter determination, is efficient in capturing both experimental and field behaviour of soft soil.

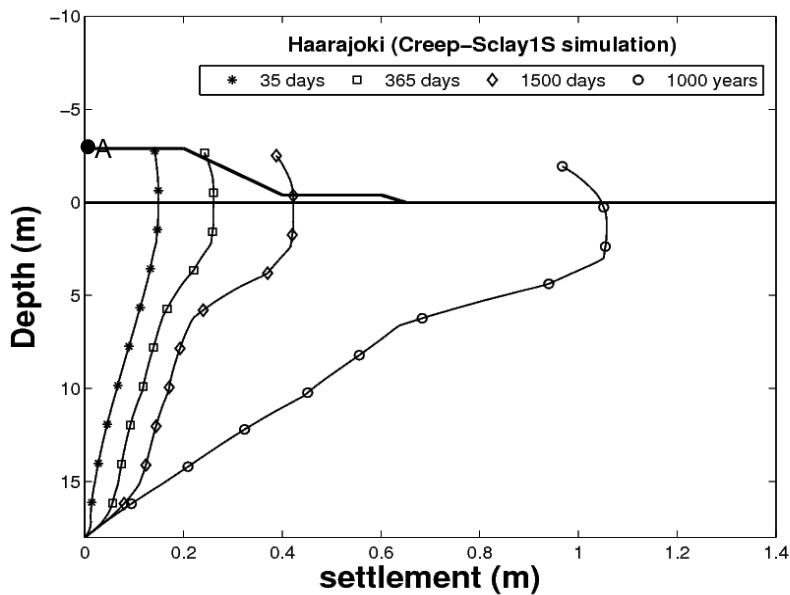


Figure 4: Predicted settlement underneath the centreline at different times.

RECOMMENDATIONS

Automated model parameter derivation should be the de facto approach for numerical modellers to increase the efficiency, and reduce the human bias in the model parameter set. Improved modelling and characterisation of the in-situ dry crust is paramount for increasing the accuracy of predictions of stability and safety of structures on soft soils.

REFERENCES

- Gmsh (2015). Gmsh reference manual. Version 2.9.3. <http://geuz.org/gmsh/doc/texinfo/gmsh.pdf>
- Sivasithamparam, N., Karstunen, M., & Bonnier, P. (2015). Modelling creep behaviour of anisotropic soft soils. *Computers and Geotechnics* 69, 46-57.
- Tochnog Professional User's manual (2015). Version 22. FEAT-Finite Element Application. Technology. url: <http://www.feat.nl/manuals/user/user.pdf>.
- Vepsäläinen, P., Lojander, M., and Koskinen, M. (1997). Competition to calculate settlements at Haarajoki test Embankment, FinnRA, Finland.
- Yildiz, A., Karstunen, M., and Krenn, H. (2009). Effect of Anisotropy and Destructuration on Behaviour of Haarajoki Test Embankment. *International Journal of Geomechanics*, 153-168.

IMPLEMENTATION OF A CRITICAL STATE SOFT SOIL CREEP MODEL WITH SHEAR STIFFNESS

M.A. Haji Ashrafi, G. Grimstad

Department of Civil and Transport Engineering, Norwegian University of Science and Technology, Trondheim, Norway

INTRODUCTION

The initial shear stiffness of soils decays non-linearly in the well-known S-shaped normalised load-deformation curves from laboratory tests e.g. Atkinson and Sällfors (1991) and Benz (2007). This work concerns primarily on the development and implementation of a viscoplastic (creep) model to reflect this behaviour of soil.

The existing creep constitutive models e.g. (i) the Soft Soil Creep model (SSC) Stolle et al. (1999), (ii) Anisotropic Creep Model (ACM) Leoni et al. (2009), (iii) non-Associated Creep Model for Structured Anisotropic Clay (n-SAC) Grimstad and Degago (2010), and (iv) Structured Anisotropic Creep Model (Creep-SCLAY1S) Sivasithanparam et al. (2015) use the Poisson's ratio as an input elasticity parameter. In this new model, instead, shear stiffness of the soil will be explicitly given by the engineer. This parameter can be easily obtained by standard geotechnical tests e.g. triaxial test or direct simple shear test. Having modified commercial Plaxis SSC model, MIT-MDPW embankment Karlsrud (1969) and Whittle (1974) is then studied to validate the model in a boundary value problem.

MODEL FORMULATION

First, a critical state soft soil creep model (CS-SSC) is implemented and verified against Plaxis SSC. Results from simulation of tests at elementary level shows that the model performance is very similar to Plaxis SSC. The CS-SSC model was then used as a basis to develop and implement a new critical state soft soil creep model with mobilised shear stiffness (CS-SSCG) where initial shear stiffness of the soil will be degraded with respect to mobilisation degree. The model has been formulated under the theory of so-called elasto-viscoplasticity. The Plaxis SSC has been subjected to two main modifications in its elasticity and viscoelasticity part; (i) elasticity part: stiffness matrix is expressed by mobilised shear stiffness, and (ii) viscoelasticity part: The model, similar to Plaxis SSC, uses the un-rotated elliptical viscoplastic reference in triaxial deviator stress q versus mean effective stress p' , however, the slope of the critical state line is set to be Lode angle dependent. This can reflect the soil strength anisotropy as expected e.g. in a triaxial compression and a triaxial tension test. Pay attention that Plaxis SSC uses Mohr-Coulomb cut-off for failure prediction, and therefore, two models' response may diverge in failure. The implicit Euler scheme is adopted for the sake of implementation in which the equivalent preconsolidation pressure and the viscoplastic multiplier are internal state variables whilst strain and the time increments are external actions.

For each soil cluster the initial shear stiffness is assumed to vary linearly with depth, see *Figure 1* and Equation(1). The parameter G_{inc} is the increment of initial shear stiffness per unit depth. For depths above the reference depth, y_{ref} , the initial shear stiffness is equal to G_{ref} . The mobilised shear stiffness G_M is formulated by Equation(2) where the degree of mobilisation f is defined by Equation(3). M_θ is the Lode angle dependent slope of the critical state line in triaxial $q-p'$ space, and $\langle \rangle$ denotes the Macaulay brackets. Mobilisation degree will be activated at stress ratios η higher than one at rest η_{K_0} , and ζ is the degradation factor which controls the decay of the initial shear stiffness with respect to mobilisation. The latter parameter can be obtained by curve fitting to the laboratory tests (numerically; $0 \leq \zeta < 1$). When using the model with $\zeta = 0$ and G_{50} (rather than G_0), nonlinear elasticity will be switched off.

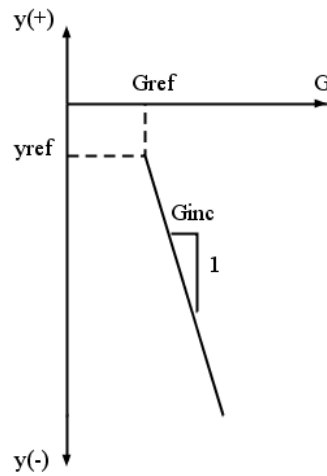


Figure 1. Increasing initial shear stiffness with depth in a soil cluster

$$G_0 = G_{ref} + \max\{(y_{ref} - y)G_{inc}, 0\} \quad (1)$$

$$G_M = G_0(1 - \xi f)^2 \quad (2)$$

$$f = \frac{\langle \eta - \eta_{K_0} \rangle}{M_\theta - \eta_{K_0}} \quad (3)$$

NUMERICAL ANALYSIS OF THE MIT-MDPW EMBANKMENT

Several researchers have studied numerical analysis of MIT-MDPW embankment, e.g. Neher et al. (2001) and Fatahi et al. (2012). Fatahi et al. (2012) use Plaxis SSC for their simulation. They are able to show a good agreement for vertical settlement under the centre of the embankment but they overestimate the vertical settlements under the embankment toe and at the deep layers. The main reason is that they do not reflect on the importance of the selection of OCR when using viscoplastic (creep) rate dependent models in settlement problems. Grimstad et al. (2013) addressed this issue and examined the embankment with focus on the 'proper' selection of OCR. The vertical displacements improved significantly both at the deeper and shallower levels and at the centre and toe of the embankment. However, prediction of the horizontal deformation under the embankment remained unsatisfactory as before. The Plaxis SSC model simulated the horizontal displacements that were considerably higher than the field measurements - the problem yet to be resolved. Results from the simulation of the MIT-MDPW embankment show that the CS-SSCG model were successful to reproduce the horizontal displacements that fits better to the field measurements compared to Plaxis SSC and CS-SSC. At the same time it can capture the vertical displacements and the pore pressure response well. Figure 2 illustrates the results from simulations and the field data profile for horizontal displacements under the embankment at I5 at construction day 620 and 2053. The inclinometer I5 is located close to the embankment toe. As can be seen, the implemented CS-SSC model predicts nearly the same profile compared to Plaxis SSC—this may verify the performance of CS-SSC in a boundary value problem. Nonetheless, both Plaxis SSC and CS-SSC predict higher horizontal displacements than the field measurements. The CS-SSCG model, on the other hand, shows a fairly good agreement with the field data. In general, this is particularly achieved in the beginning of the creep settlement (until CD 620) when elasticity dominates the deformation, and therefore, using 'proper' shear stiffness is of more significance.

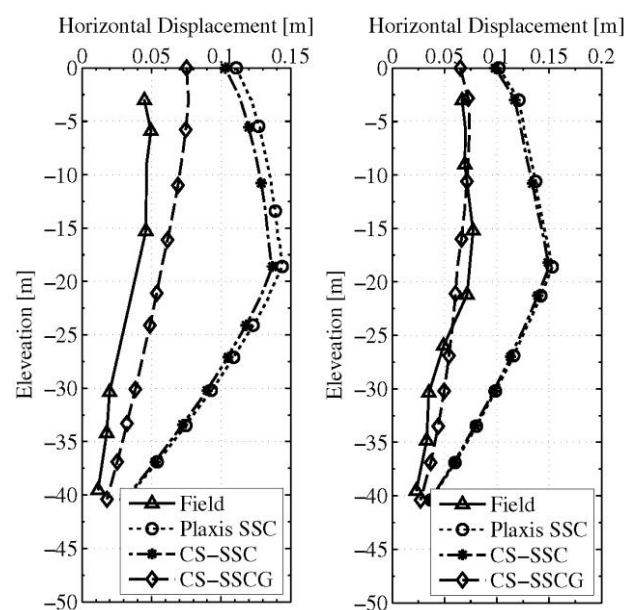


Figure 2. Simulated and measured horizontal displacements at day 620 (left) and 2053 (right)

CONCLUSION

With minor modifications in Plaxis SSC, the CS-SSCG model were successful to reproduce the horizontal displacements that fits better to the field measurements and yet it can capture the vertical displacements and the pore pressure profiles from the field measurements reasonably well. However, the model usage should be restricted for simulation of settlement problems. A similar idea is being formulated based on 'hyperelasticity' approach. This will improve the reliability of the model response when simulating other geotechnical problems dealing with loading-unloading.

ACKNOWLEDGEMENT

The research was carried out as part of CREEP (Creep of Geomaterials, PIAP-GA-2011-286397) project supported by the European Community through the programme Marie Curie Industry-Academia Partnerships and Pathways (IAPP) under the 7th Framework Programme.

REFERENCES

- Atkinson, H. & Sällfors, G. 1991. Experimental determination of soil properties. 10th ECSMFE. Florence.
- Benz, T. 2007. Small-Strain Stiffness of Soils and its Numerical consequences. Stuttgart University.
- Fatahi, B., Le, T. M., Le, M. Q. & Khabbaz, H. 2012. Soil creep effects on ground lateral deformation and pore water pressure under embankments. *Geomechanics and Geoengineering*, 8, 107-124.
- Grimstad, G. & Degago, S. A. 2010. A non-associated creep model for structured anisotropic clay (n-SAC). *Numerical Methods in Geotechnical Engineering*. Taylor & Francis Group.
- Grimstad, G., Haji Ashrafi, M. A., Degago, S. A., Emdal, A. & Nordal, S. 2013. Discussion of 'Soil creep effects on ground lateral deformation and pore water pressure under embankments' *Geomechanics and Geoengineering: An International Journal*.
- Karlsruud, K. 1969. Evaluation and interpretation of the performance of an embankment on clay. . Master, Massachusetts Institute of Technology (MIT).
- Leoni, M., Karstunen, M. & Vermeer, P. 2009. Anisotropic creep model for soft soils. *Geotechnique*, 58, 215-266.
- Neher, H. P., Wehnert, M. & Bonnier, P. G. An evaluation of soft soil models based on trial embankments. In: DESAI, C. S., ed. *Computer Methods and Advances in Geomechanics*, 2001 Rotterdam. Balkema, 373-378.
- Sivasithamparam, N., Karstunen, M., & Bonnier, P. (2015). Modelling creep behaviour of anisotropic soft soils. *Computers and Geotechnics*, 69, 46-57.
- Stolle, D. F. E., Vermeer, P. A. & Bonnier, P. G. 1999. A consolidation model for a creeping clay. *Canadian Geotechnical Journal*, 36, 754-759.
- Whittle, J. F. 1974. Consolidation behavior of an embankment on Boston blue clay. MEng, MIT.

A FRAMEWORK FOR PEAT BEHAVIOUR BASED ON HYPERPLASTICITY PRINCIPLES

D. Boumezerane, G. Grimstad

Geotechnical Division, Norwegian University of Science and Technology, Trondheim, Norway

A. Makdisi

Department of Civil & Environmental Engineering, University of Washington, Seattle, WA, USA

INTRODUCTION

Fibrous peat differs significantly from clay and sand in both its inherent properties and its resulting mechanical behavior. Peat generally consists of a network of long, hollow, flexible organic fibers in a loosely deposited, aqueous environment. Its very low initial density and extremely high natural water content result in viscous and highly compressible deformation behavior. Thus, creep deformations play a more significant role in settlement behavior of peat than for most other geomaterials. In the past, models used to describe the behavior of peat have been adapted from models originally developed to describe clay or sand, and thus may not be as inherently well-equipped to capture the complex deformation behavior of fibrous peat.

Houlsby & Puzrin (2006) developed an approach to modeling geomaterials using the principles of hyperplasticity, which involves the development of material models within a fully thermodynamically consistent framework. The formulation of a hyperplastic model must obey the principles of mass conservation, conservation of energy (First Law of thermodynamics), and the principle of work dissipation in the form of heat (Second Law of thermodynamics). The main advantage to employing this framework is that it cannot produce thermodynamically inconsistent results.

The formulation of a hyperplastic model requires the specification of two potential functions: one describing the internal energy of the system, from which the constitutive behavior is defined; and one describing how energy is dissipated from the system, from which the evolution of the internal variables is determined. By defining these two functions such that the unique and complex properties of peat are accounted for in the internal energy and energy dissipation, a thermodynamically consistent model for peat can be formulated and implemented independently of the constraints of traditional soil models.

ENERGY FUNCTIONS

The relative importance of the flow of pore fluid on the deformation response of fibrous peat necessitates the development of a hyperplastic model within a poromechanical framework. For a porous continuum (Houlsby & Puzrin, 2006), the Gibbs' free energy function, which is a form of the internal energy function, is defined as:

$$g = g^s + wg^w \quad (1)$$

where g^s and g^w are the free energy functions for the solid and water phases, respectively, and w is the water content.

$$g^s = g_0^s + (p - p_0)v_0^s - (\theta - \theta_0)s_0^s - \frac{(p - p_0)^2}{2K^s} + 3\alpha^s(\theta - \theta_0)(p - p_0)v_0^s \quad (2)$$

$$- c_p^s \frac{(\theta - \theta_0)^2}{2\theta_0}$$

$$- \frac{1}{\rho_0} \left[\frac{p_i^{2-n}}{p_r^{1-n}k(1-n)(2-n)} + \frac{\bar{\sigma}_{kk}}{3k(1-n)} + \alpha(\theta - \theta_0)\bar{\sigma}_{kk} + \bar{\sigma}_{ij}\alpha_{ij} \right]$$

- g_0^s , v_0^s , and s_0^s are the initial free energy, specific volume, and specific entropy values for the solid phase, respectively
- K^s , α^s , and c_p^s are the isothermal bulk modulus, coefficient of thermal expansion, and mass heat capacity at constant pressure (p_0) of the solid particles. p_0 , θ_0 , and ρ_0 are the initial pore fluid pressure, temperature, and density of the total system, respectively. α is the linear thermal expansion coefficient of the skeleton matrix
- α_{ij} is the internal variable, in this case, the viscoplastic strain

The bulk and shear stiffness of the skeleton matrix, K and G , are considered to be pressure-dependent:

$$\frac{K}{p_r} = k \left[\frac{p}{p_r} \right]^n \quad \frac{G}{p_r} = g_s \left[\frac{p}{p_r} \right]^n \quad (3)$$

where p_r is the reference pressure, k and g_s are dimensionless proportionality constants, and the exponent n is between 0 and 1.

$$p_i^{2-n} = \left(\frac{\bar{\sigma}_{ii}\bar{\sigma}_{jj}}{9} + \frac{k(1-n)\bar{\sigma}'_{ij}\bar{\sigma}'_{ij}}{2g_s} \right)^{\frac{2-n}{2}} \quad (4)$$

The free energy of the water phase is:

$$g^w = g_0^w + (p - p_0)v_0^w - (\theta - \theta_0)s_0^w - \frac{(p - p_0)^2}{2K^s} + 3\alpha^w(\theta - \theta_0)(p - p_0)v_0^w -$$

$$c_p^w \frac{(\theta - \theta_0)^2}{2\theta_0} \quad (5)$$

The second function required is the force potential function z , which is a form of the energy dissipation function:

$$z = \frac{(E + \psi_{ij}\bar{\sigma}_{ij})}{\rho_0} \sqrt{\tilde{\alpha}'_{ij}\tilde{\alpha}'_{ij}} + \frac{\Lambda}{\rho_0} \left(3\beta \sqrt{\tilde{\alpha}'_{ij}\tilde{\alpha}'_{ij}} + \tilde{\alpha}_{ii} \right) + \frac{v^w}{2\rho k_m} m_i m_i + \frac{\theta}{2\rho k_\eta} \eta_i \eta_i +$$

$$\frac{k_2}{b} r^{1-b} \left[(\tilde{\alpha}_{ii}\tilde{\alpha}_{ii})^{b/2} + (\tilde{\alpha}'_{ij}\tilde{\alpha}'_{ij})^{b/2} \right] \quad (6)$$

where $\tilde{\alpha}_{ij}$ and $\tilde{\alpha}'_{ij}$ are the total and deviatoric increments of the internal variable, taken here to be the plastic strain. The first term of the force potential accounts for energy dissipation due to interactions between peat fibers in the skeleton matrix,

analogous to frictional dissipation in granular materials, where E is the tensile strength of the entire skeleton matrix. ψ_{ij} is introduced to account for fabric anisotropy, and modifies the dissipation term such that at low stresses, the dissipation due to fiber interactions is insignificant, and at high stress (near failure), the dissipation term converges to $\frac{E}{\rho_0} \sqrt{\tilde{\alpha}'_{ij} \tilde{\alpha}'_{ij}}$. The second term is related to the dissipation due to dilation or contraction of the skeleton matrix, where β is related to the dilation angle of the material, and Λ is the Lagrangian multiplier. The third and fourth terms describe the dissipation due to mass flux (due to pore water flow) and entropy flux (due to temperature changes) out of the system, respectively, where k_m is the permeability coefficient and k_η is the thermal conductivity coefficient. The fourth term accounts for the viscous behavior of the material, where $k_2 = \eta/r$, and η is the viscosity of the total material. r is a constant that maintains the stress dimensions of k_2 , and b is generally in the range of 1 to 2. The viscous terms describe the long-term flow of micropore fluid across the individual fiber membranes, which can occur as a result of both deviatoric stress and volumetric compression, and is principally responsible for the significant secondary compression in peat.

CONSTITUTIVE RELATIONSHIPS

The constitutive relationships can be derived, in a finite-strain regime, from the Gibbs' free energy expression as follows:

$$\Delta_{ij} = -\rho_0 \frac{\partial g^s}{\partial \pi_{ij}} \quad \bar{\chi}_{ij} = -\rho_0 \frac{\partial g^s}{\partial \alpha_{ij}} \quad (7)$$

$$v^s = \frac{\partial g^s}{\partial p^s}, \quad v^w = \frac{\partial g^w}{\partial p^w}, \quad s^s = -\frac{\partial g^s}{\partial \theta^s}, \quad s^w = -\frac{\partial g^w}{\partial \theta^w} \quad (8)$$

where Δ_{ij} is the Green-Lagrange strain tensor, π_{ij} is the 1st Piola-Kirchhoff stress tensor, v^s is the specific volume, and s^s is the entropy. The generalized and dissipative generalized stresses are defined by:

$$\bar{\chi}_{ij} = -\rho_0 \frac{\partial g^s}{\partial \alpha_{ij}} \quad \chi_{ij} = \rho_0 \frac{\partial z^g}{\partial \alpha_{ij}} \quad (9)$$

By invoking Ziegler's condition of orthogonality, which requires the dissipated energy to be maximal (i.e. $\chi_{ij} = \bar{\chi}_{ij} = \bar{\sigma}_{ij}$), we obtain an expression for the deviatoric viscoplastic strain increment using the deviatoric form of Eq. 7:

$$\tilde{\alpha}'_{ij} = r \left[\frac{(\sqrt{\bar{\sigma}'_{kl} \bar{\sigma}'_{kl}} - (E + \psi_{ij} \bar{\sigma}_{ij} + 3\Lambda\beta))}{k_2} \right]^{\frac{1}{b-1}} S_{ij}(\bar{\sigma}_{ij}), \quad S(x) = \begin{cases} -1, & x < 0 \\ 0, & x = 0 \\ 1, & x > 0 \end{cases} \quad (10)$$

The Lagrangian multiplier, Λ , must then be solved for using the volumetric form of Eq. 7:

$$3\Lambda = \chi_{ii} - k_2 r^{1-b} \tilde{\alpha}_{ii} [\tilde{\alpha}_{ii} \tilde{\alpha}_{ii}]^{\frac{b}{2}-1} \quad (11)$$

The implicit expression for Λ can be solved within the finite-element framework using an implicit stress-update algorithm (Wang 1997), based on the consistency condition of the yield surface for a viscoplastic model:

$$\tilde{y} = \frac{\partial y}{\partial \chi_{ij}} \tilde{\chi}_{ij} + \frac{\partial y}{\partial \alpha_{ij}} \tilde{\alpha}_{ij} + \frac{\partial y}{\partial \psi_{ij}} \tilde{\psi}_{ij} + \frac{\partial y}{\partial \tilde{\alpha}_{ij}} \tilde{\tilde{\alpha}}_{ij} = 0 \quad (12)$$

where y can be obtained directly from the force potential z through:

$$y = \bar{\chi}_{ij} \tilde{\alpha}_{ij} / \rho_0 - z, \quad \bar{\chi}_{ij} = \bar{\sigma}_{ij} \quad (13)$$

CONCLUSIONS

A framework based on hyperplasticity is proposed for rate-dependent peat behavior. This thermo-poro-viscoplastic formulation accounts for fabric anisotropy, volumetric and deviatoric viscosity, and large deformations governed by pore fluid flow. The formulation is based on internal and dissipated energy function, and the constitutive relations are derived using Gibbs free energy and force potential (dissipation) functions. The model, yet to be implemented, shows promise as a thermodynamically consistent model developed specifically for peat-like materials.

ACKNOWLEDGEMENT

The research was carried out as part of CREEP (Creep of Geomaterials, PIAP-GA-2011-286397) project supported by the European Community through the programme Marie Curie Industry-Academia Partnerships and Pathways (IAPP) under the 7th Framework Programme.

REFERENCES

- Houlsby G.T. & Puzrin A.M. (2006). Principles of Hyperplasticity, An approach to Plasticity Theory Based on Thermodynamic Principles. Springer Verlag Limited, London.
- Mesri G. & Ajlouni. M. (2007). Engineering properties of fibrous peats. Journal of Geotechnical and Geoenvironmental Engineering 133, no. 7: 850-866.
- Taylor H. F. (2012). Peat Behaviour: Some Conceptual Mechanisms and Challenges. 20th Vancouver Geotechnical Society Symposium. Vancouver, B.C., Canada
- Wang W.M., Sluys L.J. & De Borst R. (1997). Viscoplasticity for instabilities due to strain softening and strain-rate softening. International Journal fo Numerical Methods in Engineering, Vol.40, 3839-3864.

A NEW CONCEPT IN DEVELOPING A CONSTITUTIVE MODEL FOR FROZEN SOILS

S. A. Ghoreishian Amiri, M. Kadivar, G. Grimstad

Norwegian University of Science and Technology (NTNU), Trondheim, Norway

INTRODUCTION

Considering the increase in engineering activities in permafrost and seasonally frozen regions, developing constitutive models for simulating the behavior of frozen materials is important. Two different approaches are commonly used to simulate the mechanical behavior of frozen soils: total stress based models and two stress-state variables approach.

Total stress models have been widely used in the literature to describe the mechanical behavior of frozen soils [e.g. Arenson & Springman (2005); Lai et al. (2008, 2009, 2010); Zhu et al. (2010); Xu (2014)]. However, deformations due to the variation of ice content and/or temperature have not been taken into account. Moreover, description of soil behavior, in the presence of unfrozen water is not described.

Considering the close analogy between the physics of saturated frozen soils and unfrozen unsaturated soils, Nishimura et al. (2009) proposed a two stress-state variables approach by adopting the Basic Barcelona Model (BBM) (Alonso et al. 1990) for the frozen state of saturated soils. In this model, the cryogenic suction and the difference of total mean stress and ice pressure are considered as the independent stress-state variables. This approach is also employed by Shastri and Sanchez (2012). They showed the ability of the model for considering the influence of cryogenic suction and temperature on the stress-strain behavior of frozen soils. However, since the Suction Increase (SI) yield curve of the BBM is ignored, there is no mechanism for considering the plastic deformation due to a freezing period, and consequently the model cannot simulate the frost heave phenomenon. Moreover, in the ice segregation phenomenon, the soil strength will decrease by increasing suction, while in the model proposed by Nishimura et al. (2009) soil strength will increase monotonically by suction.

In this paper, the solid phase stress concept will be introduced. Considering the SI curve, and defining appropriate coupled hardening rules, the model proposed by Nishimura et al. (2009) has been improved in order to provide the ability of simulating of frost heave and strength weakening due to pressure melting. Moreover, the time dependent behavior is added to the model within the framework of the over-stress method.

MODEL DESCRIPTION

Considering the frozen soil as a composition of solid materials (consists of soil particles and ice crystals) and unfrozen water, the solid phase stress tensor, σ^* , can be defined as

$$\sigma^* = \sigma - s_w p_w \mathbf{I} \quad (1)$$

where σ is the total stress, s_w and p_w are the water saturation and pressure, respectively.

The solid phase stress and cryogenic suction are proposed for the stress state variables. The cryogenic suction, S_c , is defined as

$$S_c = p_i - p_w \quad (2)$$

where p_i is the ice pressure.

In this framework, it is assumed that any strain increment, $d\epsilon$, can be additively decomposed into the following parts

$$d\epsilon = d\epsilon^{me} + d\epsilon^{se} + d\epsilon^{mvp} + d\epsilon^{svp} \quad (3)$$

where $d\epsilon^{me}$ and $d\epsilon^{mvp}$ are the elastic and viscoplastic parts of strain due to solid phase stress variation and $d\epsilon^{se}$ and $d\epsilon^{svp}$ are the elastic and viscoplastic parts of strain due to suction variation, respectively.

The elastic parts of strain can be calculated with considering the elastic parameters as a function of temperature and ice content, while for the visoplastic parts, definition of reference and dynamic surfaces are essentially required. Figure 1 shows the suction increase (SI) and Loading Collapse (LC) reference curves.

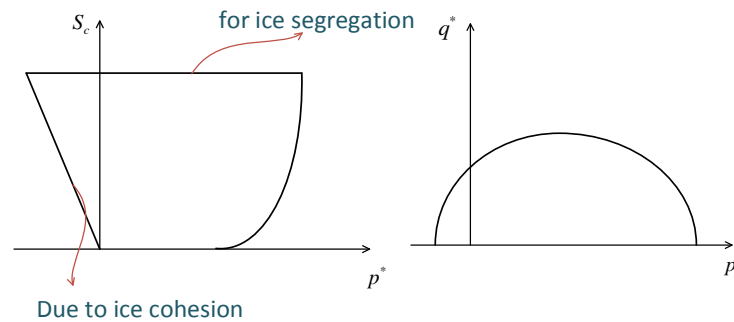


Figure 1. Representation of SI and LC reference curves in S_c - p^* and p^* - q^* planes.

The dynamic surfaces should always pass through the current stress point (σ^*, S_c) and also keeps the similar shape and orientation to that of the reference surfaces with respect to a similarity line. For defining the similarity line, the following conditions for dynamic surfaces are considered:

- The more strain rate results in the more apparent cohesion.
- For infinitely small strain rate, the apparent cohesion should approach zero.
- For unfrozen state, the similarity center should locate at origin.

The dynamic curves and similarity line are presented in figure 2.

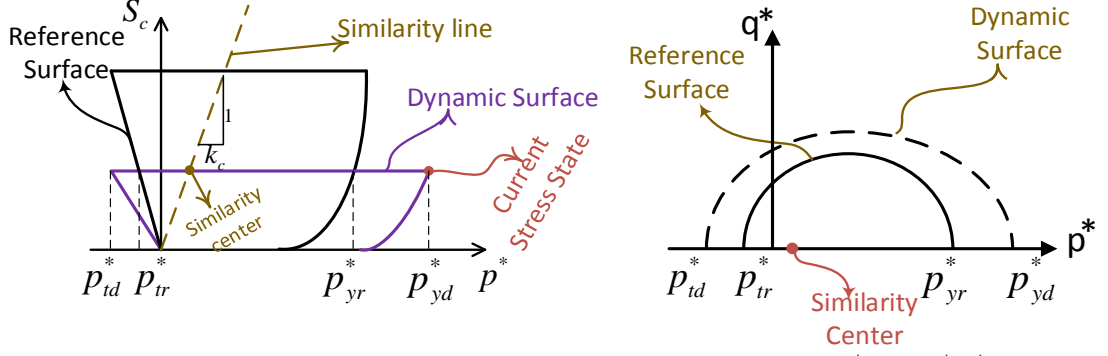


Figure 2. Representation of dynamic curves and similarity line in S_c - p^* and p^* - q^* planes.

The following formulation can describe the dynamic surfaces:

$$F_{d1} = \left[p^* - \left(\frac{p_{yd}^* - p_{td}^*}{2} \right) \right]^2 + \frac{q^*}{M^2} - \left(\frac{p_{yd}^* + p_{td}^*}{2} \right)^2 = 0. \quad \text{and} \quad F_{d2} = S_c - R_2 S_{seg} = 0. \quad (3)$$

where

$$p_{tr}^* = k_t S_c \quad \text{and} \quad p_{yr}^* = p_c^* \left(\frac{p_{y0r}^*}{p_c^*} \right)^{\frac{\lambda_0 - \kappa}{\lambda - \kappa}} \quad (4)$$

$$\lambda = \lambda_0 [(1-r)\exp(-\beta S_c) + r] \quad \text{and} \quad R_1 = \frac{p_{yd}^* - k_c S_c}{p_{yr}^* - k_c S_c} = \frac{k_c S_c - p_{td}^*}{k_c S_c - p_{tr}^*} \quad (5)$$

p^* is the solid phase mean stress, k_t is the parameter that controls the increase in apparent cohesion with suction, M is the slope of the critical state line, S_{seg} is the initial position of the SI reference curve, p_{y0r}^* is the pre-consolidation stress for unfrozen condition, p_c^* is the reference stress, λ_0 is the compressibility coefficient for the unfrozen state along virgin loading, κ is the compressibility coefficient along elastic stress paths [= $(1+e) \cdot p^*/K$], R_1 and R_2 are the over-stress ratios for LC and SI curves, respectively, β and r are the parameters that control the increase in stiffness with suction, k_c , p_{yd}^* and p_{td}^* are introduced in figure 2.

In order to complete the description, variation of the viscous parameters of the soil due to change of ice content should be taken into account. The more ice content results in the more viscous behavior (Fig. 3).

The viscoplastic parts of strain can be calculated as

$$\dot{\boldsymbol{\varepsilon}}^{mvp} = \mu_1(s) \langle R_1^{N_1(s)} \rangle \frac{\partial F_{d1}}{\partial \boldsymbol{\sigma}^*} \quad \text{and} \quad \dot{\boldsymbol{\varepsilon}}^{svp} = -\mu_2 \langle R_2^{N_2} \rangle \frac{\partial F_{d2}}{\partial S_c} \mathbf{I} = -\mu_2 \langle R_2^{N_2} \rangle \mathbf{I} \quad (6)$$

where

$$\mu_1(s) = \mu_{1(s=0)} \frac{\lambda_0 (\lambda - k)}{\lambda (\lambda_0 - k)} \quad \text{and} \quad N_1(s) = N_{1(s=0)} + b \times S_c \quad (7)$$

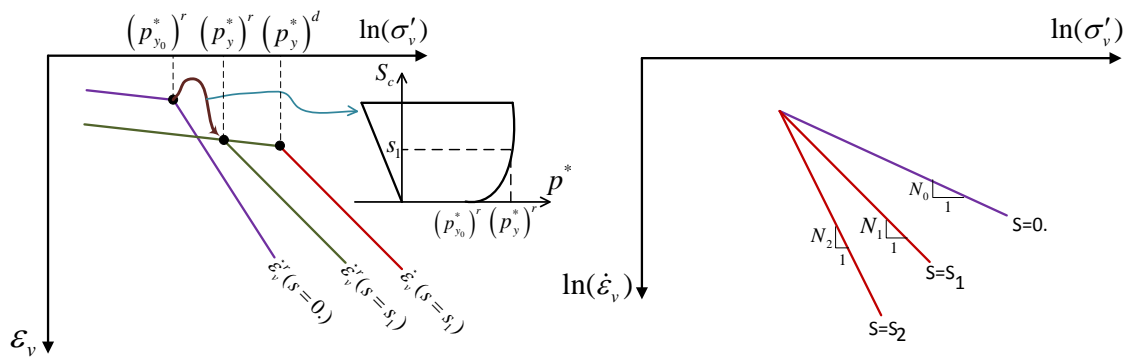


Figure 3. Schematic representation of suction dependency of viscous behavior.

where $\mu_{1(s=0)}$ and $N_{1(s=0)}$ are the viscosity parameters of the model which should be calibrated for the unfrozen state of the soil.

CONCLUSIONS

In this paper, an elastic-viscoplastic framework for describing the mechanical behavior of frozen soils is presented. The model is able to represent many of the fundamental features of the behavior of frozen soils such as strength weakening due to pressure melting and frost heave due to ice segregation phenomena. Influence of temperature and ice content variations on the behavior of the soil are implicitly considered in the model by the use of the cryogenic suction as an independent stress-state variable. Effect of unfrozen water is also considered in the model by introducing the solid phase stress as the second stress-state variable.

ACKNOWLEDGMENTS

This work is carried out under the Marie Curie Action, European FP7, CREEP project, Grant number 17 PIAG-GA-2011-286397.

REFERENCES

- Alonso E., Gens A. & Josa A. (1990). A constitutive model for partially saturated soils, *Géotechnique* 40 (3), 405-430.
- Arenson L.U. & Springman S.M. (2005). Mathematical descriptions for the behaviour of ice-rich frozen soils at temperatures close to 00 C. *Canadian Geotechnical Journal* 42(2), 431–442.
- Lai Y., Li S., Qi J., Gao Z. & Chang X. (2008). Strength distributions of warm frozen clay and its stochastic damage constitutive model. *Cold Regions Science and Technology* 53 (2), 200–215.
- Lai Y., Jin L. & Chang X. (2009). Yield criterion and elasto-plastic damage constitutive model for frozen sandy soil. *International Journal of Plasticity* 25 (6), 1177–1205.
- Lai Y., Yugui Y., Xiaoxiao C. & Shuangyang L. (2010). Strength criterion and elastoplastic constitutive model of frozen silt in generalized plastic mechanics. *International Journal of Plasticity*, 26 (10), 1461–1484.
- Nishimura S., Gens A., Jardine R.J. & Olivella S. (2009). THM-coupled finite element analysis of frozen soil: Formulation and application. *Géotechnique* 59 (3), 159-171.
- Xu G. (2014). Hypoplastic constitutive models for frozen soil. PhD thesis. University of Natural Resources and Life Sciences, Vienna.
- Zhu Z., Ning J. & Ma M. (2010). A constitutive model of frozen soil with damage and numerical simulation for the coupled problem. *Science China Physics, Mechanics and Astronomy*, 53 (4), 699-711.

ON ESTIMATION OF PARAMETERS DESCRIBING SOIL STRUCTURE AND ANISOTROPY FOR CREEP-SCLAY1S

J.-P. Gras, J. Dijkstra, M. Karstunen

Department of Civil and Environmental Engineering, Chalmers University of Technology, Gothenburg, Sweden.

INTRODUCTION

Creep-SCLAY1S is an advanced soil model developed to simulate natural soft clay behaviour. The model requires in total values for 16 input parameters. Most of these parameters are easy to determine from experimental data. Nevertheless, some are not directly measurable, such as some parameters related to describing the evolution of anisotropy and the structure (bonding). In this paper, we propose a way to estimate a range for these parameters.

ASSESSMENT OF STRUCTURE AND ANISOTROPY PARAMETERS

In the Creep-SCLAY1S model, three surfaces are used for the description of the stress state and the amount of bonding (Figure 1). The first surface is called the Normal Consolidation Surface (NCS) and represents the boundary between small and large irrecoverable strains of the natural clay (Sivasithamparam et al., 2015). The intersection of the vertical tangent to the ellipse with the mean effective stress axis is the apparent isotropic preconsolidation pressure p_m . Another ellipse called the Current Stress Surface (CSS) represents the current state of effective stress. The intersection of the CSS with the horizontal axis is called the equivalent mean stress p_{eq} . The third surface is the imaginary intrinsic yield surface (ICS) (Gens et al., 1993, Karstunen et al., 2005). The difference in sizes between the NCS and ICS is related to the amount on apparent bonding.

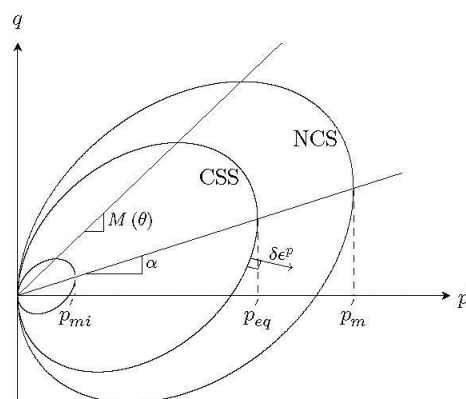


Figure 1. Description of the main characteristics of the model in the $q - p'$ plane

The Creep-SCLAY1S model takes into account three hardening processes: isotropic hardening and structural hardening which will affect the size of the NCS, and rotational hardening which will affect the orientation of both the NCS and the CSS. The evolution of structure, characterized by an increment of the amount of

bonding $\delta\chi$ as a function of an increment of volumetric creep strains $\delta\varepsilon_v^c$ and deviatoric creep strains $\delta\varepsilon_d^c$ is expressed by:

$$\delta\chi = -a\chi[|\delta\varepsilon_v^c| + b|\delta\varepsilon_d^c|]$$

where the absolute rate of destructuration a and the relative rate of destructuration b are the parameters controlling the rate of destructuration of the soil. This expression was used by Karstunen et al. (2005). Usually, people have no idea of the values of parameter a , before they start to calibrate the model by comparing to experimental results. In this paper, we propose a range of values for the estimation of a . For that, we assume that in soft clays deviatoric strains have less or equal influence than the volumetric strains on the destructuration process, which implies that $0 < b < 1$.

In Creep-SCLAY1S, the rotational hardening rule, which relates the evolution of anisotropy $\delta\alpha$ as a function of an increment in volumetric and deviatoric strain rates is (Sivasithamparam et al.):

$$\delta\alpha = \omega \left(\left[\frac{q}{4p} - \alpha \right] \langle \delta\varepsilon_v^c \rangle + \omega_d \left[\frac{q}{3p} - \alpha \right] |\delta\varepsilon_d^c| \right)$$

The evolution α of a causes a rotation of the normal consolidation surface (NCS) and the current stress surface (CSS). For the sake of simplicity, the same is assumed to apply to ICS, but given it is an imaginary surface its shape does not matter, as it is the relative size compared to NCS which controls the debonding process. ω is the absolute effectiveness of rotational hardening and ω_d is the relative effectiveness of deviatoric creep strains ε_d^c and volumetric creep strains $\delta\varepsilon_v^c$ in the rotational hardening. ω_d is usually calculated from a mathematical formula based on the value of the critical state friction angle, assuming Jaky's K_0^{nc} (Wheeler et al., 2003). ω is usually calibrated by comparison with experimental data. In this paper, we propose a method to get a range for the value of ω .

ACKNOWLEDGEMENT

The research was carried out as part of CREEP (Creep of Geomaterials, PIAP-GA-2011-286397) project supported by the European Community through the programme Marie Curie Industry-Academia Partnerships and Pathways (IAPP) under the 7th Framework Programme.

REFERENCES

- Gens A. and Nova R (1993). Conceptual bases for a constitutive model for bonded soils and weak rocks. *Geotechnical engineering of hard soils-soft rocks*, 1(1):485–494.
- Karstunen M., Krenn H., Wheeler S J, Koskinen M, Zentar R (2005). The effect of anisotropy and destructuration on the behaviour of Murro test embankment. *Int J Geomech*. 5(2):87-97.
- Sivasithamparam N., Karstunen M., and Bonnier P (2015). Modelling creep behaviour of anisotropic soft soils. *Computers and Geotechnics*, 69:46–57.
- Wheeler S.J., Nääätänen A., Karstunen M., and Lojander M (2003). An anisotropic elastoplastic model for soft clays. *Canadian Geotechnical Journal*, 40(2):403–418.

IS CREEP ANALYSIS CREEPING INTO PRACTICE?

G. Grimstad

Norwegian University of Science and Technology, Trondheim, Norway

M. Mehli

Norwegian Geotechnical Institute, Trondheim, Norway

S.A. Degago

Norwegian Public Road Administration, Trondheim, Norway

INTRODUCTION

Several researchers like Leroueil (1996) and Degago *et al.* (2011a), (2011b), (2009) have demonstrated that the isotache approach convincingly captures the rate dependent characteristics of clay. However, a good creep analysis requires good quality laboratory data and/or knowledge on how to account for sample disturbance. This is not always a straight forward procedure and makes creep-analysis in engineering practice challenging. In this paper the well instrumented Onsøy test fill (Berre, 2013) is analyzed using different constitutive models. Instrumentation data consists of settlement profiles, horizontal deformation profiles and pore-pressure measurements. The Onsøy test fill is of particular interest due to the availability of high quality block samples from the Onsøy test site. The paper demonstrates some of the effects of the assumptions regarding creep on the resulting calculations, compared to field measurements.

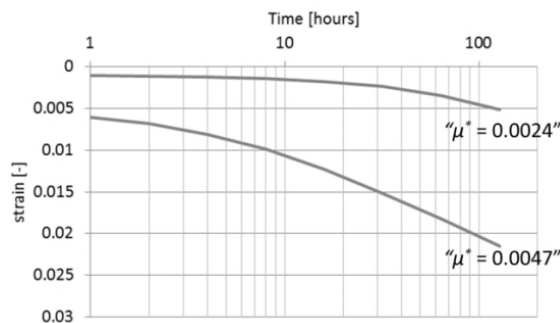


Figure 1. Illustration of time(log) vs strain plot for two different stress levels in an oedometer test

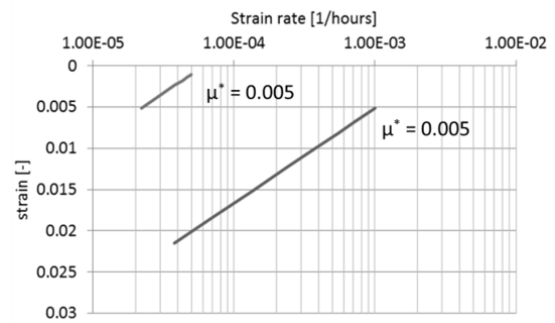


Figure 2. Data in 1 plotted in a strain rate vs strain plot, showing unique μ^*

MODELLING CREEP IN CLAY

In geotechnics there is not a common international 'language' when it comes to settlement and creep calculation. According to Janbu (1990), Terzaghi stated in 1925 that based on experiments on dry powder in the period 1916-1920, both the strength and stiffness of such a material is linearly dependent on the intergranular pressure. Terzaghi did not directly build his developments on this fundamental discovery. Instead the $e - \log p'$ concept was introduced early in the 1930's by a mere coincidence (due to a readily available semi-log paper?) and this was somehow unfortunate. Similar procedure of plotting was used for time dependency, plotting time-strain data in $e - \log t$ diagrams. From these two diagrams the C_c and C_α parameters were established. Unlike e and p' , time (t) is not an objective measure since it is dependent on when the clock starts. Therefore the C_α parameter found at relatively low stress levels, where initial strain rate is low, cannot directly be used to describe development of strain rate with occurred deformation (or time). Nash og Ryde (2001) showed that an objective determination of the creep parameter will reproduce different interpreted C_α (or its strain equivalent μ^*) in a strain – $\log t$ plot (see Figure 1 and Figure 2), as the initial strain rate for "time = 0" is different in the two cases. Using the terminology of the time resistance concept proposed by Janbu (1969): it is the time resistance, $R = 1/\dot{\epsilon}$, that is different at "t = 0" and not necessary the time resistance number, $r_s = 1/\mu^*$. This difference in terminology/interpretation is most important in cases where the expected stress state, after load application, is well below the pre-consolidation pressure determined in lab time scale (e.g. 24h load increments) (i.e. problems controlled by initial in-situ strain rate). For stresses above this pressure the in-situ 'equivalent time' and 'lab time' becomes similar (the two lowest curves in Figure 1 and Figure 2 have almost same interpreted values

Having this in mind the triaxial and oedometer tests, conducted on block sampled Onsøy clay, were evaluated with focus on initial strain rate, compressibility and creep parameter. For the "simplest" models (linear in $\log p$) the parameters must be interpreted for the actual expected stress/strain ranges that are relevant at each position in the ground. For more "advanced" models the resulting μ^* are allowed to vary with change in strain (destruction effect) or OCR (aging effect) (both experienced as change in interpreted μ^* with stress/time). In such cases it is possible to fit a wider range, of expected changes at different positions, within one parameter set.

CALCULATIONS OF THE ONSØY TEST FILL

In this paper five different models are used to simulate the Onsøy test fill (Berre, 2013). The isotropic Soft Soil Creep (SSC) model (Stolle *et al.*, 1999), the non-associated Structured Anisotropic creep model (n-SAC) (Grimstad og Degago, 2010) and the Critical State SSCG (CS-SSCG) model (with small strain) (Haji Ashrafi, 2014) are all used in the FE program PLAXIS (www.plaxis.nl) along with a model without creep (SS model). Finally the 1D creep model KRYKON (Svanø, 1986, Svanø *et al.*, 1991), available in the Geosuite package (www.geosuite.se) is used to show effect of 1D vs 2D plane strain assumption.

Figure 3 shows results from FE analyses and how they compare with the measurements. As seen in the figure including creep increases the settlement after 3 years by 70% (After 20 years the prediction tells that the increase would be 120%). SSC, SS and n-SAC distinctly over-predicted horizontal deformations

directly after application of load while the CS-SSCG model does a much better prediction of the short term deformation (undrained deformation). For the long term horizontal deformation, the n-SAC model seems to do the best prediction; this is due to the anisotropic formulation in n-SAC. Most of the models tend to show higher pore pressures directly after load application, while after three years SS model significantly under-predicted the pore pressures. The main reason for the different pore pressure prediction under the centerline of the embankment is due to differences in calculated load distribution. For the KRYKON analysis, in particular, the 1D situation (Boussinesq distribution) combined with too high initial strain rate is expected to overestimate pore pressure. The more advanced model (n-SAC) has a more contractive behavior and will therefore also give some higher pore pressure.

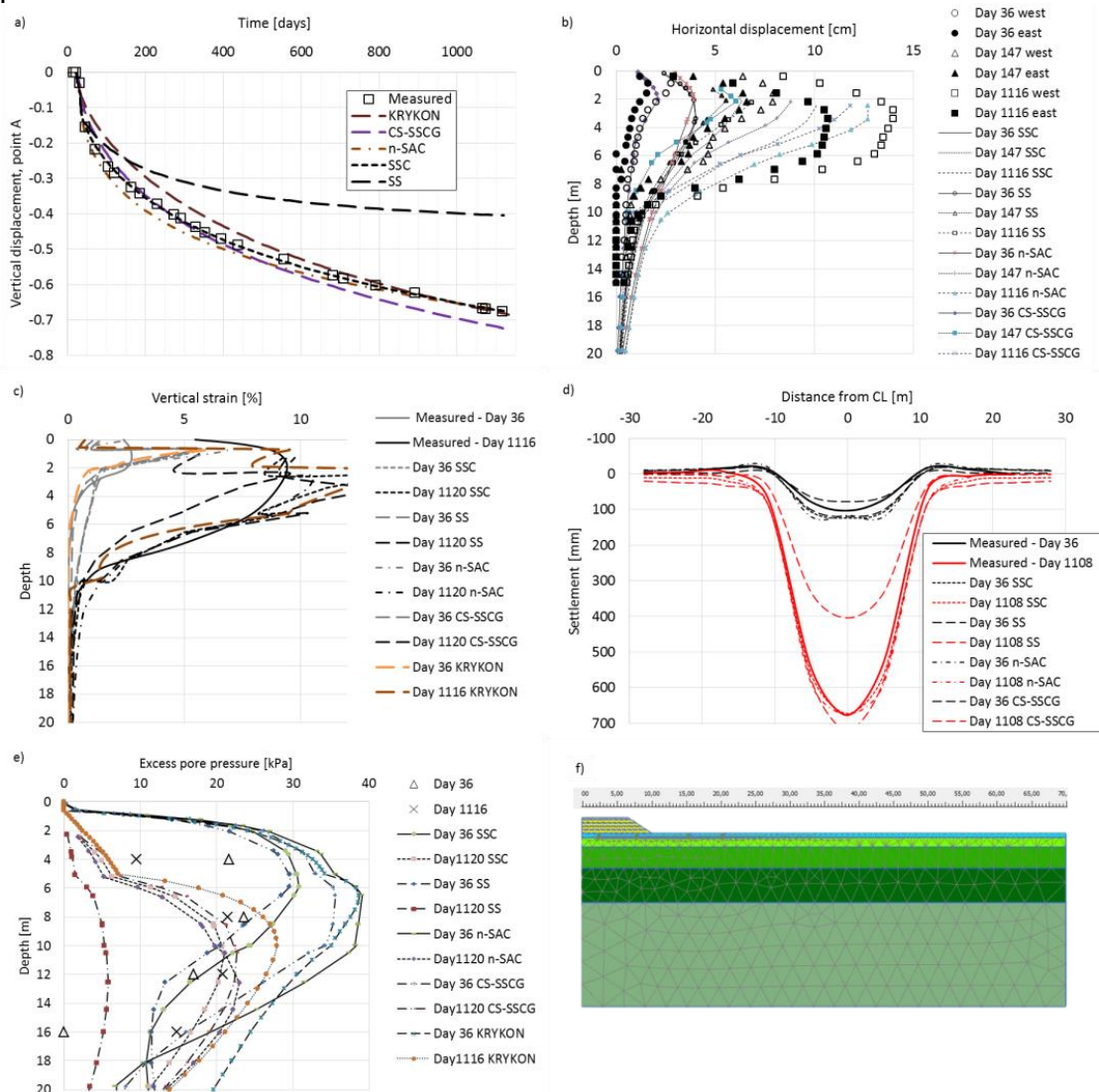


Figure 3. Results from the analyses with the different models, compared with measurements

- a) Time deformation curve (original surface under center of embankment)
- b) Horizontal deformation under toe at day 36, 147 and 1116
- c) Strain vs depth at day 26 and 1116 (1120)
- d) Settlement profiles at day 36 and 1108
- e) Excess pore pressure under embankment at day 36 and 1116
- f) Finite element model of the test fill

CONCLUSIONS

To be able to do a reasonable creep calculation, parameters must be obtained from high quality samples. The initial (prior to loading) in-situ strain rate is an important parameter (in many models this is given as OCR for a particular reference time). The assumptions regarding the initial strain rate are especially important for cases where the stress change is relatively moderate, most often the case for embankments on clay (except for directly under the embankment or the foundation). Since the OCR determined from laboratory tests are highly influenced by sample quality, creep calculations require either good samples or some method of correction of laboratory data. The predicted in-situ strain rate from the model should therefore be checked carefully. Finally, simulations including creep are demonstrated on the Onsøy test fill case. The results agrees well with measured values and shows that accounting for creep during the first three years after construction gives a 70% increase in settlement prediction as compared to the calculation without creep. The analysis without creep also significantly underestimated the pore pressures after this period.

ACKNOWLEDGEMENT

The research was carried out as part of CREEP (Creep of Geomaterials, PIAP-GA-2011-286397) project supported by the European Community through the programme Marie Curie Industry-Academia Partnerships and Pathways (IAPP) under the 7th Framework Programme.

REFERENCES

- Berre, T. (2013): Test fill on soft plastic marine clay at Onsøy, Norway. *Canadian Geotechnical Journal*, 51, 30-50.
- Degago, S.A., Grimstad, G., Jostad, H.P. & Nordal, S. (2009): The non-uniqueness of the end-of-primary (EOP) void ratio-effective stress relationship. *Proceedings of the 17th International Conference on Soil Mechanics and Geotechnical Engineering, Alexandria, Egypt* 324-327.
- Degago, S.A., Grimstad, G., Jostad, H.P., Nordal, S. & Olsson, M. (2011a): Use and misuse of the isotache concept with respect to creep hypotheses A and B. *Géotechnique*, 61, 897-908.
- Degago, S.A., Nordal, S., Grimstad, G. & Jostad, H.P. (2011b): Analyses of Väsby test fill according to creep hypothesis A and B. *Proc. 13th IACMAG, Sydney, Australia*, 307-312.
- Grimstad, G. & Degago, S.A. (2010): A non-associated creep model for structured anisotropic clay (n-SAC). *Numerical Methods in Geotechnical Engineering* CRC Press, 3-8.
- Haji Ashrafi, M.A. (2014): Implementation of a Critical State Soft Soil Creep Model with Shear Stiffness. MSc thesis. Norwegian University of Science and Technology.
- Janbu, N. (1969): The resistance concept applied to deformations of soils. *7th International Conference Soil Mechanics Foundation Engineering, Mexico city*, 191–196.
- Janbu, N. (1990): Fremtidens geotekniske utfordringer. *Geoteknikkdagen*. Oslo, Norway.
- Leroueil, S. (1996): Compressibility of Clays: Fundamental and Practical Aspects. *Journal of Geotechnical Engineering*, 122, 534-543.
- Nash, D.F.T. & Ryde, S.J. (2001): Modelling consolidation accelerated by vertical drains in soils subject to creep. *Géotechnique*. 257-273.
- Stolle, D.F.E., Vermeer, P.A. & Bonnier, P.G. (1999): A consolidation model for a creeping clay. *Canadian Geotechnical Journal*, 36, 754-759.
- Svanø, G. (1986): Program KRYKON, documentation and manual (The “Soft clay deformation” project.), STF69 F86017. Trondheim, Norway.
- Svanø, G., Christensen, S.O. & Nordal, S. (1991): A soil model for consolidation and creep Trondheim: Institutt for geoteknikk.

A PROCEDURE FOR DETERMINING LONG-TERM CREEP RATES OF SOFT CLAYS BY TRIAXIAL TESTING

H.P. Jostad

Norwegian Geotechnical Institute, Oslo, Norway

J. Yannie

Department of Civil and Environmental Engineering, Chalmers University of Technology, Gothenburg, Sweden

INTRODUCTION

Determination of creep parameters has been traditionally done by incremental loading (IL) oedometer tests. The creep rates obtained from a standard test is then typically restricted to a 24 hours domain. Thereafter, the creep rate is extrapolated with help of a constitutive framework, e.g. isotach based creep models as the Soft Soil creep model in Plaxis (www.plaxis.nl). For long-term settlement predictions this extrapolation is typically up to several decades. Consequently, the results highly depend on the validity of this extrapolation. The aim is to study this long-term creep behaviour with help of a special triaxial test presented herein.

LABORATORY TEST

The isotaches, i.e. creep rates at different stress-strain (or void ratio) states, of a soft plastic marine clay from Onsøy in the east part of Norway is determined. The tested specimens are taken from a special block-sampler (Lacasse et al. 1985) from a depth of 8 meters stored for almost 5 years. The samples did not show any signs of dryness. Furthermore, this had minor importance since they were loaded up well above the initial yield stress (apparent vertical pre-consolidation pressure). The latter is done in this first trial test in order to avoid the additional complex behaviour of de-structuration of natural clays. In order to study the important effect of de-structuration close to the initial yield stress one would need several tests loaded up to different ratios of the pre-consolidation pressure with fresh samples. The behaviour of this clay is already well documented in Berre (2012).

TRIAXIAL TEST

The purpose of the proposed special triaxial test is to establish the distance between isotaches with different creep rates by reducing the effective vertical stress, instead of a long-term creep test at a constant effective vertical stress, as illustrated in Figure 1. Another advantages of performing the test in a triaxial apparatus is that one avoid the effect of side friction present in a standard oedometer apparatus, which may become significant at very low creep rates. In addition, one also controls the effective horizontal stress.

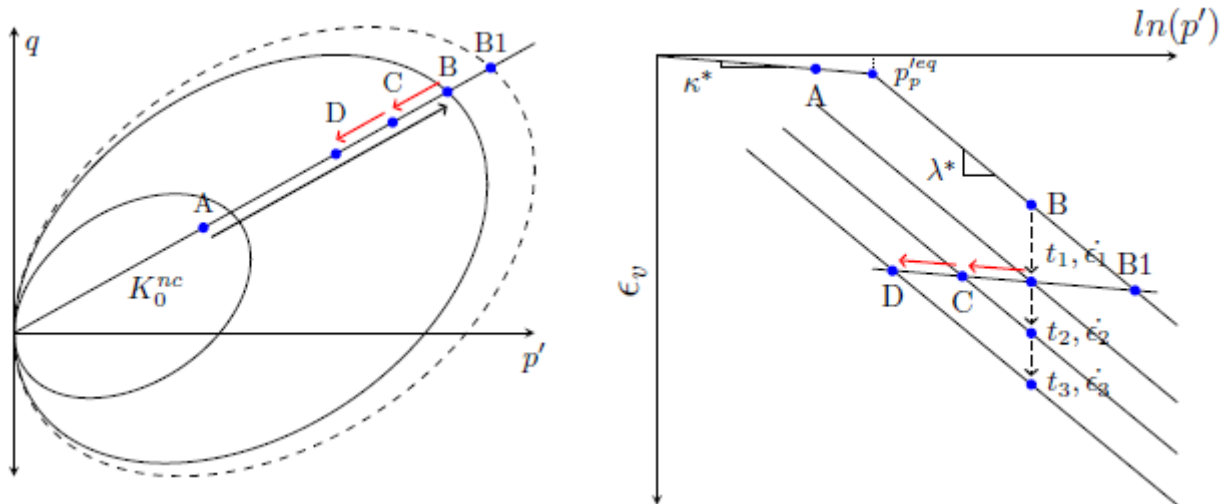


Figure 1. Concept of special triaxial creep test with unloading.

The test was done with a specimen of Ø70mm and height 140mm in a standard triaxial apparatus, at room temperature and with drainage at the top and bottom. It was loaded following a $K_0^{nc}=0.54$ up to a final vertical stress level of 100 kPa (see Figure 2). After that the sample was left to creep for 23 days. This creep time was helpful to understand the relation of the creep parameter (e.g. μ^* in the Soft Soil Creep Model) with respect to time. The first unloading was to 95 kPa, again following the K_0^{nc} line and this new stress level was held for another 35 days and then again unloaded to 90 kPa. The new effective stress state corresponds theoretically to continuing the creep phase for about 55 days and 180 days respectively, under constant effective vertical stress (i.e. the equivalent times). The unloading steps were done until the creep rate became too small to be measured within a reasonable time.

In order to back-calculate the test, the isotaches constitutive framework (Bjerrum, 1967) was used. The parameters κ^* , λ^* and μ^* in the Soft Soil Creep Model were back-calculated from the test and listed in Table 1. The parameter λ^* exhibited a non-linear relation versus strains, while κ^* obtained from the unloading steps, was rather constant. For the calculation of the creep strains, a reference time of 3 days was chosen. This was done since some consolidation was still ongoing after 1 day of the last load step. It was found that a constant μ^* did not fit the change of creep rate with time. On the other hand, an almost perfect match was found using a tangential μ^* as a linear function of accumulated creep strains. After the first unloading step, the creep rate reduced significantly, with rather small increase in accumulated creep strains. It is therefore appropriate to assume that the parameters κ^* , λ^* and μ^* should be fairly constant during the unloading steps.

Table 1. Parameters for Onsøy clay at 8 meters depth.

σ'_{vpc} (kPa)	κ^*	λ^*	$\mu_{ini}^{* \dagger\dagger}$	$\mu_{t_1}^{* \dagger\dagger\dagger}$	$m=\Delta\mu^*/\Delta\epsilon_{cr}$	t_{ref} (days)
53.5 [†]	0.003	0.087	0.0052	0.0042	0.115	3

[†]Some disturbance, ^{††}Tangential parameter at $t_{ref} = 3$ days, ^{†††}Tangential at start of unloading.

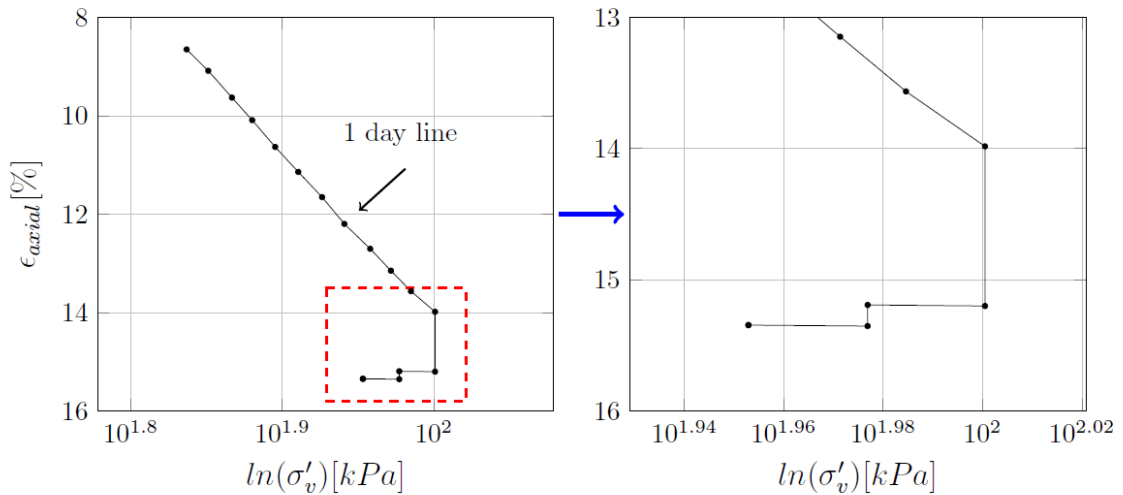


Figure 2. K0nc triaxial test with unloading steps.

INCREMENTAL LOADING OEDOMETER TEST

A parallel oedometer test was carried out on a specimen from the same block sample with the same reference vertical stress. The results did not show any clear transition from the over-consolidated to the normally consolidated condition. This is an indication that the sample had already significant disturbance before the test. An additional sign was the back calculated μ^* , constant equal to 0.0033, which is much lower than that found in the triaxial test. The constant value could be due to sample disturbance and the creep parameter being close to the intrinsic μ^* . The vertical stress was held for more than 3 months, after that the creep rate reduced significantly and there was a problem with the measurement. One possible source could be that for very low creep rates the friction between the clay and the oedometer ring becomes dominant.

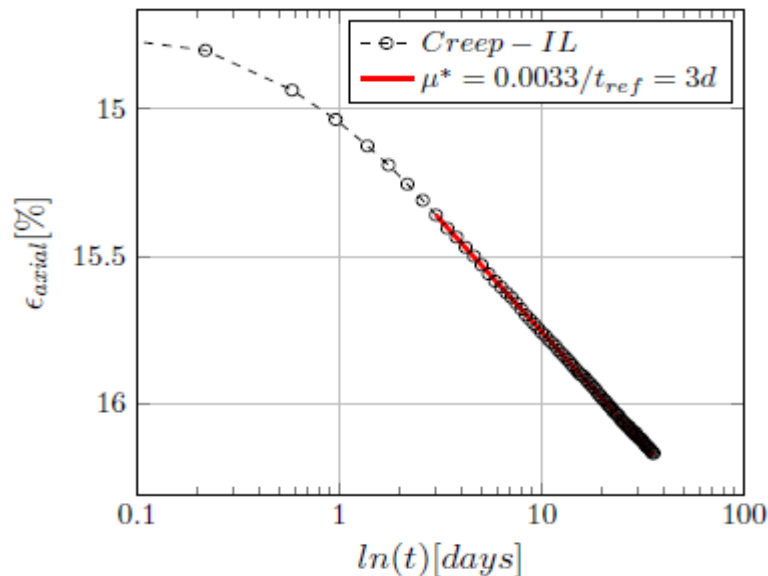


Figure 3. Long-term creep test in a standard oedometer apparatus. Creep at $\sigma_v=100\text{kPa}$.

CONCLUSIONS

A special triaxial testing procedure for determining isotaches for a significantly larger range of creep rates than what can be determined from a standard oedometer test with a maximum creep phase of typically one month is proposed. The procedure is tested on a soft Norwegian marine clay from Onsøy.

It appears that λ^* and μ^* are nonlinear functions. This can be related to the de-structuration of the soil. In addition one can also argue that they might be function of stress level since it is not very clear of what will be the effect of creep strains close to the initial yield point, where de-structuration is a significant phenomenon. The effect of time can only be determined from long-term tests. However, a reasonable assumption seems to consider the isotaches parallels with respect to strain level.

ACKNOWLEDGEMENT

The research was carried out as part of CREEP (Creep of Geomaterials, PIAP-GA-2011-286397) project supported by the European Community through the programme Marie Curie Industry-Academia Partnerships and Pathways (IAPP) under the 7th Framework Programme.

REFERENCES

- Lacasse, S., Berre, T., and Lefebvre, G. (1985). Block sampling of sensitive clays. Proceedings of the 11th International Conference on Soil Mechanics and Foundation Engineering, San Francisco, 12–16 August 1985. A.A. Balkema, Rotterdam, the Netherlands. Vol. 2, pp. 887–982.
- Berre, T. (2012). Test fill on soft plastic marine clay at Onsøy, Norway. In *Canadian Geotechnical Journal*, 51 (1), 2012, pp. 30-50.
- Bjerrum, L. (1967). Engineering geology of Norwegian normally-consolidated marine clays as related to settlements of buildings. Seventh Rankine Lecture, *Geotechnique* 17, 81-118.

EFFECT OF SAMPLE DISTURBANCE ON EVALUATED CREEP PARAMETERS FOR A HIGH PLASTICITY CLAY

M. Karlsson, A. Bergström, J. Dijkstra

Department of Civil and Environmental Engineering, Chalmers University of Technology, Gothenburg, Sweden

A. Emdal

Norwegian University of Science and Technology (NTNU), Trondheim, Norway

INTRODUCTION

When geotechnical analyses are performed based on test results on disturbed samples, the accuracy of deformations predictions is potentially poor, and often expensive ground improvement solutions have to be introduced. Sample quality affects namely both the apparent stiffness and strength of the soil. With improved soil characterisation and more representative high quality sampling and testing, there is a potential for major savings and reduced risk for damage, when combined with numerical analyses with state-of-the-art constitutive models. However, until now no one has attempted to quantify the effects of sample disturbance on (long-term) deformation predictions.

The latter requires obtaining a large number of samples on which a wide variety of laboratory tests need to be performed to acquire all relevant model parameters. Herein is highlighted some first findings on the effect of sample disturbance on the creep index for a high plasticity Swedish clay.

SAMPLE DISTURBANCE

The effects of sample disturbance are well known in the research community and led to several sampling techniques (e.g. Rochelle et al. 1981; Hight (1993); Lefebvre et al. 1997; Tanaka et al. 1996). However, to have any chance of industry acceptance the 'best' sampler should be compatible with existing field rigs and achieve a reasonable sample yield (4 blocks/day). As a result the team at the Norwegian University of Science and Technology (NTNU) developed a scaled down version of the Sherbrooke sampler (Lefebvre et al. 1997).

Up to now the most reliable sample disturbance metric is the one proposed by Lunne et al. (1997) based on extensive testing of primarily low plasticity soft marine clays (e.g. Lunne et al. 2006). This still requires testing in the laboratory, where the change in volume during re-consolidation of the sample to the field effective vertical stress is measured. Alternative non-destructive procedures such as shear wave velocity and suction measurements are pioneered as well (Landon et al. 2007), but are difficult to interpret, as they are relative measures.

METHODOLOGY

Several samples of a high plasticity clay with high sensitivity (CH classification; $S_f = 23$) are taken up to a depth of 10 meters using the Swedish 50 mm diameter STII

piston sampler and the NTNU mini-block sampler at the Utby test site near Gothenburg. The mini-block sampler is a down sized Sherbrooke sampler that acquires samples of 165 mm diameter and 250-300 mm height.

In both cases the best practice procedures as set out by the respective organizations are followed by an experienced team of technicians. The Norwegian technicians came to the test site to ensure the required quality for the mini-block. The time between sampling and testing was not longer than 10 days and the samples were transported and stored appropriately. Some pictures of the sampling process of the mini-block are shown in Figure 1.



a) Mini-block sampling tool



b) Pre-augering



c) Retrieved soil sample



d) Almost ready for transport

Figure 1 Some stages in the mini-block sampling process.

The laboratory program comprised a wide range of tests ranging from oedometer constant rate of strain to CADC triaxial tests, all performed in a climatized laboratory (7 ± 0.5 °C). For the creep parameters, however, the incremental loading oedometer results are most useful. The incremental loading oedometer cells at Chalmers are directly axially loaded (no cantilever) with dead

weight. The sample is contained in a 50 mm diameter and 20 mm high Teflon ring to minimise wall friction. Two-sided drainage and load steps of 24 hours have been used. The displacements are automatically logged following a progressive (quadratically increasing) measurement interval.

RESULTS

A typical result is shown in Figure 1 where the load – compression, time – compression and evaluated creep index C_α curves are presented for an incremental loading test on a STII piston sample and a mini-block sample. The legend presents the sample disturbance metric as proposed by Lunne et al. (1997). The creep index is evaluated and plotted for each load step in Figure 2d. The stress level in Figure 2d is normalised with the in-situ vertical effective stress.

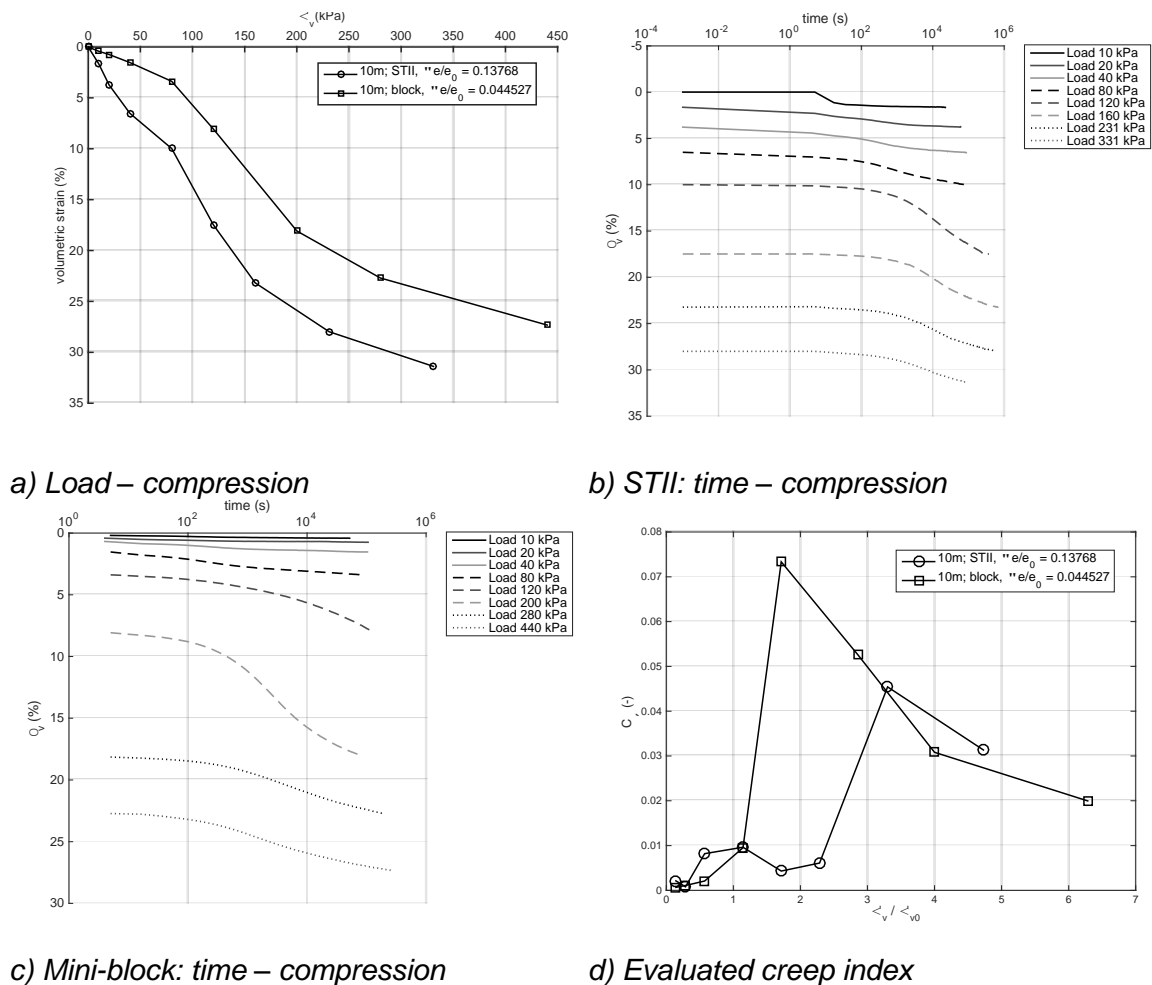


Figure 2. Comparison of creep rates from STII and miniblock samples from 10 meters depth at Utby test site.

In terms of the Lunne sample quality metric the mini-block sample is clearly superior to the 50 mm Swedish piston sampler. However, even the mini-block would only classify as very good for this depth (other depths show values < 0.02). The load-compression curve for the mini-block indicates a stiffer response and larger pre-consolidation pressure than the STII, however the pre-consolidation pressure is hard to evaluate for the strongly disturbed STII sample.

A closer look at the creep index tentatively shows what can be expected, i.e.: (1) small differences at low loading magnitudes, (2) large differences around the pre-consolidation pressure and (3) the creep index tends to a similar value at large loads (intrinsic value). Similar results are observed for the other tested samples (not shown).

Currently, the effects of sample disturbance on predictions of long-term settlements using advanced constitutive models (such as those developed by Sivasithamparam et al. 2015) are being investigated.

CONCLUSIONS

The mini-block sampler has proven to be suitable for sampling the Swedish high plasticity clays up to depths of 10 m. The incremental loading oedometer tests and the evaluated creep index show marked differences between the STII and mini-block samples.

ACKNOWLEDGMENTS

The financial support from Trafikverket in the framework Branch samverkan i Grund and EC/FP7 CREEP PIAG-GA-2011-286397 is greatly acknowledged. Finally, the Authors would acknowledge the support of NTNU in providing the mini-block sampler and the technicians and NCC for the test site. JD is supported by a Fellowship grant EC/FP7-MC-IEF 623613 EMPIRC.

REFERENCES

- Lefebvre, G., & Poulin, C. (1979). A new method of sampling in sensitive clay. *Canadian Geotechnical Journal*, 16(1), 226-233.
- Hight, D. W. "A review of sampling effects in clays and sands." In *Offshore site investigation and Foundation behaviour*, pp. 115-146..
- Landon, M. M., DeGroot, D. J., & Sheahan, T. C. (2007). Nondestructive sample quality assessment of a soft clay using shear wave velocity. *Journal of Geotechnical and Geoenvironmental Engineering*, 133(4), 424-432.
- Lunne, T., Berre, T., & Strandvik, S. (1997). Sample disturbance effects in soft low plastic Norwegian clay. In *Symposium on Recent Developments in Soil and Pavement Mechanics, Rio de Janeiro, Brazil, 25-27 June 1997. Edited by M. Almeida. pp. 81-102.*
- Lunne, T., Berre, T., Andersen, K. H., Strandvik, S., & Sjursen, M. (2006). Effects of sample disturbance and consolidation procedures on measured shear strength of soft marine Norwegian clays. *Canadian Geotechnical Journal*, 43(7), 726-750.
- Rochelle, P. L., Sarrailh, J., Tavenas, F., Roy, M., & Leroueil, S. (1981). Causes of sampling disturbance and design of a new sampler for sensitive soils. *Canadian Geotechnical Journal*, 18(1), 52-66.
- Sivasithamparam, N., Karstunen, M., & Bonnier, P. (2015). Modelling creep behaviour of anisotropic soft soils. *Computers and Geotechnics*, 69, 46-57.
- Tanaka, H., Oka, F., & Yashima, A. (1996). Sampling of soft soils in Japan. *Marine georesources & geotechnology*, 14(3), 283-295.

CREEP OF SAND IN FILLED OPEN CAST MINING PITS

F. Levin, S. Vogt

Faculty of Civil, Geo and Environmental Engineering, Technische Universität München, Germany

INTRODUCTION

Lignite open surface mining in large open cast mines contribute to 25 % of the total electricity production in Germany. In order to gain 180 million tons of lignite per year, depending on the geological boundary conditions of the open cast mine, a three- to fivefold magnitude of overburden must be excavated and dumped, giving an immense bulk flow of about 700 million tons per year. These dumps cover large areas of land that are to be regained for nature reserve, agriculture, constructions and infrastructure.

OPEN CAST MINES

In the context of the reuse of dumps resulting from open cast mines the aspect of surface deformations plays an important role for the planning of infrastructure projects and the design of foundations for structures to be built on dumped soils. The open cast mines under consideration can reach depths of up to 370 m and are filled by dumping soils with large scale spreaders without any further compaction. The density of the soils is influenced only by the drop height from the spreader during dumping and the stresses resulting from the overburden (Lange 1980). Results from cone penetration testing show generally medium to low relative densities even in great depths. The dumped soils under consideration are sands with different grain size distributions defined by the percentage of fines and the content of the different sand fractions fine, medium and coarse. Due to their loose density these sands exhibit a high compressibility, which includes time-dependent deformations (Kothern and Knufinke 1990, Vogt et al. 2013). Due to dewatering of the open cast mine the soils in situ are in a drained state. Thus no consolidation takes place and the long-term strains result from secondary compression or creep defined by the volume change under constant stress. Furthermore, experiences and field tests show no significant influence of water infiltrating to the dump body. Even though the creep strains in sand compared to clay or even peat are very small, due to the great depth of the dumps significant deformation accumulates resulting in time dependent settlements of more than 1 m to be measured on the surface. Also possible differential settlements due to the different resting time (age) of dumped soil layers have to be considered. The prediction of these deformations is very important mainly for the long-term serviceability of engineering structures. Secondary compression of soils can be influenced by different factors such as soil type, mineralogy, grain size and in situ external influences such as change of water content, human activity or seismic activity. The deformation mechanisms in sand include sliding at inter-particle contacts, particle breakage and expulsion of water from microfabric structures in the fines content (Leung et al. 1996) (Mitchell & Soga 2005). In naturally deposited granular soils secondary deformations have usually

already reduced to a negligible rate. However in freshly dumped soils these deformations are still predominant.

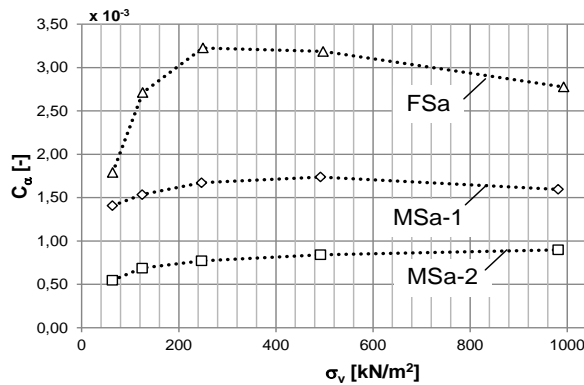


Figure 1: Stress-dependency of C_α -coefficient of sands prepared with the same relative density $D = 35\%$

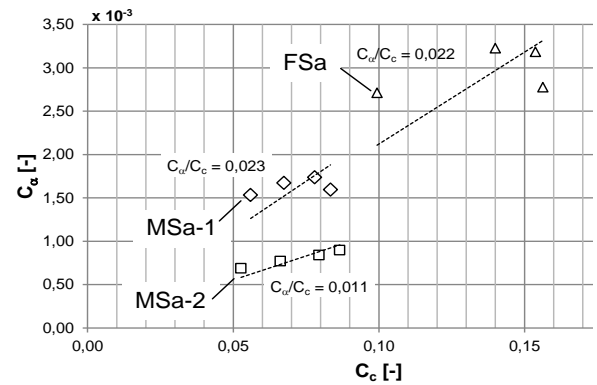


Figure 2: Ratio C_α / C_c of sands prepared with the same relative density $D = 35\%$

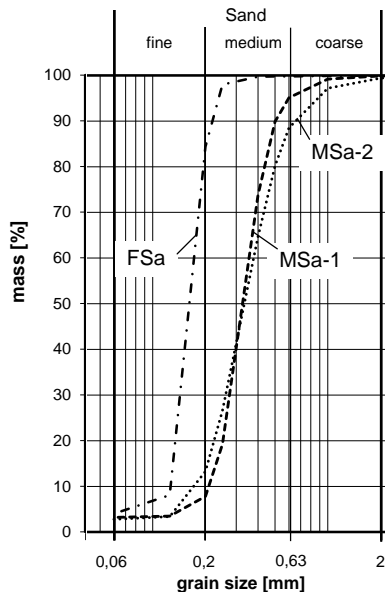


Figure 3: Grain size distribution of the three sands in figure 1 and 2

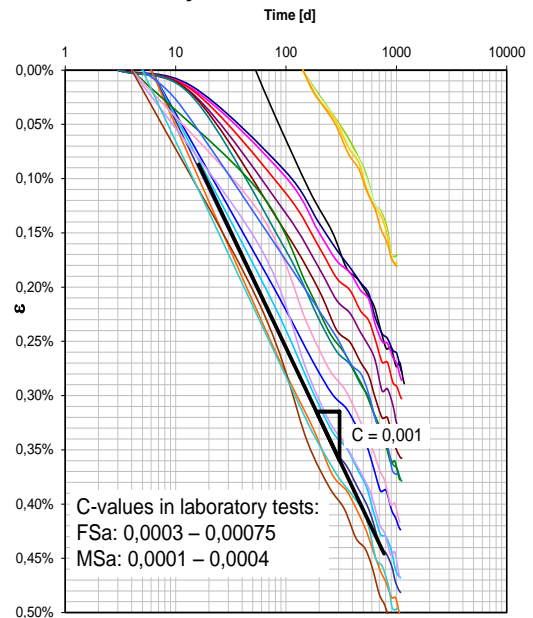


Figure 4: Deformation measurements at different locations on top of the dump and C -values from laboratory tests

For a better understanding of the deformation behaviour of dumped sands a series of one-dimensional compression tests on representative specimens were conducted with variety in initial density, stress-level, stress path and grain size distribution (e.g. figure 1, 2 and 3). The tests were performed in standard size apparatus with diameter of 100 mm and large size apparatus with 300 mm diameter. One unique aspect of the work was the high stress level of up to 2.5 MPa under which the soils were studied. This is not a common stress level in geotechnical application, which is why the behaviour of sand under these stress levels has not been studied sufficiently from a geotechnical point of view.

Furthermore the constitutive soft-soil-creep-model of Vermeer and Neher (1999) was calibrated with available field data (figure 3) and used for prediction of deformations of sands (Vogt et al. 2014).

CONCLUSIONS

The results of the laboratory tests show a considerable dependency of the creep-factor on several of the mentioned parameters (Figures 1 and 2) and also a big difference to the values conducted from available field deformation measurements. This implies the necessity for further investigations especially in triaxial tests to investigate the reason for these deviations.

The results of the numerical calculations generally show the applicability of the soft-soil-creep-model for sands. But these results could only be obtained with parameters calibrated with field measurements. The calibration based on laboratory tests would have resulted in an underestimation of the creep strains.



Figure 5: Impression of an open cast mining pit near Cologne, Germany

REFERENCES

- Kothen, H.; Knufinke, H.(1990): Restsetzungen auf Neulandflächen. Braunkohle 1990 (10), 1990, p. 24 - 29.
- Lange, S. (1980): Eine Modellstudie über Lockergesteinskippen im linksrheinischen Braunkohlenrevier mit Folgerungen für deren Bebaubarkeit. Kolloquium Angewandte Geomechanik, TU-Clausthal.
- Leung, C.F.; Lee, F.H.; Yet N.S. (1996): The role of particle breakage in pile creep in sand. Canadian Geotechnical Journal, Ottawa, vol. 33, p.888 - 898.
- Mitchell, J.K.; Soga, K. (2005): Fundamentals of Soil Behavior. 3rd ed., John Wiley & Sons. Hoboken, New Jersey.
- Vermeer, P.A.; Neher, H. (1999): A soft soil model that accounts for creep. In R.B.J. Brinkgreve, Beyond 2000 in Computational Geotechnics, Balkema, Rotterdam, pp. 249–261.
- Vogt, N.; et al. (2013): Special Aspects for Building a Motorway on a 185 m Deep Dump; Proc. 18th ICSMGE, Paris, vol.1, p. 1377 - 1380.
- Vogt, S.; Birle, E.; Vinzelberg, G. (2014): Zeitabhängige Setzungen von Sand und FE-Simulationen einer Tagebaukippe; Proceeding of the Ohde-Kolloquium 2014, TU Dresden, p. 93 – 108.

THERMO-HYDRO-MECHANICAL SIMULATION OF AN ENERGY PILE IN SOFT CLAY WITH A RATE-DEPENDENT ANISOTROPIC CONSTITUTIVE MODEL

Y. Li, J. Dijkstra, M. Karstunen

Department of Civil and Environmental Engineering, Chalmers University of Technology, Gothenburg, Sweden

INTRODUCTION

With the on-going interest in sustainable development, energy piles have received a lot attention in recent years because they can utilize geothermal energy for thermal control of buildings in an environmental friendly and economic way. Until now energy piles have been mainly employed in stiff subsoils where the primary function of the pile, such as mobilization of sufficient pile resistance and reduction of the settlements of the super structure, are typically not compromised. In soft sensitive clays, however, long-term stability during the lifetime for the soil adjacent to the pile needs to be ensured, considering both mechanical and thermal loading. Therefore, a thorough understanding on thermal processes and geomechanics of the energy pile system is needed to predict the pile-soil response to temperature change, e.g. the load transfer between the pile and soil, the generation and dissipation of excess pore pressures during heating and cooling, and potential thermal effects on the creep rate in the soil.

ENERGY PILES

Recent studies on energy pile calculations were focused on the structural behaviour of piles, (Amatya et al., 2012), such as the load transfer process during heating (Knellwolf et al., 2011, Suryatriyastuti et al., 2014), and the extra strain within the pile caused by temperature increase (Akrouch et al., 2014). Nevertheless, the soft soil around the pile will also be influenced by the thermal load introduced by temperature. The deformations of the soil in turn affect the stability of piles. In real-world energy pile system temperature cycles monthly, seasonally or yearly in a limited range (0-50°C) (Laloui, & Di Donna, 2011). During heating and cooling process, the structure of the soil skeleton can be destroyed by thermal consolidation effects. Meanwhile, viscous properties such as creep rate of soft sensitive clay could also be influenced. Depending on the number of loading cycles and permeability, the effect of thermal loading cycles on the accumulation of excess pore pressures should be considered as well, especially in soft contractive clays. This implies that modelling soft sensitive clay around an energy pile with a simplified elasto-plastic constitutive model is not sufficient to ensure a safe design.

Thermo-mechanical behaviour of clay has been investigated both theoretically and numerically. Advanced models were proposed to predict stress-strain behavior of saturated clay under thermal load (among others (Gera et al., 1996; François et al., 2009; Hueckel et al., 2009; Hong et al., 2013). The focus is on coupling the

convection-diffusion equation and the storage equation with an advanced constitutive model for soft soils, rather than explicitly model the thermal effects in a thermo-plastic constitutive model. At this stage the thermal convection is set equal to the groundwater flow velocity and the effects of thermal loads on the generation of additional pore water pressures by water expansion (Campanella, & Mitchell, 1968). The Creep-SCLAY1S model (Sivasithamparam et al, 2015) was used to model the soft sensitive clay. Example results of a pipe-pile-soil system in a simplified analysis using elasticity for the soil are shown in Fig.1. The temperature and excess pore pressures development in time is shown in Fig. 2. More advanced modelling will present creep rate and volumetric plastic strain in soft clay which are observed in simulation.

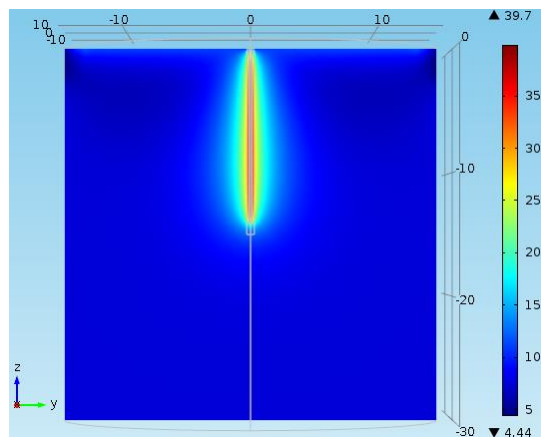


Figure 1. Temperature distribution around one single pile.

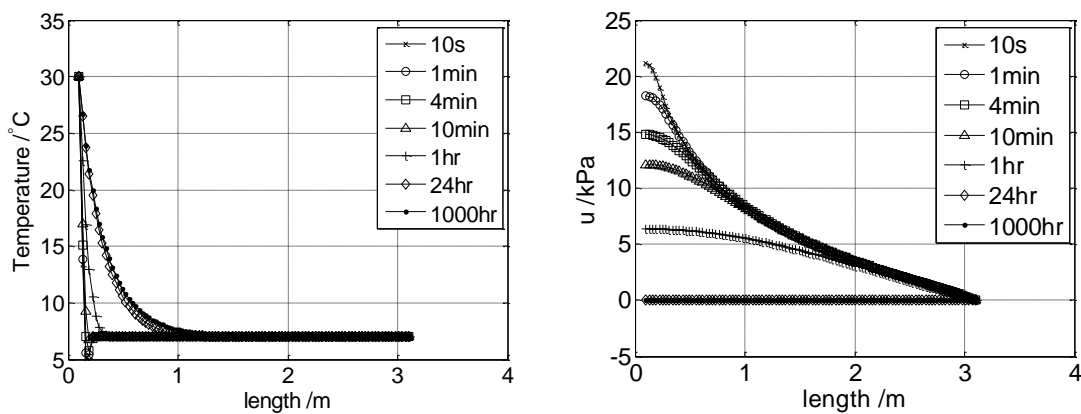


Figure 2. Temperature (left) and excess pore pressure (right) development.

CONCLUSIONS

The calculation results showed that under thermal load, excess pore pressure would be generated in soft clay, which is highly dependent on the mechanical and thermal properties of the soil and can be linked with cyclic thermal loads. Therefore, laboratory tests need to be carried out to study the effect of thermal load cycles on compressibility and creep behavior, as well as thermal properties of soft sensitive clay.

ACKNOWLEDGEMENTS

The financial support from FORMAS (Grant number 2013-771) for project Geothermal Foundation in Soft Clay is gratefully acknowledged.

REFERENCES

- Akrouh, G. A., Sánchez, M., Briaud, J.-L. (2014). Thermo-mechanical behavior of energy piles in high plasticity clays. *Acta Geotechnica*, 9(3), 399-412.
- Amatya, B., Soga, K., Bourne-Webb, P., Amis, T., & Laloui, L. (2012). Thermo-mechanical behaviour of energy piles. *Géotechnique*, 62(6), 503-519.
- Campanella, R. G., Mitchell, J. K. (1968). Influence of temperature variations on soil behavior. *Journal of Soil Mechanics & Foundations Div.*
- François, B., Laloui, L., & Laurent, C. (2009). Thermo-hydro-mechanical simulation of ATLAS in situ large scale test in Boom Clay. *Computers and Geotechnics*, 36(4), 626-640.
- Gera, F., Hueckel, T., Peano, A. (1996). Critical issues in modelling the long-term hydro-thermomechanical performance of natural clay barriers. *Engineering geology*, 41(1), 17-33.
- Hong, P., Pereira, J., Tang, A., Cui, Y.-J. (2013). On some advanced thermo-mechanical models for saturated clays. *International Journal for Numerical and Analytical Methods in Geomechanics*, 37(17), 2952-2971.
- Hueckel, T., François, B., Laloui, L. (2009). Explaining thermal failure in saturated clays. *Géotechnique*, 59(3), 197-212.
- Knellwolf, C., Peron, H., Laloui, L. (2011). Geotechnical analysis of heat exchanger piles. *Journal of Geotechnical and Geoenvironmental Engineering*, 137(10), 890-902.
- Laloui, L., & Di Donna, A. (2011). Understanding the behaviour of energy geo-structures. Paper presented at the Proceedings of the ICE-Civil Engineering.
- Sivasithamparan, N., Karstunen, M., Bonnier, P. Modelling creep behaviour of anisotropic soft soils. *Computers and Geotechnics*, 69:46–57, 2015.
- Suryatriyastuti, M., Mroueh, H., Burlon, S. (2014). A load transfer approach for studying the cyclic behavior of thermo-active piles. *Computers and Geotechnics*, 55, 378-391.

VISCOPLASTIC SUBLOADING MODELLING OF STRAIN RATE CHANGE EFFECTS IN LONDON CLAY

J.R. Maranhã

Geotechnical Department, National Laboratory for Civil Engineering, Lisbon, Portugal

C. Pereira

Geotechnical Department, National Laboratory for Civil Engineering, Lisbon, Portugal

A. Vieira

Geotechnical Department, National Laboratory for Civil Engineering, Lisbon, Portugal

INTRODUCTION

Time dependence of soil behaviour plays an important role in the prediction of the performance of geotechnical structures. Concerning only the strain rate change effects, several studies reported in the literature (e.g., Yin and Cheng, 2006, Sorensen et al., 2007, Li et al., 2009) show that the soil response to changes in the strain rate is characterised by an isotach behaviour, i.e. the stress-strain response curve approaches the same constant strain rate (isotach) stress-strain curve. Under certain conditions, during the transition between two strain rates, the stress-strain response curve presents temporarily values above (overshooting) or below (undershooting) the corresponding isotach curve, respectively with an increase or decrease in the strain rate. The cause of this behaviour is presently not clear.

In this paper the capability of a new viscoplastic subloading soil model to represent the strain rate change effects is evaluated. The stress-strain response from an undrained triaxial compression test on a normally consolidated reconstituted London Clay, presented by Sorensen et al. (2007), is simulated and compared with the experimental results.

VISCOPLASTIC MODELLING OF LONDON CLAY

The new viscoplastic subloading soil model used in this paper is based on an overstress generalisation using the subloading surface concept with a mobile centre of homothety, allowing the occurrence of viscoplastic strains inside the yield surface and avoiding the abrupt change in stiffness of the traditional overstress viscoplastic models. The model was formulated to reproduce the soil rate dependent behaviour under cyclic loading and incorporates both initial and induced anisotropy. Fig. 1 represents, schematically, in the effective stress space, σ , the several homothetic surfaces that define the model, where p is the effective mean stress and s the deviatoric stress tensor. The subloading surface is defined geometrically simply as being homothetic to the yield surface relative to a given mobile centre of homothety, a , which is always located inside the yield surface. The effective stress state is always located on the dynamic loading surface, inside or outside the yield surface. It can never be inside the subloading surface. The overstress is a measure of the distance between the dynamic loading and the subloading surfaces. Finally, the infinite strain rate yield surface, ISRYS, defines a limit to the evolution of σ for increasing values of the strain rate.

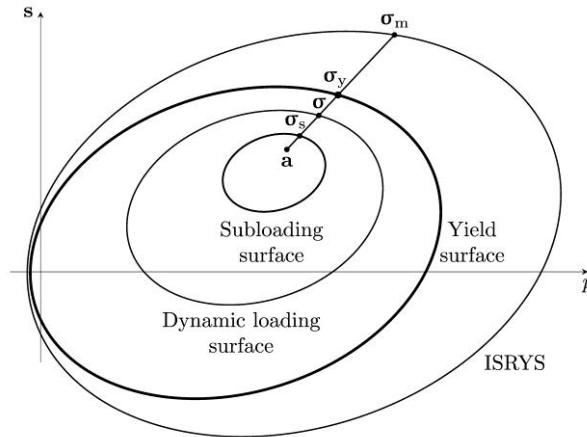


Figure 1. Schematic representation of the homothetic surfaces that define the viscoplastic subloading overstress model with a mobile centre of homothety.

It is not an objective of this paper to present the formulation of this new model. A preliminary version of the model was briefly presented by Maranha et al. (2014), where the response of the model was compared with the laboratorial results of a triaxial undrained test with an unloading-reloading deviatoric stress cycle at constant total mean stress equal to 200 kPa, that incorporates a series of staggered fast loading, approximately $6 \times 10^{-6} \text{ s}^{-1}$ axial strain rate, followed by 24 h creep stages. The evolution of deviatoric stress q with time is represented in Fig. 2.

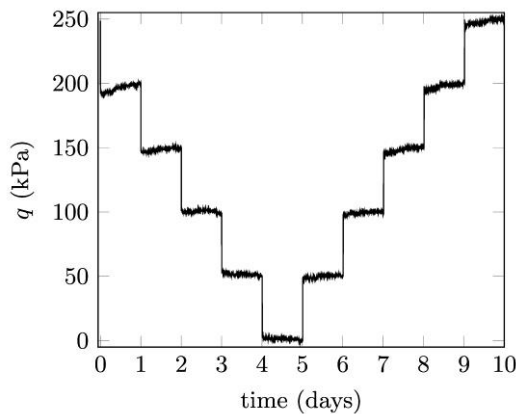


Figure 2. Evolution of deviatoric stress with time of a triaxial undrained test with an unloading-reloading deviatoric stress cycle at constant total mean stress (Maranha & Vieira 2011).

Fig. 3 presents the comparison between the experimental and numerical results obtained in Maranha et al. (2014). As can be seen, a good agreement with the measured response was achieved in (ε_a, q) representation space (Fig. 3a), where ε_a is the axial strain. The model has clearly been able to reproduce the main observed aspects of the stress-strain response of a stiff overconsolidated clay. The observed pore pressure, p_w , evolution was qualitatively well reproduced by the model. After that, the model has been updated and its capabilities greatly improved. Its current version is in the process of publication.

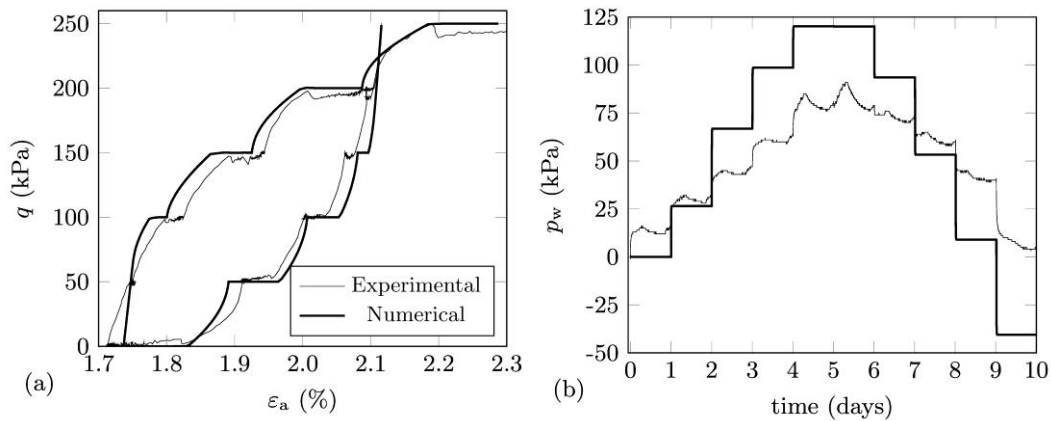


Figure 3. Comparison between the experimental and numerical results. (a) Results in (ε_a, q) representation space. (b) Results in (p_w, time) representation space (Maranha et al., 2014).

After a brief presentation of the new viscoplastic subloading model and its performance reproducing complex laboratorial tests, the capability of the same model to reproduce the strain rate change effects is evaluated. In this study an undrained triaxial compression test on reconstituted London Clay presented by Sorensen et al. (2007) is simulated. The sample was isotropically consolidated to a mean effective stress $p = 300$ kPa, corresponding to a normally consolidated state. The sample was then sheared in undrained conventional triaxial compression from the initial isotropic stress state. To characterise the viscous behaviour in shearing the axial strain rate, $\dot{\varepsilon}_a$, was changed in a stepwise manner between three distinct values, $\dot{\varepsilon}_a = 0.05\%/h$, $0.2\%/h$ and $0.9\%/h$, as indicated in Fig. 4.

Fig. 4 shows the stress-strain response of the normal consolidated reconstituted London Clay, obtained by Sorensen et al. (2007). With this type of laboratorial tests, with loading only, it is not clear if the response to strain rate changes depends on the strain level, the deviatoric stress level, both or any other factor. In fact, their results suggest that the behaviour is different during unloading. Fig. 4 also represents the numerical simulation results and the corresponding isotach curves obtained with the viscoplastic subloading model. The material model constants and initial values of state and internal variables were obtained through the application of a genetic algorithm (Pereira et al., 2014). A good adjustment was obtained. The main characteristics of the soil response were correctly reproduced by the model: (i) the existence of an isotach behaviour at the beginning of the test, (ii) the increase in the overshooting and undershooting magnitude with increasing axial strain and (iii) the shape of the stress-strain curve during strain rate changes. This result was achieved without any specific modification of the model regarding this type of behaviour.

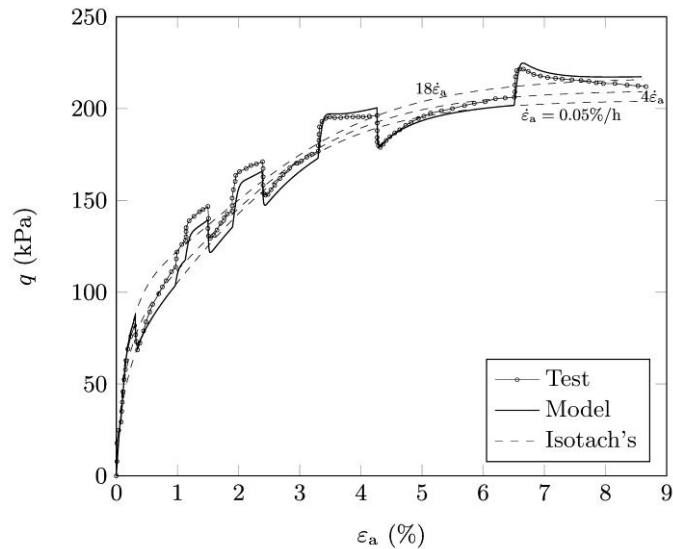


Figure 4. Illustration of stepwise change effects in strain rate on undrained triaxial compression test of normal consolidated reconstituted London Clay. Comparison between the experimental and numerical results.

CONCLUSIONS

This paper presents a study where the capability of a new viscoplastic subloading model to represent the strain rate change effects is evaluated. The stress-strain curve from an undrained triaxial compression test on a normal consolidated reconstituted London Clay is simulated. A good adjustment was achieved. The main characteristics of the soil response are correctly reproduced by the model without any specific modification of the model regarding this type of behaviour.

REFERENCES

- Li, F.-L., Peng, F.-L., Li, J.-Z. & Kongkitkul, W. (2009). Strain rate effects on sand and its quantitative analysis. *Journal of Central South University of Technology*, 16(4), 658-662.
- Sorensen, K. K., Baudet, B. A. And Simpson, B. (2007). Influence of structure on time-dependent behaviour of a stiff sedimentary clay. *Géotechnique*, 57(1), 113-124.
- Maranha, J. R., Pereira, C. & Vieira, A. (2014). A viscoplastic subloading overstress model with a moving centre of homothety. In *Proceedings 14th International Conference of the International Association for Computer Methods and Advances in Geomechanics*, Kyoto, Japan, 243-248.
- Maranha, J. R. & Vieira, A. (2011). An elastoplastic-viscoplastic soil model for cyclic loading. In *Proceedings 11th International Conference on Computational Plasticity. Fundamentals and Applications. COMPLAS XI*, Barcelona, Spain, 1201-1211.
- Pereira, C., Maranhã, J. R. & Brito, A. (2014). Advanced constitutive model calibration using genetic algorithms: some aspects. In *Proceedings 8th European Conference on Numerical Methods in Geotechnical Engineering*, Delft, The Netherlands, 485-490.
- Yin, J.-H. & Cheng, C.-M. (2006). Comparison of strain-rate dependent stress-strain behaviour from K0-consolidated compression and extension tests on natural Hong Kong marine deposits. *Marine Georesources & Geotechnology*, 24(2), 119-147.

CREEP MECHANISMS IN SOIL AND CRYSTALLINE ROCK AND MATHEMATICAL FORMULATION OF THEM BASED ON STOCHASTICAL MECHANICS

R. Pusch

Luleå University of Technology, Luleå, Sweden

INTRODUCTION

The nature of interaction of crystallites is naturally different in soil and rock but they have one thing in common: the strength of interparticle bonds represents an energy spectrum ranging from very low to high levels, meaning that material in bulk exposed to a deviatoric stress condition undergoes time-dependent strain on the microstructural level by activation of slip units to an extent that is determined by local shear stresses, strain, and rates of strain and loading – provided that the material does not disintegrate and no longer coheres. The problem in taking this into account in practical soil and rock mechanics is the definition of boundary conditions, macroscopic heterogeneity and stress distribution in the materials, but testing in the lab and in well instrumented field tests of long duration can give an indication of whether recorded long-term strain will retard or end up in failure.

The particle system in a clay element remains stable if the bulk shear stresses do not exceed a certain critical stress level, which is believed to be on the order of 2/3 of the conventionally determined bulk strength. The bulk strain represents the integrated very small slips leading to “primary creep” with attenuating strain rate for stresses lower than the critical value. Applying Eyring’s principle that the frequency of slip is given by Arrhenius’ rate equation and introducing Feltham’s transition probability parameter to describe the time-dependent energy shifts and assuming furthermore the condition that each transition of a slip unit between consecutive barriers gives the same contribution to the bulk strain, one gets a mathematical expression of creep strain as a function of time that implies that the creep starts off linearly with time, retards and then dies out. This corresponds to primary creep. For medium high stresses the rate of mobilization of new particle bonds is too low to maintain microstructural coherence, and “secondary” creep, ultimately leading to bulk failure, is reached. For thermodynamically appropriately defined limits of the energy barrier spectrum the expression of creep strain represents the commonly observed logarithmic type. This model implies, for moderate deviatoric stresses, microstructural recovery. For high stresses the creep rate of clays follows the same trend of initial retardation but becomes linear for some time, which can be very long for smectite clay, and then increases leading to failure if the boundary conditions permit. The fluid-like behaviour of smectites is explained by the extremely large number of hydrogen bonds between particles and water films that can be activated.

For rock, the stress/strain behaviour is controlled by its content of weaknesses in the form of fissures and voids. The principle of creep is similar to that of soils: a bulk shear stress is carried by a certain number of strong bonds between the crystallites, representing energy barriers, and primary creep with very small strain

that eventually stops for low bulk shear stresses. For medium high stresses breakage and disintegration of a limited number of crystals take place and give slip bands starting from voids or from chlorite or muscovite/biotite micro-lenses. The damaged microzones propagate with time and by increasing the bulk shear stress by which neighbouring bonds become activated and eventually overloaded, leading to further breakage. At this stage the shear resistance increases by the formation of new bonds between the disintegrated particles, making the whole process more soil-like and complex.

CONCLUSIONS

The overall conclusion of the study is that both clay and crystalline rock obey the theoretical model of quickly retarding creep if the stress level does not exceed about 50 % of the stress at failure, and that exceeding about 70 % of this stress leads to creep of log-time type that can be followed by creep and ultimate failure. As to clay one finds that:

- The particle system in a clay element remains stable if the bulk shear stresses do not exceed a certain critical level, which is believed to be on the order of 2/3 of the conventionally determined bulk strength,
- For lower bulk stresses than about 30 % of the conventionally determined shear strength the integrated very small slips lead to “primary” creep with attenuating strain rate, while for stresses ranging from 30 to 50 % of the bulk shear strength, the creep strain rate is of the commonly observed log-time type, implying microstructural recovery. For higher stresses than about 50-70 % the rate of mobilization of new particle bonds is too low to maintain microstructural coherence, and “secondary” creep takes place, ultimately leading to bulk failure,

As concerns crystalline rock the study indicates that:

- The role of chlorite in rock seems to be important; in gneiss it provides vast numbers of slip units and initiation of creep and in both gneiss and granite it does the same as phyllosilicate minerals by being a dominant fracture filling mineral,
- The stress/strain behaviour is controlled by the content of weaknesses in the form of fissures and voids. The principle of creep is similar to that of soils: a bulk shear stress is carried by a certain number of strong bonds between the crystallites, representing energy barriers, causing “primary” creep with very small strain that eventually stops for low bulk shear stresses. For medium high stresses breakage and disintegration of a limited number of crystals take place causing vibrations and slip bands starting from voids or from chlorite or muscovite/biotite micro-lenses,
- The scale dependence of the strength and creep potential is very strong and controlled by the rock structure. For apparently homogeneous laboratory-sized samples trimmed from drill cores to cubic-meter sized rock objects with no through-going fractures or lenses of phyllosilicate minerals, the latter still control

the bulk creep behaviour, implying that a lower compressive stress than 50 % of the conventionally determined strength gives “primary creep” with attenuating strain rate. For stresses of about 50-75 % of the bulk compressive strength, the creep strain rate is of the commonly observed log-time type, implying microstructural recovery. For even higher stresses the rate of mobilization of activated crystal bonds is too low to maintain microstructural coherence, and “secondary” creep takes place, ultimately leading to “tertiary” creep and bulk failure.

REFERENCES

- Bernander, S., 2011. Progressive landslides in long natural slopes. Doct. Thesis, Luleå University of Technology (ISBN: 978-91-7439-283-8; ISSN: 1402-1544), Luleå, Sweden.
- Chunlin, Li., 1993. Deformation and failure of brittle rocks under compression. Doct. Thesis, Luleå Technical University. 118d, ISSN 0348-8373.
- Martin, D., 1994. Brittle Rock Strength. TVO & SKB Workshop, Nuclear Waste Management, TVO technology project, Work Report TEKA-94.07, Helsinki.
- Feltham, P., 1968. A stochastic model of creep. *Phys. Stat. Solidi*, Vol.30 (pp.135-146).
- Pusch, R. 1962. Clay Particles. PhD Thesis, Royal Technical Institute (KTH), Stockholm.
- Pusch, R., Feltham, P., 1980. A stochastic model of creep of soils. *Géotechnique*, Vol.30, No.4 (pp.497-506).
- Pusch, R., 1984. Creep in rock as a stochastic process. *Engineering Geology*, Vol.20 (pp.301-310).
- Pusch, R., 1995. *Rock Mechanics on a Geological Base. Developments in Geotechnical Engineering*, 77. Elsevier Publ. Co, ISBN: 0-444-89613-9.
- Pusch, R., Yong, 2006. *Microstructure of smectite clays and engineering performance*. Taylor & Francis, London and New York. ISBN10: 0-415-36863-4.
- Pusch, R., Weston, R., Knutsson, S., 2015. Impact of scale on rock strength. *J. Earth Sciences and Geotechnical Engng*. ISSN 1792-9040.
- Pusch, R., Knutsson, S., 2015. Strain mechanisms in illitic clay – long-term slope stability. *Eng. Geol.* (In print).

BACK CALCULATION OF TRIAXIAL EXTENSION CREEP TESTS ON A TERTIARY CLAY

N. Sivasithamparam, H.P. Jostad, P. Fornes

Division of Computational Geomechanics, Offshore Energy, Norwegian Geotechnical Institute (NGI), Oslo, Norway

INTRODUCTION

Natural soils can behave in a highly anisotropic manner due to the deposition process and subsequent loading history, and show rate-dependent (creep) behaviour. An accurate description of anisotropy and rate-dependent behaviour of soils is necessary for safe and economic design. Hence, a constitutive model which can model these features is essential. Further, the constitutive model should be simple and easy to understand, and determination of the key model parameters should be possible from standard laboratory tests.

In this paper, laboratory test results on a medium to high-plasticity and fully saturated Tertiary clay were used to study the importance of modelling anisotropy and rate-dependency. In this context, two rate-dependent constitutive models were considered; the Soft Soil Creep (SSC) model which assumes isotropic behaviour and the Creep-SCLAY1 model which can model initial inherent anisotropic behaviour and induced anisotropy due to creep strains.

CONSTITUTIVE MODELS

The Soft Soil Creep (SSC) model (as available within the PLAXIS software) is developed by Vermeer and Neher (1999) to represent the isotropic behaviour of normally consolidated clays. The SSC uses isotropic ellipses around the effective mean stress as contours of volumetric strain rates which is given by the following power law:

$$\dot{\varepsilon}_v = \frac{\mu^*}{\tau} \left(\frac{1}{OCR^*} \right)^\beta \quad \text{where } \mu^* = \frac{C_\alpha}{\ln 10(1+e_0)} \quad \text{and} \quad \beta = \frac{\lambda^* - \kappa^*}{\mu^*} \quad (1)$$

Here μ^* is referred to as modified creep index and τ is the reference time. OCR^* is ratio between mean preconsolidation pressure and equivalent stress as a measure on the isotropic axis of the distance between the current stress and the mean preconsolidation pressure. C_α is the secondary compression index and, λ^* and κ^* are the modified compression and swelling indexes respectively.

The Creep-SCLAY1 model (Sivasithamparam et al., 2015) is an anisotropic rate-dependent model which uses rotated ellipses for the creep rate. Furthermore, the creep strain rates are formulated using the concept of a constant rate of a viscoplastic multiplier $\dot{\lambda}$ as

$$\dot{A} = \frac{\mu^*}{\tau} \left(\frac{1}{OCR^*} \right)^\beta \left(\frac{M^2 - \alpha_{K_0}^{nc}}{M^2 - \eta^2_{K_0}^{nc}} \right) \quad (2)$$

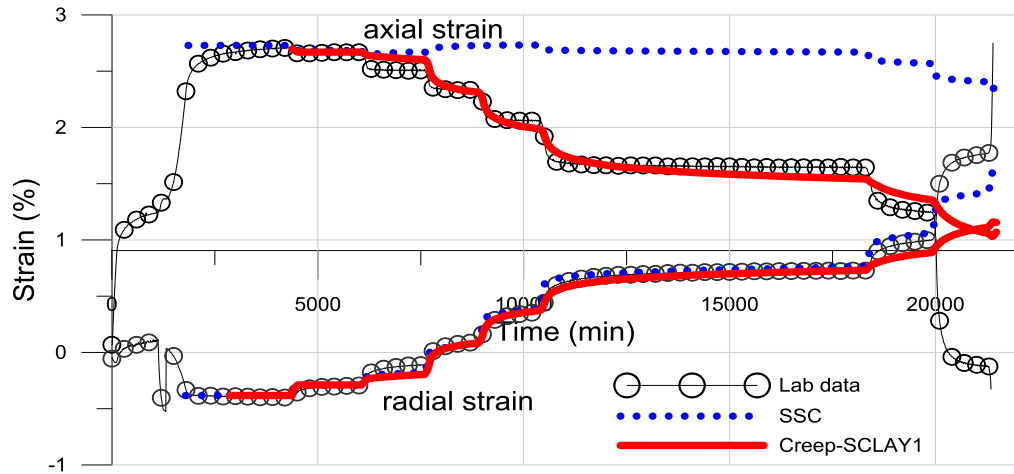
where M is the stress ratio at critical state, the actual stress ratio $\eta = q/p'$ and $\alpha_{K_0}^{nc}$ defines the inclination of the ellipses in normally consolidated state. For further details of the SSC model and the Creep-SCLAY1 model are given in Vermeer and Neher (1999) and Sivasithamparam et al. (2015), respectively.

TRIAXIAL EXTENSION CREEP TESTS AND BACK CALCULATION

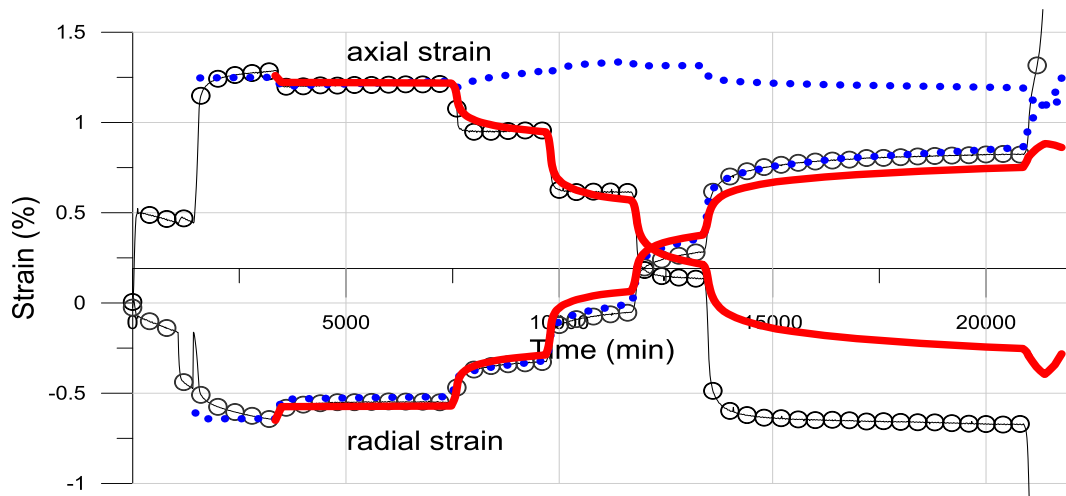
Three triaxial extension creep tests on Tertiary clay are presented. The intact samples were obtained using block sampler. Two tests were performed with intact samples and one was performed with remoulded sample, under drained condition at NGI's laboratory (NGI report, 2012). In the triaxial tests, the vertical stress was first applied to reach the assumed in-situ effective vertical stress, and then the effective horizontal stress was incrementally applied until failure was achieved while the effective vertical stress was kept constant. The time for each load step varied between a few hours and more than a week in order to investigate the creep behaviour of the tertiary clay. The soil test samples were experiencing swelling when saturated with water, and the initial part of the laboratory test were not reliable. Therefore, the laboratory test results in the start of each test were neglected in the FEA back calculation.

The comparison of the FEA back calculation of the triaxial extension creep tests on the two intact samples and one remoulded sample using Creep-SCLAY1 and SSC, with the laboratory test results are shown in Figure 1. Axial and radial strain versus time for the FEA back-calculation were presented in the figures using a best fit parameter set for each test. The anisotropic Creep-SCLAY1 model prediction is in good agreement with the laboratory data for both axial and radial strains with time. By contrast, the SSC model could not be able to predict development of axial strains with time (and radial strain) for the case of the two intact samples (Figures 1-a and 1-b). In the case of remoulded sample, axial strain development with time was predicted by SSC much better than for the intact samples (Figure 1-c). This can be due to that the remoulded sample behaviour is more isotropic. Both models were not very good to predict the measured strains with time toward failure.

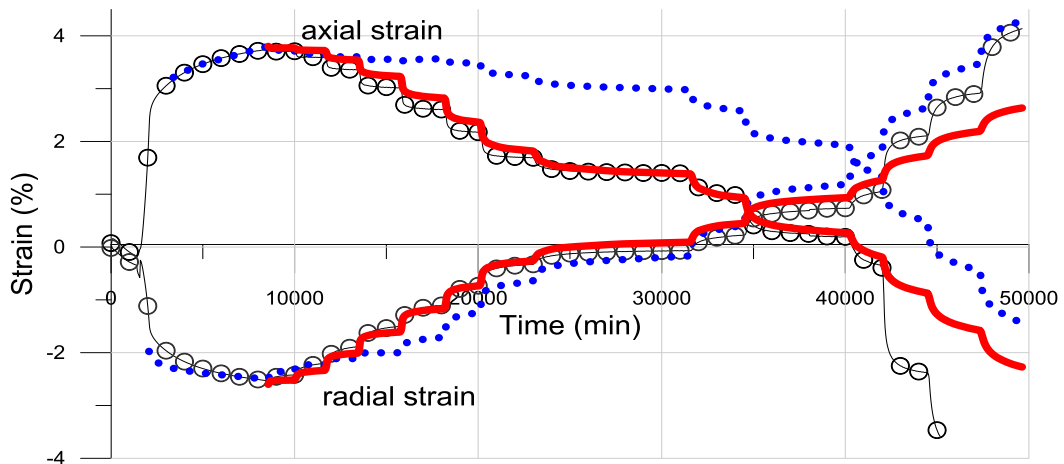
Table 1 summarizes the best fit set of parameters for the laboratory tests for both the Creep-SCLAY1 and SSC models. The best fit parameter set for the Creep-SCLAY1 model is very similar for all three tests except the modified compressibility parameter λ^* . In contrast, the SSC model was not able to predict a good fit using a similar parameter set for all three tests. In addition to the modified compressibility parameters, there is a significant variation the modified creep index and pre-overburden-pressure POP . Further, the POP value used in SSC is much lower than the values used in Creep-SCLAY1 model.



(a) Intact sample – EXVII-3A,3B,3C



(b) Intact sample – P0-XIVa-1E-2



(c) Remoulded sample – EXIV-4A,4B,4C

Figure 1. Comparison of axial and radial strain versus time from the FEA back calculation using SSC and Creep-SCLAY1, and the laboratory test results

The Tertiary clay has experienced several ice sheet advances in the past and as a consequence which may correspond to a higher *POP* than used in the back-calculation. However, it should be noted that sample disturbance can cause underestimation of the *POP* value and inconsistency in modified compressibility parameter when back calculating laboratory tests. The EXIV-4A,4B,4C laboratory test was carried out on a remoulded sample therefor a lower value of *POP* (5 kPa) was used in both models in this case.

Table 1. Summary of model parameters used in back calculation

Parameters	EXVII-3A,3B,3C		P0-XIVa-E-2		EXIV-4A,4B,4C	
	Creep-SCLAY1	SSC	Creep-SCLAY1	SSC	Creep-SCLAY1	SSC
Depth	68.7		70.6		47.7	
κ^*	0.008	0.012	0.008	0.014	0.008	0.018
ν'	0.2	0.2	0.2	0.2	0.2	0.2
λ^*	0.018	0.06	0.022	0.07	0.028	0.09
M	0.94		0.94		0.94	
α_0	0.61		0.70		0.66	
ω	10		10		4	
ω_d	0.42		0.42		0.42	
μ^*	0.0005	0.0005	0.0005	0.001	0.0005	0.001
<i>POP</i>	1600	120	1620	56	5	5

CONCLUSIONS

This paper studies the performance of two rate-dependent models namely SSC and Creep-SCLAY1 during back-calculation of three triaxial extension creep tests. The SSC model is an isotropic model and the creep strain rate is formulated using contours of volumetric creep strain rates whereas Creep-SCLAY1 is an anisotropic model and the creep strain rate is formulated using concept of rate of viscoplastic multiplier. Though both models were able to predict the radial strains with time, in contrast to the Creep-SCLAY1 model, the SSC model was not able predict the axial strains with time. The back-calculation demonstrates that the Creep-SCLAY1 model, which accounts for anisotropic behaviour predicted best the measured behaviour.

ACKNOWLEDGEMENT

The research was carried out as part of CREEP (Creep of Geomaterials, PIAP-GA-2011-286397) project supported by the European Community through the programme Marie Curie Industry-Academia Partnerships and Pathways (IAPP) under the 7th Framework Programme.

REFERENCES

- NGI report. (2012). Laboratory tests on tertiary clay samples. Report No. 20110039-00-2-R.
- Jamiolkowski, M. (2014). Soil mechanics and the observational method: challenges at the Zelazny Most copper tailings disposal facility. *Geotechnique* 64(8), 590-619.
- Sivasithamparam N., Karstunen M. & Bonnier P. (2015). Modelling creep behaviour of anisotropic soft soils. *Computers and Geotechnics* 69, 46-57.
- Vermeer P.A. & Neher H.P. (1999). A soft soil model that accounts for creep. In: *Pro. of the int. symposium on 'Beyond 2000 in Computational Geotechnics'*. Amsterdam, 249–261.

A PROBABILISTIC APPROACH FOR CALCULATION OF LAND SUBSIDENCE ON A MACRO-SCALE

J. Sundell, L. Rosén, C. Alén, M. Karlsson

Department of Civil and Environmental Engineering, Chalmers University of Technology, Gothenburg, Sweden

E. Haaf

Department of Earth Sciences, University of Gothenburg, Gothenburg, Sweden.

INTRODUCTION

In the years to come, several major infrastructure projects are planned in central Stockholm and Gothenburg that require tunneling and deep excavations. Sub-surface constructions generally involve drainage of groundwater, which can induce land subsidence in compressible soil deposits and lead to excessive cost for damage in urban areas. The influence area for a groundwater drawdown affecting pressure heads can be very large (square kilometers), see e.g. Huang et al. (2012). By contrast, predictive calculations of ground subsidence with compression parameters obtained from sampling points are typically assumed to be valid for small areas close to the sampling point itself, see e.g. Larsson and Ahnberg (2005), Wong and Varatharajan (2014) or Yin et al. (2002).

Geotechnical uncertainties can be divided into three primary sources where the first two are parameter uncertainties and the third is a model uncertainty: (1) inherent variability due to geological processes (2) measurement errors caused by equipment, procedural-operator and random testing effects; (3) model uncertainties such as laboratory measurements transformed into design properties (Kok-Kwang & Kulhawy, 1999). Model uncertainties can also include the capability of a model to represent reality. Numerous studies have focused on reducing the second and third source of uncertainty by improving sampling equipment and routines and models that better describe the natural processes see e.g. Olsson (2013), Sivasithamparam et al. (2015) and Yin et al. (2002). The first source can be minimized by taking more samples, but since very large areas need to be considered, precise information cannot be obtained for all objects at risk without considerable costs.

The relationship between groundwater drawdown and ground subsidence on a city-scale have been evaluated in several studies, see e.g. Shen et al. (2013). These studies, however, focus on the evaluation of historical observations of groundwater drawdown and subsidence and not predictions for future events.

In order to prioritize risk reduction measures for planned groundwater drawdown and ensuing subsidence damage, a modelling approach has to be established which has the capacity to: (1) couple a hydrogeological groundwater drawdown model with a geotechnical subsidence model, (2) perform calculations within reasonable computation time as well as (3) consider and quantify the

uncertainties in the system. This paper presents a novel modelling approach including three parts. First, a study of the variability of compression parameters evaluated from Constant Rate of Strain (CRS) tested (Larsson & Ahnberg, 2005) piston samples taken along a planned 14 km long tunnel in Stockholm is presented. Second, based on the result of the first investigation, the model by Sällfors (2001) without creep was adjusted for performing probabilistic calculations of subsidence. Moreover, possibilities for including creep in the model are presented.

DATA TREATMENT AND MODEL

The study area in Stockholm (59°19'N 18°4'E) is located on the East Coast of Sweden and covers approximately 4.5 x 9.5 km². The geology in the area consist of several valleys in pre-Cambrian crystalline bedrock, partly filled with glacio-fluvial sediments such as sand, gravel and clay. To find a representation of the geotechnical properties of the clay, three criteria were set defining the spatial target areas for sampling: (1) within clay-covered valleys where thick layers of clay could be expected; (2) within a predicted influence area for groundwater drawdown; and (3) where constructions sensitive for subsidence damages are located within (1) and (2). Seventy-nine piston samples from 38 locations were taken during 2013-2014 and evaluated with CRS-tests. Compression parameters (preconsolidation pressure, σ'_c ; the pressure where the modulus ends being constant, σ'_L ; Over Consolidation Ratio, OCR; and the modules, M_0 , M_L and M') were then evaluated.

Although the number of samples were few in relation to the size of the investigated area, the sampling density was similar to other major tunnel projects in Stockholm with corresponding investigation aims, such as Bypass Stockholm (Lindberg, 2011), Norra Länken (Bergab, 2004) and City Line (Aqualog, 2007). For projects with low sampling density, it is important to evaluate how representative the samples are for the whole study area. According to a literature review by Li et al. (2015), the distance for which geotechnical parameters of clay are significantly correlated typically fall within the ranges of 10-90 m (horizontally) and 0.1-8.0 m (vertically). To investigate if horizontal correlations exist for the samples in the case study, the data was first detrended vertically, then transformed to a normal distribution (N-dist) and finally a variogram analysis, see e.g. Isaaks et al. (1989), was conducted. No spatial correlations were found, which could be due to low sampling density.

Compression properties of clay are affected by their history, from the sedimentation environment to loading/unloading from e.g. erosion, changes in groundwater levels and constructions. Although precise information of these external factors are difficult to find, it was investigated if the samples from the case study are correlated, based on the following general assumptions: (1) clay from the same valley represent the same sedimentological unit and have similar properties; and (2) the load history is different between clay sampled in a heavily urbanized area compared to a peri-urban area. This investigation was conducted by a categorization of the urbanization ratio and sedimentological units for the different samples. To investigate whether these two categories have any impact on the clay properties, an ANOVA (analysis of variance) was carried out for the data (detrended and converted to N-dist). The null hypothesis is that there is no difference in mean value of the parameter values for the different groups. Since the significance level was lower than five percent for all parameters, it could not be

proven that a difference in mean value of the parameters exists between the categories.

As no spatial correlation, nor correlation to other known factors was found in the available data, all data is considered to belong to the same population. Consequently, all data is used for subsidence predictions at all locations. Although no dependencies could be proven for the external factors, it was investigated with regression methods if internal dependencies among the parameters exist. Internal dependencies are important to consider in simulations using a probabilistic model. If these are ignored, there is a risk for overestimating the uncertainties in the model. Prior to regression analysis, the data is transformed to assure the following conditions to be fulfilled: (1) no inconsistencies in the relation among different parameters in a continuous simulation should appear (e.g. σ'_L can be simulated to be greater than σ'_C); and (2) the residuals of the predicted value can be described by a normal distribution. Correlations with various correlation strength (e.g. correlation coefficient $R = 0.9$ between M_L and σ'_L , and $R = 0.4$ between M' and a combined model with σ'_L , and σ'_C), were found. Since internal dependencies exist, the respective formulas and standard deviations that describe the relations between predicted and dependent parameter, rather than the parameters themselves, are used for the simulations.

OCR was found to vary according to the natural logarithm along depth. From OCR, the other soil parameters needed for calculation with the model by Sällfors are simulated with the formulas from the regression analysis. The soil stratigraphy and ground water table are simulated as grid layers for the entire study area with a novel approach that considers both dependencies and uncertainties in the simulations. Groundwater drawdowns of 0.5, 1 and 2 meters are used for describing the additional effect in the soil profile. In each realization a soil profile is first simulated at every calculation point, then the compression parameters are simulated and the ground subsidence calculated. This process is repeated for 1000 iterations at about 800,000 calculation points.

With the obtained calculation result, a risk map of where a groundwater drawdown could be expected to cause subsidence is created. The risk area is defined as calculation points where the 95th percentile of the simulations show a land subsidence exceeding two centimeters.

In the case study, only permanent groundwater drawdowns are considered and creep effects are left out of the model. In order to improve the calculations, a more advanced one-dimensional finite difference model that considers creep and time-dependencies will be integrated. Moreover, the model is planned to be calibrated with history matching to subsidence observations. Commonly, relatively dense subsidence observations exist in many urban areas. In the cities Stockholm and Göteborg there are thousands of subsidence observation points. With history matching, it is expected that probability density functions for soil parameters valid for local areas can be found. This approach is expected to reduce both model and parameter uncertainties. Model uncertainties are planned to be reduced by including time dependencies and creep effects.

CONCLUSIONS

This paper presents an evaluation of the validity of soil parameters for simplified probabilistic simulation of subsidence on a macro scale where reduction in groundwater pressure head is the additional action. Since no spatial correlation, nor correlation to other known factors were found in the case study, parameters from all samples were considered to belong to the same population. Although an evaluation of the uncertainties in the calculation parameters was carried out, further development is needed in order to reduce model uncertainties.

ACKNOWLEDGEMENTS

We gratefully acknowledge the funding of this work by FORMAS (contract 2012-1933), BeFo (contract BeFo 333) and the COWI-fund.

REFERENCES

- Aqualog. (2007). PM Hydrogeology, Railway tunnel Tomtebodavägen-Riddarholmen (translated from Swedish). Stockholm.
- Bergab. (2004). Hydrogeological investigation Norra länken Project. Stockholm.
- Huang, B., Shu, L., & Yang, Y. S. (2012). Groundwater Overexploitation Causing Land Subsidence: Hazard Risk Assessment Using Field Observation and Spatial Modelling. *Water Resources Management*, 26(14), 4225-4239. doi: <http://dx.doi.org/10.1007/s11269-012-0141-y>
- Isaaks, E. H., Srivastava, R. M., & Knovel. (1989). *Applied geostatistics*. New York: Oxford University Press.
- Kok-Kwang, P., & Kulhawy, F. H. (1999). Characterization of geotechnical variability. *Canadian Geotechnical Journal*, 36(4), 612-624.
- Larsson, R., & Ahnberg, H. (2005). On the evaluation of undrained shear strength and preconsolidation pressure from common field tests in clay. *Canadian Geotechnical Journal*, 42(4), 1221-1231. doi: <http://dx.doi.org/10.1139/T05-031>
- Li, D.-Q., Jiang, S.-H., Cao, Z.-J., Zhou, W., Zhou, C.-B., & Zhang, L.-M. (2015). A multiple response-surface method for slope reliability analysis considering spatial variability of soil properties. *Engineering Geology*, 187(0), 60-72. doi: <http://dx.doi.org/10.1016/j.enggeo.2014.12.003>
- Lindberg, M. (2011). *GeoB, Geotekniska beräkningar, Redovisning av beräkningsresultat, Geoteknik*.
- Olsson, M. (2013). *On rate-dependency of Gothenburg clay*. Chalmers University of Technology, Göteborg.
- Shen, S.-L., Ma, L., Xu, Y.-S., & Yin, Z.-Y. (2013). Interpretation of increased deformation rate in aquifer IV due to groundwater pumping in Shanghai. *Canadian Geotechnical Journal*, 50(11), 1129-1142. doi: 10.1139/cgj-2013-0042
- Sivasithamparan, N., Karstunen, M., & Bonnier, P. (2015). Modelling creep behaviour of anisotropic soft soils. *Computers and Geotechnics*, 69(0), 46-57. doi: <http://dx.doi.org/10.1016/j.compgeo.2015.04.015>
- Sällfors, G. (2001). *Geoteknik, Jordmateriallära - Jordmekanik*. Göteborg: Chalmers Tekniska Högskola.
- Wong, R. C. K., & Varadarajan, S. (2014). Viscous behaviour of clays in one-dimensional compression. *Canadian Geotechnical Journal/Revue Canadienne de Geotechnique*, 51(7), 795-809. doi: <http://dx.doi.org/10.1139/cgj-2013-0198>
- Yin, J.-H., Zhu, J.-G., & Graham, J. (2002). A new elastic viscoplastic model for time-dependent behaviour of normally and overconsolidated clays: theory and verification. *Canadian Geotechnical Journal*, 39(1), 157-173. doi: 10.1139/t01-074

AN OVERLAY MODEL FOR PEAT

J.A.M. Teunissen, C. Zwanenburg
Deltares, Delft, The Netherlands

INTRODUCTION

Peat is fibrous material. Dependent on its level of decay, it is to be expected that the fibres influence the mechanical behaviour of peat. For daily engineering, no material model, especially developed for peats, is available. This paper describes a constitutive model for peats with an approach to the anisotropy due to the fibres as by Teunissen (1995). The basis of the assumed constitutive model for the mechanical behaviour of peat is based on the overlay or fraction model. In this approach the general behaviour results from a set of parallel chain of sub models. Here the sub models represent fibres and the soil matrix. The total effective stress is the summation of both sub model stresses. The strains and the strain rates of the soil matrix and the fibres are equal.

$$\sigma'_{ij} = \sigma'^m_{ij} + \sigma'^f_{ij}, \quad \dot{\epsilon}_{ij} = \dot{\epsilon}^m_{ij} = \dot{\epsilon}^f_{ij} \quad (1)$$

The superscript m relates to the matrix and the superscript f to the fibres. This concept allows incorporating the behaviour of fibres and soil matrix into a general model. The overlay model described in this paper combines the CREEP-SCLAY1S model, one of most prominent models for soft soils, with a fibre model. The CREEP-SCLAY1S model is among others, extensively described by Karstunen et al (2014), Sivasithamparam et al. (2013, 2015). The next sections discuss the formulation used for the fibres and show calculation results. The overlay model is available as a user defined model in for computer program PLAXIS 2D.

FIBRE MODEL

It is assumed that the organic tissues have only stiffness and strength in one direction. The fibre stiffness E^f describes the uniaxial stiffness for the complete area. In the direction of the fibres the following relationship holds:

$$\dot{\sigma}^f = E^f \dot{\epsilon}^f \quad (2)$$

Note that this expression is one dimensional and linear elasticity is assumed. The elastic stress is limited by the ultimate tension stress and compression stress. Beyond these limits the fibres behave perfectly plastic:

$$\begin{aligned} \sigma^f \leq \sigma^f_{tension} &\rightarrow \sigma^f = \sigma^f_{tension} \\ \sigma^f \geq \sigma^f_{compres} &\rightarrow \sigma^f = \sigma^f_{compres} \end{aligned} \quad (3)$$

The fibre model is expressed in local coordinates, in which x' is parallel to the fibres, y' perpendicular and α is the angle between the local and global

coordinates. The relation between stress respectively strain in local and general Cartesian coordinate system is given by:

$$\dot{\boldsymbol{\sigma}} = \boldsymbol{\Omega}^\sigma \dot{\boldsymbol{\sigma}}^f \quad \dot{\boldsymbol{\varepsilon}} = \boldsymbol{\Omega}^\varepsilon \dot{\boldsymbol{\varepsilon}}^f \quad (4)$$

In which $\boldsymbol{\Omega}^\sigma$ represents the rotation matrix for stress and $\boldsymbol{\Omega}^\varepsilon$ for strain. The fibre stiffness is defined with respect to the local axis:

$$\dot{\boldsymbol{\sigma}}^f = \mathbf{D}^f \dot{\boldsymbol{\varepsilon}}^f \quad \text{or} \quad \begin{pmatrix} \dot{\sigma}^f \\ 0 \\ 0 \end{pmatrix} = \begin{pmatrix} E^f & 0 & 0 \\ 0 & 0 & 0 \\ 0 & 0 & 0 \end{pmatrix} \begin{pmatrix} \dot{\varepsilon}^f \\ 0 \\ 0 \end{pmatrix} \quad (5)$$

With respect to the general Cartesian coordinates it is found:

$$\dot{\boldsymbol{\sigma}} = \left((\boldsymbol{\Omega}^\sigma)^{-1} \mathbf{D}^f \boldsymbol{\Omega}^\varepsilon \right) \dot{\boldsymbol{\varepsilon}} \quad (6)$$

The actual stiffness of the fibres depends on the tangent stiffness of the fibres and the orientation of the fibres. Zero fibre stiffness is found when the ultimate tension or compression is reached.

Table 1, Calculation input

Parameters matrix	Value	Parameters matrix	Value	Parameters fibres	values
κ^*	6.70E-03	OCR	1.5	E^f [kN/m ²]	10000
N	0.2	POP [kN/m ²]	0	$\sigma_{tension}^f$ [kN/m ²]	1.5
λ^*	0.1	e_0	2	$\sigma_{compres}^f$ [kN/m ²]	-1.0
M_c	1.5	α_0	0.59	α^f	varies
M_e	1.5	χ_0	0		
ω	50	t [day]	1		
ω_d	1	μ^*	5.07E-03		

SIMULATIONS

To show the fibre influence a biaxial test and a Direct Simple Shear test are simulated. The biaxial test simulation consists of a 1 × 1 m sample. First, a 10 kPa horizontal and vertical consolidation stress is applied for 20 000 days. Next a vertical displacement of 0.6 m is applied undrained in 1 day. The simulated DSS sample has a measure of 0.2 × 0.02 m. A vertical consolidation stress of 10 kPa is applied for 20 000 days followed by a shearing phase with a shear displacement of 0.01 m in which the vertical load is kept constant. For both cases the consolidation phase is simulated using the Mohr-coulomb model. The shearing phase uses the overlay model. Table 1 shows the parameters.

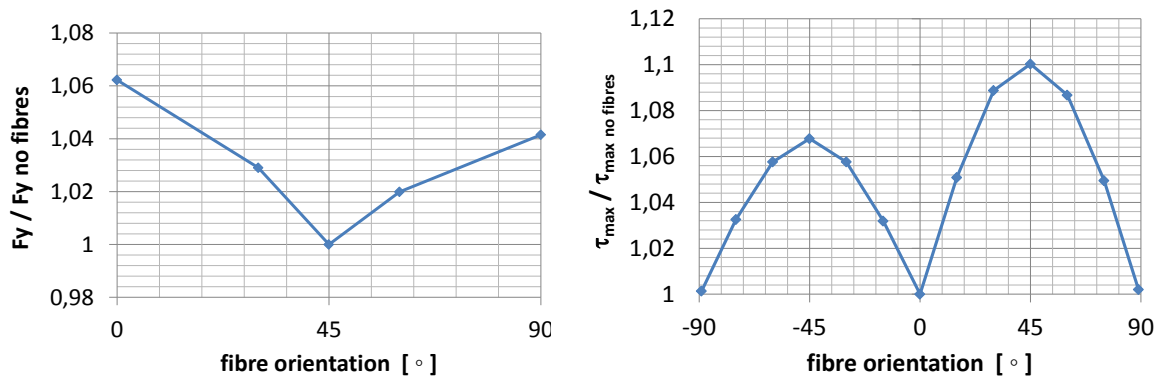


Figure 1, Fibre influence, left normalized failure vertical failure load for biaxial test, right normalized maximum shear stress in DSS test

Figure 1 shows the influence of the fibre orientation on the calculated maximum failure or shear load. For the different loading conditions, biaxial or DSS, the maximum or minimum influence of the fibres is found for different orientations. It is remarkable that for both tests a non-symmetrical pattern is found.

CONCLUSIONS

This paper presents a novel and innovative step in modelling peat behaviour. It shows that with a relative simple extension of an existing model for soft soils the fibre influence can be modelled. The lack of a proper material model for peat is hampering the application FEM in simulations peat related engineering problems.

It can be concluded that the fibres have a significant effect on the strength. This depends on the orientation of the fibres and the loading conditions.

The orientation of the fibres plays a dominant role in the mechanical behaviour of the material model.

ACKNOWLEDGEMENT

The Authors would like to express their gratitude to N. Sivasithamparam and M. Karstunen and for using their code of the CREEP-SCLAY1S model for the matrix part of the overlay model. The research was carried out as part of CREEP (Creep of Geomaterials, PIAP-GA-2011-286397) project supported by the European Community through the programme Marie Curie Industry-Academia Partnerships and Pathways (IAPP) under the 7th Framework Programme.

REFERENCES

- Karstunen M., Rezaia M., N. Sivasithamparam & Z.-Y Yin (2014). Comparison of anisotropic rate-dependent models for modelling consolidation of soft clays. *Int. J. of Geomechanics* DOI: 10.1061/(ASCE)GM.1943-5622.0000267
- Sivasithamparam N., M.Karstunen, R.B.J. Brinkgreve & P.G. Bonnier (2013). Comparison of two anisotropic creep models at element level. *Installation effects in Geotechnical Engineering* eds Hicks, CRC press, 72-78.
- Sivasithamparam, N., Karstunen, M., & Bonnier, P. (2015). Modelling creep behaviour of anisotropic soft soils. *Computers and Geotechnics*, 69, 46-57.
- Teunissen J.A.M. (1995). Modelling of peat. *Compression and Consolidation of Clayey Soils*, eds Yoshikuni & Kusakabe, Balkema, 367-372.

MODELLING DEEP FOUNDATIONS IN SOFT GOTHENBURG CLAY

T. Wood, M. Karstunen

Department of Civil and Environmental Engineering, Chalmers University of Technology, Gothenburg, Sweden

INTRODUCTION

The city of Gothenburg lies on the Swedish west coast. Planned investment in infrastructure and urban construction schemes over the next 10 years within the city itself are currently estimated to cost 4.5 billion euro. Many of these schemes include buildings and underground structures which are deeper, wider and taller than previously carried out in Sweden on thick deposits of soft highly plastic glacio-marine clays. The basement of these structures will be typically founded on driven piles connected by a stiff concrete slab or raft. Historically in Sweden mainly empirical methods have been used in the design of deep foundations (see Ericsson et al. 2004). Generally, the predictions have been highly inaccurate, in particular with regard to the long term deformations. For the projects that lie ahead, a more reliable method of design for deep foundations is required. Therefore, a stepwise approach is proposed which stems from the concept of performance based design. It is shown that with the proposed approach, it is for the first time possible to perform representative back analyses of the long term response of deep foundations in Gothenburg clays. This is achieved with simplified 2D finite element analyses, tailored to the specific case by carefully validating each design assumption or simplification against existing case studies nearby.

STEPWISE APPROACH FOR DEEP FOUNDATION DESIGN

The complexity of natural soft clay behaviour, combined with unknowns surrounding pile-soil-raft behaviour, requires an integrated approach. The engineer has to first understand the individual components that then build together to form the geotechnical structure. The numerical model that is created is verified by comparison with real test data, and if required, adjusted. Once realistic modelling of characteristic behaviour is established, the model can be used to investigate the design.

The proposed approach breaks the design of piled rafts into 8 stages as shown in Table 1. In practice stages 2, 4, and 6 can be omitted, once the designer is familiar with the proposed approach. Each stage is independently verified by comparing numerical predictions with the measured behaviour, in this example from 8 sites indicated by Figure 1.

FE simulations of laboratory tests at single element level using different commercially available constitutive models helped to highlight the model limitations. Based on this work, the FE simulations of long term field behaviour were carried out in 2D plain strain with the Soft Soil Creep model (Vermeer and Neher, 1999). Piles were modelled using an embedded pile concept in 2D (Engin & Brinkgreve 2003), evolved from work by Sadek and Shahrour (2004). The piles

are modelled “wished in place”. However, local experience was used to define the maximum allowable shear forces and mobilised shear stiffness at the pile-soil interface, thus some effects of installation have been implicitly incorporated.

Table 1: Overview of the modelling stages

Stage Number	Design Task	Verification of design assumptions
1	Specify ground & hydrological profile and understand variability	Review multiple site and profiling methods in the area
2	Understand real soil behaviour	Review relevant field and laboratory test data from multiple sites
3	Model characteristic soil behaviour and determine limitations	Comparison with high quality test data
4	Understand individual pile behaviour	Review relevant case studies and identify trends
5	Model characteristic individual pile behaviour and determine limitations	Comparison of FE results with relevant full scale pile tests
6	Understand deep excavation and pile group behaviour	Review relevant case studies and identify trends
7	Model characteristic piled raft behaviour and determine limitations	Comparison of FE results with relevant long term case studies
8	Sensitivity analysis of piled raft behaviour to uncharacteristic loads, ground and hydrological profile, material properties and construction methods	Compare results with well winnowed experience and traditional ULS calculation results

The ground profile used in the FE analyses has been derived based on a review of local sedimentary geology studies, and consideration of results from different methods of field testing at 8 sites indicated in Fig. 1. High quality soil samples were taken at Site 1 at depths representative of the main geological layering. Following extraction, index tests and CRS oedometer tests were started within 1 hour following extraction. Triaxial tests were started on samples from four of the six sample levels within 1-2 hours after extraction, and almost all triaxial samples were tested within 7 days. Stepwise oedometer tests at each level were carried out within 4 to 24 days. Testing was done as quickly as possible to reduce storage effects which had been found to be significant, in particular for undrained shear strength and small strain stiffness.

The structure chosen to verify the proposed method was built in 1988 and consists of a 22 storey tower located at Site 3. The basement slab was generally 1.8m thick and founded 5 m below ground level. The cross section studied is illustrated in Fig. 2. Piles were spaced fairly evenly with an average raft area/pile=4.3 m². The long term pile stiffness was assessed to be 21 MPa in 1999 by Claesson et al. (2007). Settlement of the basement slab was monitored at 26 positions between 1988 and 2002. Further measurements of differential settlements were taken in 2014.

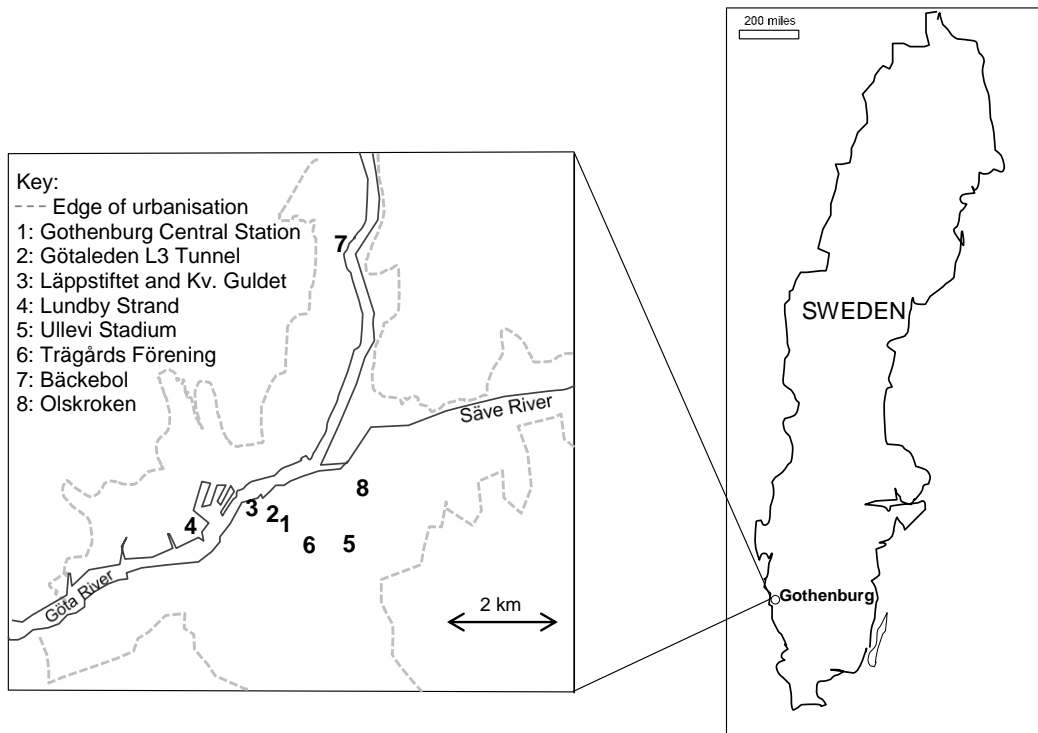


Figure 1. Location of sites used for validation of design method.

The vertical settlement of the raft at Site 3 were greatest close to the river, consistent with shorter drainage lengths and in-situ stresses prior to construction. The values predicted with FE follow the same trend. The central raft settlement predictions with $ISF_{axial\ shaft} = 1$ tended to underestimate observed settlements by approximately 5% while predictions with value of 0.1 were only marginally greater than measured. Adjacent to the river settlement predictions with $ISF_{axial\ shaft} = 1$ were marginally lower than observed settlements in 2002 (-2.2 %), whilst predictions with $ISF_{axial\ shaft} = 0.1$ were marginally greater (+2.3 %). In 2014 measurement of the differential settlement between the existing ground level and the piled raft was carried out. The maximum values agreed well with FE analyses (within 10%).

CONCLUSIONS

Until now, none of the back-analyses have been able to reproduce the measured responses of deep foundations in soft Gothenburg clays. Therefore, a stepwise approach is proposed which stems from the concept of performance based design. The local geological knowledge has been combined with model parameters interpreted from carefully conducted laboratory tests on high quality “fresh” samples for non-linear soil models available in commercial FE code. It is shown that with the proposed approach, it is for the first time possible to perform representative back analyses of the long term response on deep foundations in Gothenburg clays and that this design is fairly insensitive to the embedded pile interaction factor in 2D plain strain analyses. For detailed design, more rigorous 3D analyses with a more comprehensive constitutive model and better description of the soil-pile interface are recommended.

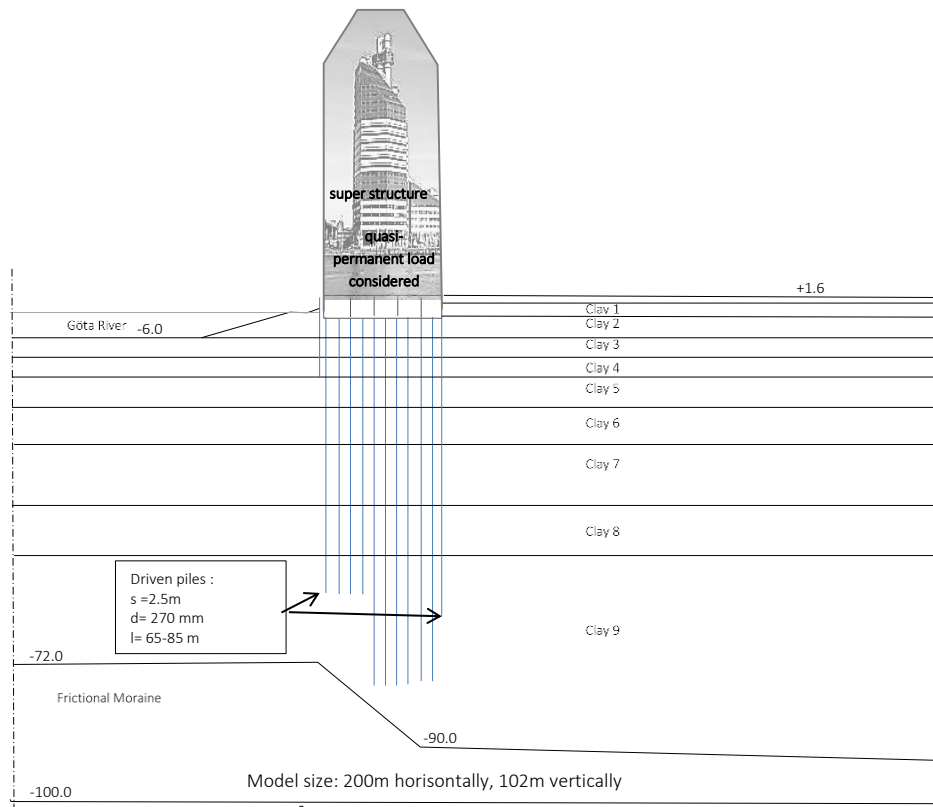


Figure 2. Simplified geometry and foundation layout in FE analyses for piled raft at Site 3.

ACKNOWLEDGEMENTS

This study is part of the BIG (Better Interaction in Geotechnics) project funded by the Swedish Transport Administration. Furthermore, the authors would like to acknowledge the financial support provided by Jernhusen, SBUF, NCC Construction and Chalmers University of Technology.

REFERENCES

- Claesson P, Holmberg G and Romell J (2007). Höghus Lilla Bommen, Göteborg: Uppföljning av kohesionspålning i mäktiga lerlager, SBUF Rapport 1034, pp. 1-36.
- Engin HK and Brinkgreve RBJ (2009). Investigation of Pile Behaviour Using Embedded Piles. In Proc.17th ICSMGE, pp. 1189-1192.
- Eriksson P, Jendeby L, Olsson T and Svensson T (2004). Kohesionspålar, Pålkommisionen Rapport 100, Linköping, Sweden.
- Sadek M and Shahrour I (2004). A three dimensional embedded beam element for reinforced geomaterials. Int. J. Num. Anal. Meth. in Geomechanics 28(9), 931-946.
- Vermeer PA and Neher HP (1999). A soft soil model that accounts for creep. In Proceedings of the International Symposium "Beyond 2000 in Computational Geotechnics pp. 249-261.

A HYPOPLASTIC CREEP MODEL FOR FROZEN SOIL

G.F. Xu, W. Wu

Institute of Geotechnical Engineering, University of Natural Resources and Life Sciences, Vienna, Austria

J.L. Qi

School of Civil and Transportation Engineering, Beijing University of Civil Engineering and Architecture, Beijing, P.R. China

INTRODUCTION

Creep is one of the most important time-dependent behaviors of frozen soil and is crucial in various engineering problems in permafrost regions. Modeling the creep behavior of frozen soil has become a hotspot issue in frozen soil mechanics. Following the creep theories for unfrozen soils and metals, remarkable progress has been made in creep models for frozen soils. Based on the aging theory for the creep of metals, a power relationship was proposed by Vyalov (1965) to describe the creep process of frozen soil. It is found that the model is primarily valid for the primary creep stage. Besides, the model is not suitable for the case with large variation of creep stress. Based on the work by Hult (1966) for the creep of metals, Ladanyi (1972) developed a secondary creep theory for frozen soils. However, this theory is obtained by approximating the creep strain curve in the primary creep stage with a straight line, which has the same slope as that in the secondary creep stage. This means that the theory can only account for creep process at moderate creep stress. In order to describe the typical three-stage creep process, some unified models were developed, such as by Assur (1980) and Fish (1982). Fish showed that the creep behavior of frozen soil at different creep stresses can be described by his model. However, as the time to creep failure is introduced as a known quantity, the model cannot predict the long term stability of structures on permafrost, as pointed out by Zhu and Carbee (1983). Based on the unified models (Assur, 1980; Fish, 1982), another unified creep model was proposed by Ting (1983). The model can give fairly accurate fits of strain (rate) - time behavior of frozen sand. However, it can only be applied to the case in which the creep deformation is large enough to cause creep rupture.

In this paper, a hypoplastic creep model is proposed for frozen soil based on the model by Wu (1992). The proposed creep model is superior in that not only accurate fit of test data can be made for creep tests, the methods for handling cases with and without failure are even not distinguished.

HYPOPLASTIC CREEP MODEL

The basic hypoplastic constitutive model proposed by Wu (1992) had the following form

$$\dot{\mathbf{T}} = c_1(\text{tr}\mathbf{T})\mathbf{D} + c_2 \frac{\text{tr}(\mathbf{T}\mathbf{D})}{\text{tr}\mathbf{T}} \mathbf{T} + c_3 \frac{\mathbf{T}^2}{\text{tr}\mathbf{T}} \|\mathbf{D}\| + c_4 \frac{\mathbf{T}_d^2}{\text{tr}\mathbf{T}} \|\mathbf{D}\| \quad (1)$$

in which c_i ($i = 1, \dots, 4$) are material parameters, \mathbf{T} is the Cauchy stress tensor, \mathbf{D} is the strain rate tensor, $\dot{\mathbf{T}}$ is the time derivative of stress tensor, \mathbf{T}_d is the deviatoric stress tensor. Constitutive equation (1) was proposed for sand. For frozen soil, this model needs to be modified to include the temperature dependent cohesion. Further analysis of the basic model shows that the model cannot describe the creep behavior of materials owing to its rate independence and stress homogeneity. Let us consider the following hypoplastic model

$$\dot{\mathbf{T}} = c_1[\text{tr}(\mathbf{T}-s)]\mathbf{D} + c_2 \frac{\text{tr}[(\mathbf{T}-s)\mathbf{D}]}{\text{tr}(\mathbf{T}-s)}(\mathbf{T}-s) + f(D) \cdot [c_3(\mathbf{T}-s)^2 + c_4(\mathbf{T}-s)_d^2] \quad (2)$$

where s is an isotropic tensor and is determined by a scalar s as $s = s \cdot \delta_{ij}$, in which s can be regarded as the cohesion of frozen soil, δ_{ij} is the Kronecker delta. $f(D)$ is a scalar function of deformation. It can be found that model (2) is not homogeneous in either stress or strain rate. The inhomogeneity of model (2) makes it possible to describe the creep and relaxation behaviors of frozen soil.

For the deformation function, the following equation can be abstracted from some creep test results (Orth, 1986; Wu and Ma, 1994),

$$\log[f(D)] = a[\log(l) + d] + \frac{b}{\log(l) + d} + c \quad (3)$$

in which a , b , c and d are parameters depending on stress, $l = \int_0^t \|\mathbf{D}(\tau)\| d\tau$ is the length of strain path (Wu et al., 1993). Further study of this equation shows that, the first term on the r.h.s. of Eq. (3) dominates in the primary creep stage and the second term is dominant in the tertiary creep stage. Similar constitutive equation was proposed by Okubo et al. (1991) for various rocks.

VALIDATION OF THE HYPOPLASTIC CREEP MODEL

The hypoplastic creep model is validated by simulating some creep tests. Before the simulation, the parameters in the model are determined.

Calibration of the creep model

The determination of the material parameters c_i ($i = 1, \dots, 4$) can be found in the publication by Wu and Bauer (1994). As the norm of strain rate in the basic model is removed, c_3 and c_4 in the creep model should be adjusted by multiplying the original ones by a factor equivalent to the norm to balance the removal. The determination of the 4 introduced parameters is given below. As stated above, the creep rate in the primary creep stage can be approximated by

$$\log[f(D)] = a[\log(l) + d] \quad (4)$$

It can be easily found from (4) that parameter a can be determined from the slope of the creep rate - deformation curve. In the tertiary creep stage, the creep rate can be approximated by

$$\log[f(D)] = \frac{b}{\log(l) + d} \quad (5)$$

Based on an optimal fit to the creep test results, parameter b in (5) can then be obtained from the intercept at a relatively large time point in the creep rate -

deformation curve. Once parameters a and b are determined, parameters c and d can also be obtained by substituting the minimum creep rate and its derivative into (3), then solving the equation system with respect to variables c and d .

Simulation of compression creep tests

Uniaxial creep tests at the temperatures of -2 and -10 °C were simulated. The tests were conducted by Orth (1986) on frozen Karlsruhe medium sand at different creep stresses. Taking the tests at the temperature of -10 °C as an example, the four material parameters in the hypoplastic creep model can be obtained as: $c_1 = -68.82$, $c_2 = -673.56$, $c_3 = 0.0768 \text{ kPa}^{-1} \cdot \text{s}^{-1}$, $c_4 = -0.0256 \text{ kPa}^{-1} \cdot \text{s}^{-1}$, and the cohesion of the frozen sand $s = 3061.9 \text{ kPa}$. For the creep stress at 10 MPa , the 4 introduced parameters were obtained as: $a = -0.3753$, $b = -0.1086$, $c = -8.1151$, $d = -3.435$. When more sets of parameters for other creep stresses were determined, four linear relationships can be drawn between each parameter and the creep stress. It was interesting to find that the linear relationships were also applicable to the cases without creep failure.

Using the stress boundary conditions in a uniaxial creep test and based on (2), the axial strain rate can be calculated with

$$D_1 = -\frac{c_3 + \frac{4}{9}c_4}{c_1 + c_2}(T_1 - s_1) \cdot f(D) \quad (6)$$

Substituting (3) into (6), then taking the logarithm of both sides of the equation, we can get

$$\log(D_1) = a[\log(l) + d] + \frac{b}{\log(l) + d} + c + \log\left[-\frac{c_3 + \frac{4}{9}c_4}{c_1 + c_2}(T_1 - s_1)\right] \quad (7)$$

Substituting the parameters determined for different creep stresses, the axial strain rate can be obtained from (7). Furthermore, when integrating the axial strain rate such obtained, we can get the axial strain in the uniaxial creep tests. The simulated axial strain and strain rate were presented in Figures 1 and 2, respectively.

From Figures 1 and 2 it can be seen that: 1) the specimen experienced only the primary creep stage at low creep stress, in which the creep strain increased continuously with time, but the increase rate became lower and lower; 2) at relatively high creep stress, typical three-stage creep curves can be observed. In these tests, the creep rate firstly decreased and then increased with an almost constant creep rate (steady-state) in between, which can be seen clearly in a Cartesian coordinate system; and 3) at higher creep stress, the creep strain increased with time and the creep rate changes in a similar pattern to that at relatively high stress in the log-log coordinate system, but without the steady creep stage in the Cartesian coordinate system, i.e. the primary creep stage is followed closely by the tertiary creep stage. From the two figures it can be concluded that the hypoplastic creep model showed a good ability in describing the creep behavior of the frozen medium sand.

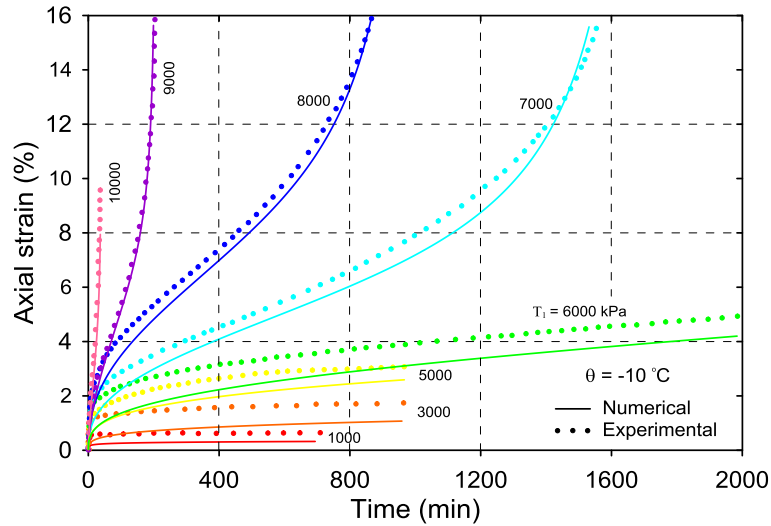


Figure 1. Evolution of the creep strain

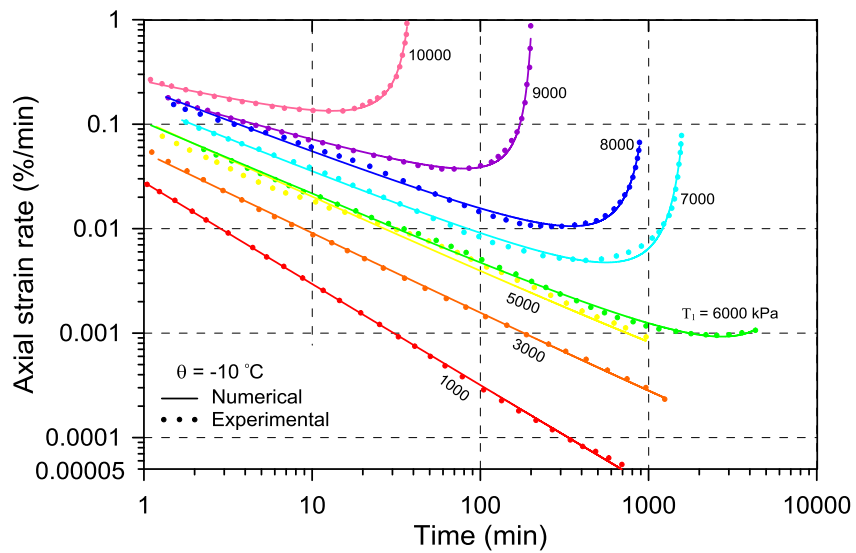


Figure 2. Evolution of the creep strain rate

CONCLUSION

In this paper, the following conclusions can be drawn. (1) The proposed hypoplastic creep model showed a good ability in describing the creep deformation and creep rate of frozen soil. (2) The creep model can indiscriminately handle the cases with or without failure in creep tests.

ACKNOWLEDGEMENT

The authors wish to thank the European Commission (Creep of Geomaterials, PIAP-GA-2011-286397) and the National Natural Science Foundation of China for their financial supports to the projects Reinforced Vegetation Numerical Evaluation of Slopes (Grant Agreement No. 324466) and Hypoplastic Constitutive Model for Warm Frozen Soils (No. 41172253).

REFERENCES

- Assur, A. (1980). Some promising trends in ice mechanics. IUTAM Symposia, Physics and Mechanics of Ice, 1-15.
- Fish, A. (1982). Comparative analysis of the USSR construction codes and the US Army technical manual for design of foundations on permafrost. Report 14. U.S. Army, Cold Regions Research and Engineering Laboratory.
- Hult, J. (1966). Creep in engineering structures. Blaisdell Publishing Company: Waltham, Mass., pp.115.
- Ladanyi, B. (1972). An engineering theory of creep of frozen soils. Canadian Geotechnical Journal 9 (1), 63-80.
- Okubo S., Nishimatsu Y. & Fukui K. (1991). Complete creep curves under uniaxial compression. International Journal of Rock Mechanics and Mining Sciences and Geomechanics Abstracts 28 (1), 77-82.
- Orth, W. (1986). Gefrorener Sand als Werkstoff: Elementversuche und Materialmodell. PhD thesis. Karlsruhe University, Institute of Soil Mechanics and Rock Mechanics, Germany.
- Ting, J. (1983). Tertiary creep model for frozen sands. ASCE Journal of Geotechnical Engineering 109 (7), 932-945.
- Vyalov, S. (1965). Rheological Properties and Bearing Capacity of Frozen Soils. Report 74. U.S. Army, Cold Regions Research and Engineering Laboratory.
- Wu, W. (1992). Hypoplasticity as a mathematical model for the mechanical behavior of granular materials. PhD thesis. Karlsruhe University, Institute of Soil Mechanics and Rock Mechanics, Germany.
- Wu W. & Bauer E. (1994). A simple hypoplastic constitutive model for sand. International Journal for Numerical and Analytical Methods in Geomechanics 18 (12), 833-862.
- Wu W., Bauer E., Niemunis A. & Herle I. (1993). Visco-hypoplastic models for cohesive soils. Modern Approaches to Plasticity. 365-383.
- Wu Z. & Ma W. (1994). Strength and Creep of Frozen Soil. Lanzhou University Press, P.R. China.
- Zhu Y. & Carbee D. (1983). Creep behavior of frozen silt under constant uniaxial stress. In Proceedings of the 4th International Conference on Permafrost, Alaska, 1507-1512.

A NEW ELASTO-VISCOPLASTIC MODEL FOR 1-D COMPRESSIVE BEHAVIOR OF CLAYS

Y. Yuan

*Department of Civil and Environmental Engineering, Massachusetts Institute of
Technology, Cambridge, USA*

A.J. Whittle

*Department of Civil and Environmental Engineering, Massachusetts Institute of
Technology, Cambridge, USA*

INTRODUCTION

The compression behavior of saturated clays is of great importance for many geotechnical projects, especially those entailing reliable predictions of the long-term deformation in underlying clay layers. The predictive accuracy depends on a realistic description of the inherent viscous behavior of clays. A great number of elasto-viscoplastic (EVP) frameworks have been used to account for this constitutive behavior. The most popular are based on 'isotache-type' formulations, which assume a unique relationship between effective stress, strain (void ratio) and viscoplastic strain rate, $\sigma'_v - \varepsilon - \dot{\varepsilon}^{vp}$ (after Suklje, 1957).

Although many researchers have experimentally validated the isotache framework (e.g., Leroueil et al., 1985), its limitations become apparent when used in practical predictions. For instance, existing isotache models tend to overestimate the initial creep rate for the consolidation of thicker clay layers due to the assumption that field-scale viscoplastic strain rate is the same as that observed in laboratory tests (typically around 1%/day for normally consolidated (NC) clay). This causes the model to predict unrealistic increases in pore pressure at points distant from drainage horizon (Yuan & Whittle, 2013). Other measured results from lab tests with step-changes in strain rate in CRS tests also deviate from the isotache framework (Deng & Tatsuoka, 2005; Tsutsumi & Tanaka, 2011), and suggests further limitations of these models.

This paper introduces a novel elasto-viscoplastic model for 1-D compressive behavior of clays. The new formulation aims to overcome the drawbacks of existing isotache models and provides a unified description for a wide range of time-dependent properties of clays.

FORMULATION OF PROPOSED MODEL

The proposed EVP formulation decomposes the total strain rate, $\dot{\varepsilon}$ into elastic and viscoplastic components, $\dot{\varepsilon}^e$ and $\dot{\varepsilon}^{vp}$. The model defines a bilinear constitutive relation in a double logarithmic, void ratio versus effective stress, $\log e - \log \sigma'$ space, following the framework by Pestana and Whittle (1995). The elastic recompression curve is linearized with a slope of ρ_r , whereas the NC regime (virgin consolidation) is characterized by a constant slope, ρ_c . This framework incorporates a physically based, viscoplastic strain evolution law:

$$\dot{\varepsilon}^{vp} = R_a \left(\frac{\sigma'_v}{\sigma'_{eq}} \right) \quad (1)$$

where R_a [1/time] is introduced as an internal strain rate representing the historical straining effects on the soil skeleton, which is assumed to be non-negative. σ'_{eq} is a stress history variable, which increases upon strain hardening.

Equation 1 assumes viscoplastic strain rate, $\dot{\varepsilon}^{vp}$ not only depends on the current stress ratio, σ'_v/σ'_{eq} , but also the internal strain rate R_a . Therefore, it distinguishes from the unique σ'_v - ε - $\dot{\varepsilon}^{vp}$ relationship of the isotache theory and allows different $\dot{\varepsilon}^{vp}$ at given effective stress and strain, σ'_v - ε states.

The determination of the new state variable, R_a necessitates an additional evolution equation, as expressed in Eqn.2. Here we assume that R_a increases with the perturbations of external straining expressed by the function, $f(\dot{\varepsilon})$, but it also decays at a rate proportional to the current internal strain rate (i.e., $-R_a$). A migration coefficient, m_t [1/time] controls the rate of change of R_a :

$$\dot{R}_a = [f(\dot{\varepsilon}) - R_a] \cdot m_t \quad (2)$$

The function $f(\dot{\varepsilon})$ is determined by considering the relation between the steady state of Eqn.2 and the NC behavior observed in constant rate of strain consolidation (i.e., CRS) tests:

$$f(\dot{\varepsilon}) = \left(\frac{\rho_c - \rho_r}{\rho_c} \dot{\varepsilon} \right) \left(\frac{\dot{\varepsilon}}{\dot{\varepsilon}_{ref}} \right)^{-\beta} \quad (3)$$

where $\dot{\varepsilon}_{ref}$ is the reference strain rate.

The exponent β controls the rate-sensitivity and has great impacts on explaining a wide range of rate-dependent characteristics.

The coefficient, m_t , can enable realistic descriptions of relaxation and secondary compression behavior and is proposed as follows,

$$m_t = \left(\frac{\rho_c}{\rho_\alpha} - 1 \right) \frac{\dot{\varepsilon}^{vp}}{\rho_r \cdot n} + \dot{\varepsilon} \quad (4)$$

where parameter ρ_α is introduced as a viscous property, similar to the secondary compression coefficient, C_α (but defined in double logarithmic void ratio-time, loge-logt space).

The model uses five material parameters, ρ_r , ρ_c , ρ_α , β and $\dot{\varepsilon}_{ref}$, that can all be determined experimentally using CRS and Incremental Loaded (IL) oedometer tests. The initial values of two internal state variables, σ'_{eq0} and R_{a0} , must also be estimated by examining the stress history and strain rate at the end of prior consolidation events, respectively. Detailed procedures are available in Yuan (2015).

DEMONSTRATION

A key advantage of the proposed formulation is that it allows realistic initial creep rates (i.e., different values of R_{a0} , can be used for incremental loading of consolidation with different drainage heights). This is demonstrated in the simulation of IL consolidation tests for 2cm and 20cm thick specimens, which are both NC at the same effective stress and void ratio (σ'_{v0} - e_0 fixed). The R_{a0} are

obtained by estimating the creep rate at the end of the prior phase of consolidation ($\approx \rho_a n / t_{99}$, where n is porosity; and t_{99} is the estimated time to 99% dissipation of excess pore pressure for each specimen). Figure 1 compares predictions of base pore pressures (for one way top drainage) using two different values of R_{a0} in the proposed model with results obtained by an isotache approach (R_{a0} same for both specimens). The latter produces an unrealistic rise in the base pore pressure, while the proposed model provides a more realistic estimate of expected changes in pore pressures.

Figure 2 illustrates another advantage of the proposed model, which is its capability of describing a full range of rate-dependent behavior in CRS tests. Figure 2b shows computed results of CRS tests with step changes in strain rate with the input parameter, $\beta = \rho_a / \rho_c$ (corresponding to the ratio, C_a / C_c). The results show parallel shifts in the compression curve for each strain rate, corresponding to the conventional isotache framework. In contrast, when $\beta = 0$ (Figure 2a) the proposed model predicts a transient decay in the compression response induced by step-changed strain rates, i.e., the strain rate has a temporary effect on compression behavior, while steady state conditions imply a unique virgin compression behavior of the NC clay.

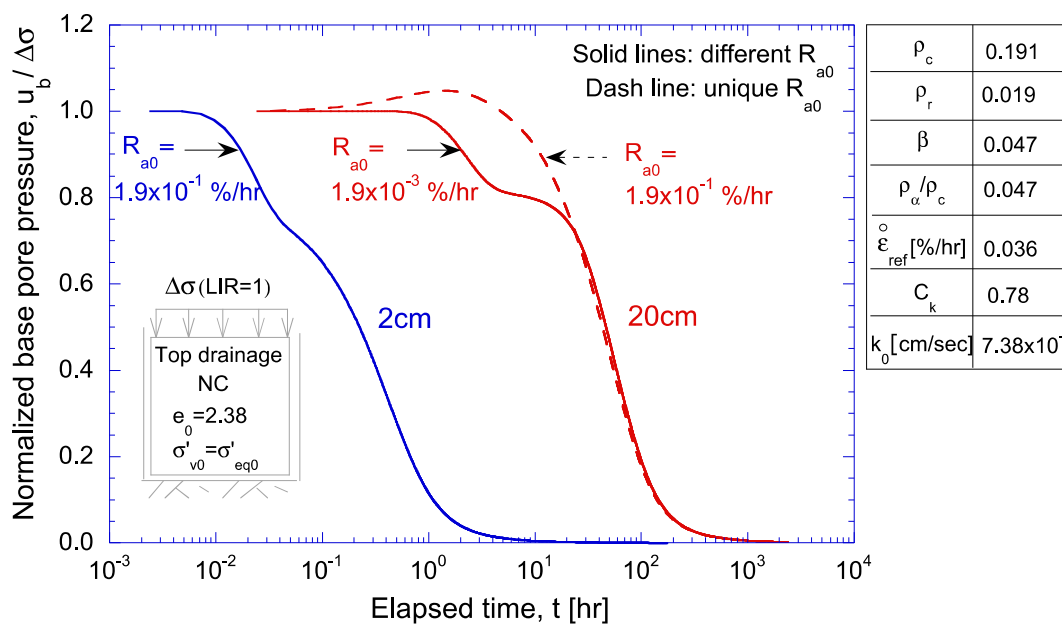


Figure 1. Effect of using estimated initial creep rate on the pore pressure response of the consolidation of specimens with different thicknesses

CONCLUSIONS

The new elasto-viscoplastic model proposed in this paper incorporates a natural description of viscoplastic deformation, which evaluates the current viscoplastic strain rate in terms of the historical straining effects. The model has overcome the drawback of existing isotache framework by enabling more realistic estimates of initial creep rate in IL consolidation predictions. Without significantly increasing the number of parameters the model extensively expands its predictive capabilities over a wide range of time-dependent compression behavior.

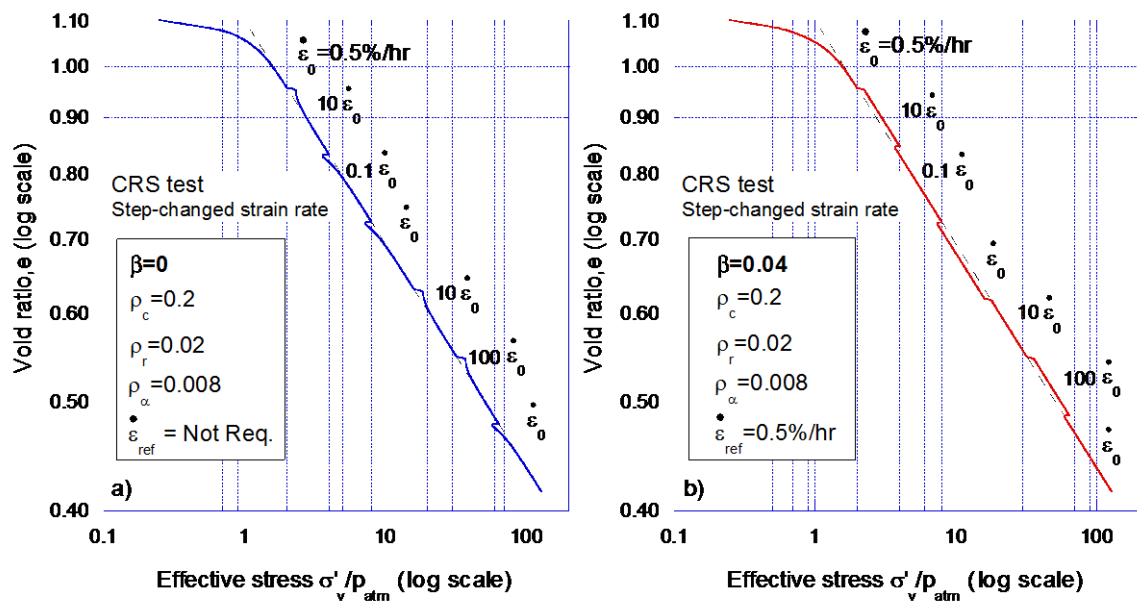


Figure 2. Effect of rate-sensitivity parameter β on the compression behavior of CRS tests with step-changed strain rates: a) $\beta=0$; b) $\beta= \rho_\alpha/\rho_c=C_\alpha/C_c$

ACKNOWLEDGEMENTS

The Authors are grateful for support provided by Ferrovial-Agromán through the Ferrovial-MIT program.

REFERENCES

- Deng, J. L., and Tatsuoka, F. (2005). Aging and viscous effects on the deformation of clay in 1D compression. *Site Characterization and Modeling*, 1–12.
- Leroueil, S., Kabbaj, M., Tavenas, F., and Bouchard, R. (1985). Stress-strain-strain rate relation for the compressibility of sensitive natural clays. *Géotechnique*, 35(2), 159–180.
- Pestana, J. M., and Whittle, A. J. (1995). Compression model for cohesionless soils. *Geotechnique*, 45(4), 611–631.
- Suklje, L. (1957). The analysis of the consolidation process by the isotaches method. *Proceedings of the 4th International Conference on soil mechanics and foundation engineering*, 201–206.
- Tsutsumi, A., and Tanaka, H. (2011). Compressive behavior during the transition of strain rates. *Soils and Foundations*, 51(5), 813–822.
- Yuan, Y., (2015). A new elasto-viscoplastic model for time-dependent behavior of clays. PhD thesis. Massachusetts Institute of Technology, Cambridge, USA
- Yuan, Y., and Whittle, A. J. (2013). Examination on time-dependent soil models in one-dimensional consolidation. *Constitutive Modeling of Geomaterials*, 159–166.

UNDRAINED TRIAXIAL RELAXATION TESTS ON A FIBROUS PEAT

L. Zhang, B.C. O'Kelly

Department of Civil, Structural and Environmental Engineering, Trinity College Dublin, Dublin 2, Ireland

T. Nagel

Department of Environmental Informatics, Helmholtz Centre for Environmental Research GmbH - UFZ, Leipzig, Germany

INTRODUCTION

The long-term creep with comparatively great strain magnitudes makes peat a distinctive as well as problematic geomaterial in geotechnical engineering practice. Hobbs (1986) claimed the effective stress strength of peat is also state dependent as the void ratio continuously decreased under the maintained load. The inelastic behavior of peat materials consists of the hysteresis of the organic solid structure as well as the delayed pore water dissipation. Here, the rate-dependent hysteresis related to a viscous effect in the soil structure is investigated. Conventionally, creep behavior of peat was studied in one-dimensional (1D) drained fashion such as oedometer tests (den Haan 1996), whereas the effective stress strength parameters were obtained in undrained tests including undrained triaxial (Hendry et al. 2014) and simple shear (Farrell et al. 1998). It was found that peat continues to creep for years or even decades (Barden and Perry 1968) without reaching its creep limit/equilibrium state. Also, the creep rate increases at a critical point termed as tertiary compression (Dhowian and Edil 1980) which complicates the laboratory investigation as well as the mathematical formulation of creep models for peat. The result from drained creep tests is a hybrid effect of solid hysteresis and the delayed micro-pore/adsorbed water movement. Albeit the 1D creep behavior (secondary and tertiary compression) of peat has been well studied for decades, information reported in the literature about the solid structure rate-dependent hysteresis, which plays a crucial role in effective stress evolution, is still incomplete. For the advancement of constitutive modelling and a better understanding of peat, undrained triaxial relaxation tests were carried out in this study to investigate the inelasticity of peat organic solid structure.

The state-of-art in modelling the rate-dependency of peat is based on the isotache concept. A linear relationship is assumed between the Hencky strain and the logarithm of virgin compression stress. On each of the equidistant isotaches, the creep rate is constant (den Haan 1996). Elasto-viscoplastic models based on the Modified Cam Clay model have been extended using the isotache concept to predict peat elasto-viscoplastic behavior. In the above mentioned models, creep was taken to start simultaneously with the hydrodynamic consolidation process. The mechanism behind peat creep was assumed to be the micro-pore water dissipation occurring at a slower rate than the macro-pore water dissipation during the consolidation stage. This paper demonstrates a set of experimental data on undrained triaxial relaxation tests on a fibrous peat collected from Clara bog,

Ireland. The suitability of such tests as an alternative experimental means to investigate peat inelasticity is evaluated.

TESTING PROGRAM

Saturated undisturbed peat specimens were trimmed into diameter of 38 ± 1 mm and height of 76 ± 1 mm from the undisturbed peat block. Saturation was confirmed by a Skempton B value of larger than 0.95. The properties of the undisturbed peat can be found in Zhang and O'Kelly (2013). Unconsolidated undrained (UU) triaxial tests were carried out with and without pore water pressure measurements at a room temperature of 20°C . The testing program is listed as following:

1. Undrained loading and unloading (*lu*) with relaxation tests (relaxation duration of 1000 s) at two axial strain rates (2.032 mm/min (2.67 %/min) and 0.2032 mm/min (0.267 %/min)) were carried out without pore water measurement at a cell pressure of 30 kPa.
2. Two undrained triaxial relaxation tests were investigated with two axial strain rates, namely 2.032 mm/min and 0.2032 mm/min, with pore water pressure measured and zero cell pressure. The relaxation time period was 10 hours.
3. The loading-unloading-reloading (*lur*) UU triaxial relaxation tests without pore water pressure measurement at axial strain rate of 2.032 mm/min were compared with *lur* UU triaxial tests at a strain rate of 0.06096 mm/min.

RESULTS AND ANALYSIS

The UU triaxial *lu* tests with relaxation of 1000 s were compared between axial strain rates of 2.032 mm/min and 0.2032 mm/min. Figure 1(a) shows the strain rate effect on the deviator stress during undrained compression and relaxation. At the very start of the compression, the two curves showed very similar slope. Higher deviator stress was achieved with the higher strain rate at the same level of axial strain. The deviator stress relaxations during loading stage decayed $14.6 \pm 0.5\%$ and $8.9 \pm 0.9\%$ of their original values for 2.032 mm/min and 0.2032 mm/min strain rates for the duration of 1000 s, respectively. Some stress points measured at the lower strain rate were below the relaxed values at the higher strain rate, which indicates incomplete relaxations. The deviator stress relaxation ratio (defined in Equation 1, where q : value after relaxation; q_0 : value before relaxation) is presented in Figure 1 (b). It can be seen that the relaxation ratio of deviator stress during the loading stage is nearly constant for the same duration whereas the relaxation ratio during unloading stage approaches 100% due to the zero value of q . The rate-dependent behavior can be represented by an overstress concept (Haupt 2002). Rate-independent hysteresis was recorded at the end of unloading, although the unloading results of the two tests are difficult to compare due to the different strain levels reached. The virtual elastic strain calculated using the stress relaxation increase during unloading divided by the tangent modulus of the unloading stress-strain curve is plotted in Figure 1 (c). A linear relationship can be found between the virtual elastic strain and the total strain during the unloading stage.

$$R\% = \frac{q_0 - q}{\max\{q_0, q\}} \% \quad (1)$$

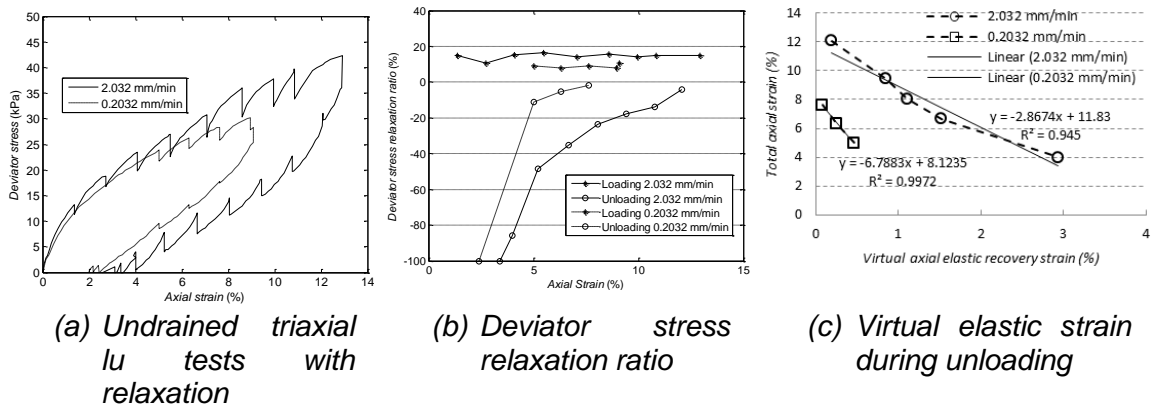


Figure 1. Undrained relaxation tests at two axial strain rates

Figure 2 presents the triaxial compression tests at strain rates of 2.032 mm/min and 0.2032 mm/min followed by a 10 hour relaxation phase with pore water pressure measurement and zero cell pressure. From Figure 2, the pore pressure variations were very small; the noise recorded was rooted in the 1 kPa resolution of the pore pressure transducer. Since the pore water pressure was practically zero, the relaxation behavior could be taken as solely from the peat organic solid structure. The tenfold increase of strain rate resulted in a deviator stress increase of 20.1 % to reach an axial strain of 5%. A linear relationship can be found between deviator stress and logarithm of time after an initial time period. Figure 2 also indicates that after 10 hour relaxation period the deviator stress tends to decrease continually for the 2.032 mm/min test.

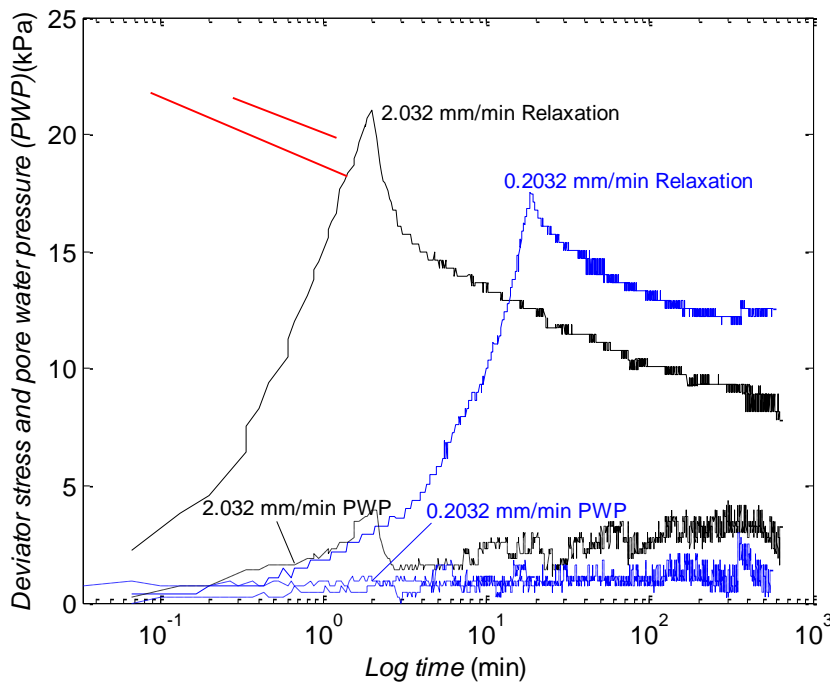


Figure 2. Undrained relaxation tests at two axial strain rates

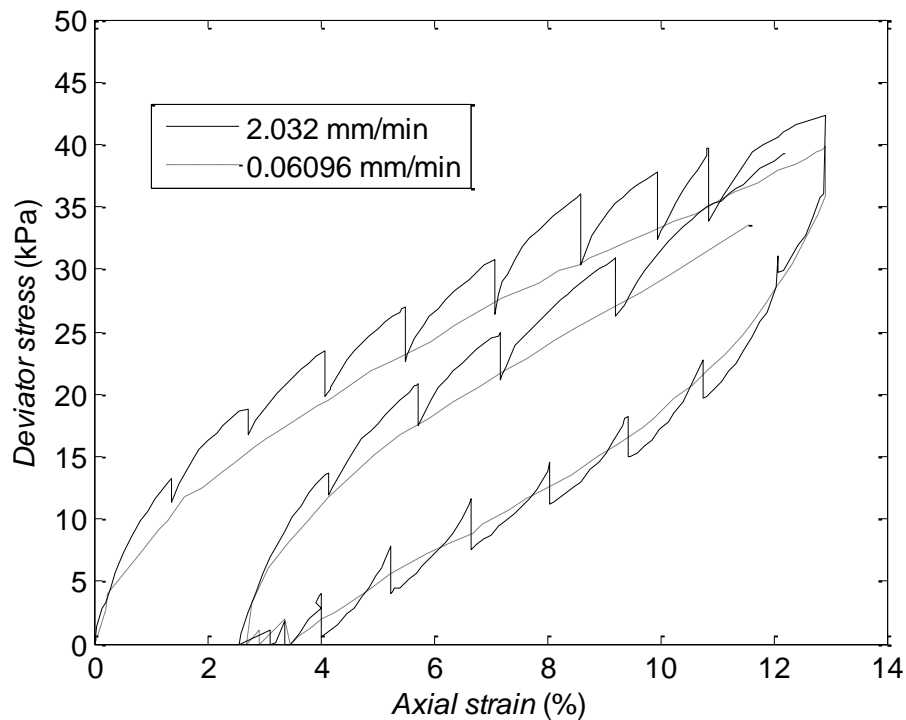


Figure 3. Comparison of *lur* relaxation test at 2.032 mm/min and *lur* test at 0.06096 mm/min

The triaxial *lur* relaxation test at an axial strain rate of 2.032 mm/min was compared with the triaxial *lur* test at a strain rate of 0.06096 mm/min (presented in Figure 3). Provided the relaxation time of 1000 s for the test at 2.032 mm/min, the termination points of the relaxation asymptotically approximated *lur* test at 0.06096 mm/min. It is reasonable to assume that if the relaxation test was leaved long enough, it would reach its creep limit, which according to Haupt (2002) is defined as *state of equilibrium*. For peat, however, creep continues for an extremely long period of time. Relaxation test provides a suitable means for the study of peat inelasticity.

CONCLUSIONS

From the results of the undrained triaxial relaxation tests of a fibrous peat with unloading, the following conclusions can be made:

- (1) Rate-dependent and -independent hystereses were observed in the undrained triaxial tests on the fibrous peat;
- (2) The pore water pressure variations during uniaxial stress relaxation tests were very small. Lower strain rate resulted in a time delay prior to the initiation of the deviator stress decay. A linear relationship can be found between deviator stress and logarithm of time after an initial time period;
- (3) Relaxation tests provide a suitable means for investigating strain rate effects in peat, especially for slow strain rates.

In order to investigate the creep limit, further relaxation tests should be carried out with longer relaxation time.

ACKNOWLEDGEMENTS

The first author gratefully acknowledges an Embark Initiative Postgraduate Scholarship from the Irish Research Council and a Postgraduate Research Award from Trinity College Dublin.

REFERENCES

- Barden L. & Perry P.L. (1968) Models of the consolidation process in peat soils. Proceedings of the 3rd International Peat Congress, Quebec. International Peat Society, Finland, 119-127.
- Den Haan E.J. (1996). A simple compression model for non-brittle soft clays and peat. *Géotechnique* 42(3), 465-483.
- Dhowian A.W. and Edil T.B. Consolidation behavior of peats. *Geotechnical Testing Journal* 3(3), 105-114.
- Farrell E.R., Jonker S.K., Knibbler A.G.M. & Brinkgreve R.B.J. (1998) The use of a direct simple shear test for the design of a motorway on peat. XII European Conference on Soil Mechanics and Geotechnical Engineering, 1027-1033.
- Haupt P. (2002) Continuum mechanics and theory of materials. Berlin Heidelberg: Springer-Verlag.
- Hendry M., Barbour S. & Martin, C. (2014). Evaluating the effect of fiber reinforcement on the anisotropic undrained stiffness and strength of peat. *Journal of Geotechnical and Geoenvironmental Engineering* 140(9), 04014054.
- Hobbs N.B. (1986). Mire morphology and the properties and behavior of some British and foreign peats. *Quarterly Journal of Engineering Geology* 19, 7-80.
- Zhang L. & O'Kelly B.C. (2013) The principle of effective stress and triaxial compression testing of peat. *Proceeding of ICE – Geotechnical Engineering* 167(1), 40-50.

